GL01133

DEPARTMENT OF GEOLOGY AND GEOPHYSICS

REPORT: TECHNICAL - 77-6

CONTRACT: EY-76-S-07-1601

AGENCY: ERDA

TITLE: GRAVITY AND GROUND MAGNETIC SURVEYS OF THE THERMO HOT SPRINGS KGRA REGION BEAVER COUNTY, UTAH

AUTHORS: ROBERT F. SAWYER AND KENNETH L. COOK

DATE: AUGUST 1977

UNIVERSITY OF UTAH SALT LAKE CITY, UTAH

GRAVITY AND GROUND MAGNETIC SURVEYS OF THE THERMO HOT SPRINGS KGRA REGION BEAVER COUNTY, UTAH

By

Robert F. Sawyer and Kenneth L. Cook

PREFACE

The attached report was submitted by Robert F. Sawyer in partial fulfillment of the requirements for the degree of Master of Science in Geophysics, Department of Geology and Geophysics at the University of Utah. The work was performed under the direction of Dr. Kenneth L. Cook.

CONTENTS

CONTENTS (CONT'D)

ABSTRACT

During the period June to September 1976, gravity and ground magnetic surveys were made in the Thermo Hot Springs KGRA region which is located southwest of the town of Milford, Beaver County, Utah. The regional surveys comprised 273 new gravity and magnetic stations and incorporated 104 previous gravity stations over an area of approximately 620 km^2. The detailed surveys consisted of 9 east-west profiles in the immediate vicinity of the Thermo Hot Springs KGRA.

The gravity data were reduced and are presented as terrain-corrected Bouguer gravity anomaly maps. Terrain corrections were made to a distance of 18.8 km. The regional gravity map shows the following features: 1) a large north-south trend with total relief of 5 mgal extending through the central portion of the study area; 2) an east-west trend with relief of about 7-8 mgal south of the Star Range and Shauntie Hills; 3) a north-south trend with 5 mgal relief east of Blue Mountain; and 4) a broad low of approximately 5 mgal closure southwest of the Shauntie Hills. The trends are probably caused by major faults and the gravity low is probably caused by the southern end of the Wah Wah Valley graben.

The detailed gravity map indicates two possible east-west trending faults intersecting a major north-south trending fault in the immediate vicinity of the Thermo Hot Springs. The location of the hot springs appears to be fault controlled.

To facilitate interpretation of the gravity data, the following processing and modeling techniques were used: 1) high-pass frequency filtering; 2) polynomial fitting; 3) second derivative; 4) strike filtering; 5) two-dimensional modeling; and 6) three-dimensional modeling. These techniques proved helpful as they more clearly delineated features of interest. The residual maps outlined an elongate north-south graben that extends through the survey area. The strike-filtered maps emphasize the major north-south and east-west faults of the region. Modeling provided reasonable depth estimates for bedrock in the vicinity of the hot springs and supported the structural interpretation for the hot springs area.

The magnetic data are presented as total magnetic intensity anomaly maps for both the regional and detailed surveys. The regional map delineates a magnetic high with 600-gammas closure that corresponds to a Tertiary quartz monzonite intrusive in the northeast part of the survey area. An east-west trend with about 300-gammas relief is delineated south of the Shauntie Hills and Star Range and possibly corresponds to an east-west fault.

The detailed magnetic map outlines an anomalous low with nearly 100-gammas closure associated with the Thermo Hot Springs. This magnetic low may reflect an alteration zone which is structurally controlled.

The following processing and modeling techniques were applied to aid interpretation of the magnetic data: 1) low-pass frequency filtering; 2) strike-filtering; 3) pseudogravity; 4) two and one-half dimensional modeling; and 5) three-dimensional modeling. The low-pass filtering clearly delineates the intrusive and the east-west trend south of the Star Range. The strike-filtering outlines north-south and east-west trends which correlate with faults implied by gravity data. The pseudogravity map indicates that the magnetic and gravity anomalies are not caused by the same bodies. The two and one-half dimensional modeling in the hot springs area provides a possible model for an alteration zone which appears to be structurally controlled. The three-dimensional model of the Tertiary quartz monzonite intrusive indicates a relatively shallow, slightly elongate intrusion that continues to a depth of at least 1 km.

LIST OF ILLUSTRATIONS

List of Illustrations (Continued)

List of Illustrations (Continued)

List of Illustrations (Continued)

ACKNOWLEDGMENTS

I would like to express my gratitude to the members of my supervisory committee, Dr. Kenneth L. Cook, Dr. William T. Parry, and Dr. David S. Chapman. Their time, supervision, and critical reading of this manuscript have proven invaluable. John H. Snow, James D. Klein, John A. Stodt, James A. Carter, and Philip E. Wannamaker assisted in the acquisition of field data or interpretation phases of this research. John H. Snow and Terry J. Crebs provided portions of the computer software used in the data processing phase.

I wish to thank the students of the gravity and magnetic classes of 1974 and 1975 (GG 521 under the supervision of Dr. Kenneth L. Cook), whose efforts helped provide a portion of the data incorporated in this thesis.

Dr. J. R Montgomery of ASARCO generously provided the polynomial fitting gravity programs used in data processing. Dr. Manik Talwani developed and provided the 3D modeling programs utilized in this study.

My sincere appreciation is given also to my wife, Melinda, who spent many hours of work assisting in various ways in the compilation of the data and manuscript of this thesis.

Financial assistance for this work was provided by the Energy Research and Development Administration under Contract No. EY-76-S-07-1601.

INTRODUCTION

During the period June to September 1976, gravity and ground magnetic surveys were made in the Thermo Hot Springs region, which is located southwest of the town of Milford, in Beaver County, Utah (Fig. 1). The survey consisted of both regional and detailed gravity and ground magnetic data acquisition. The total region surveyed was approximately 620 km^2.

The surveyed area lies in the northern portion of the Escalante Desert and is bordered by the Star Range and Shauntie Hills on the north, Blue Mountain on the west, and the Black Mountains on the southeast (Fig. 2). The hot springs, situated approximately 26 km west of the town of Minersville, are located in the south central part of the thesis area.

Most of the thesis area has little topographic relief. Elevations in the Escalante Desert typically range from 1525 to 1700 m. Blue Mountain rises to an elevation of approximately 2320 m. The Shauntie Hills, which are west of the Star Range, are more gently rolling hills and typically vary from 1700 to 1890 m. The Black Mountains have elevations ranging from approximately 1700 to 1900 m for the area of interest of this report.

Purpose of the Study

The primary objectives of the gravity survey were to determine the regional structural features of the area, to delineate the

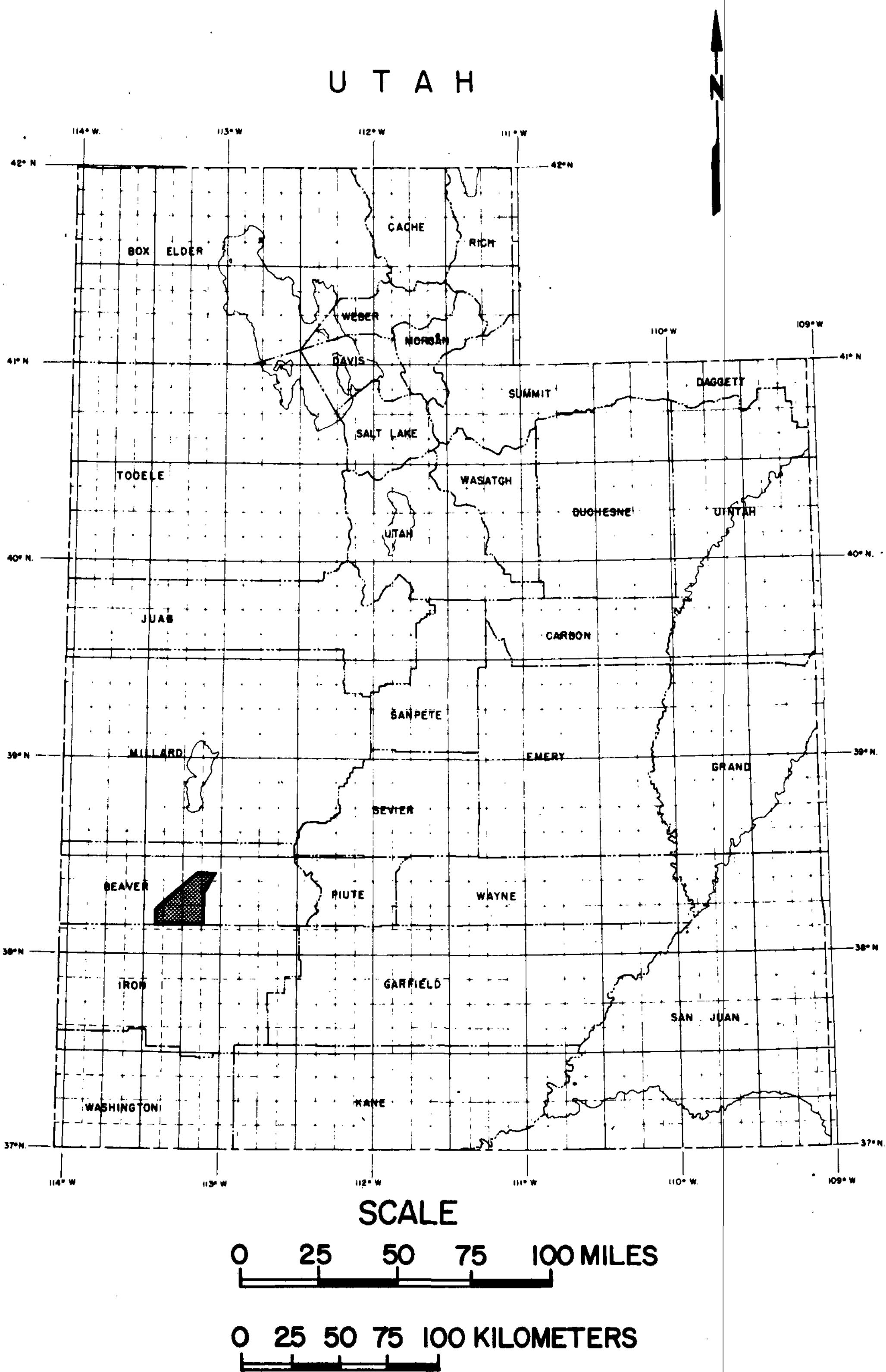

Figure 1. Map of Utah showing the surveyed area.

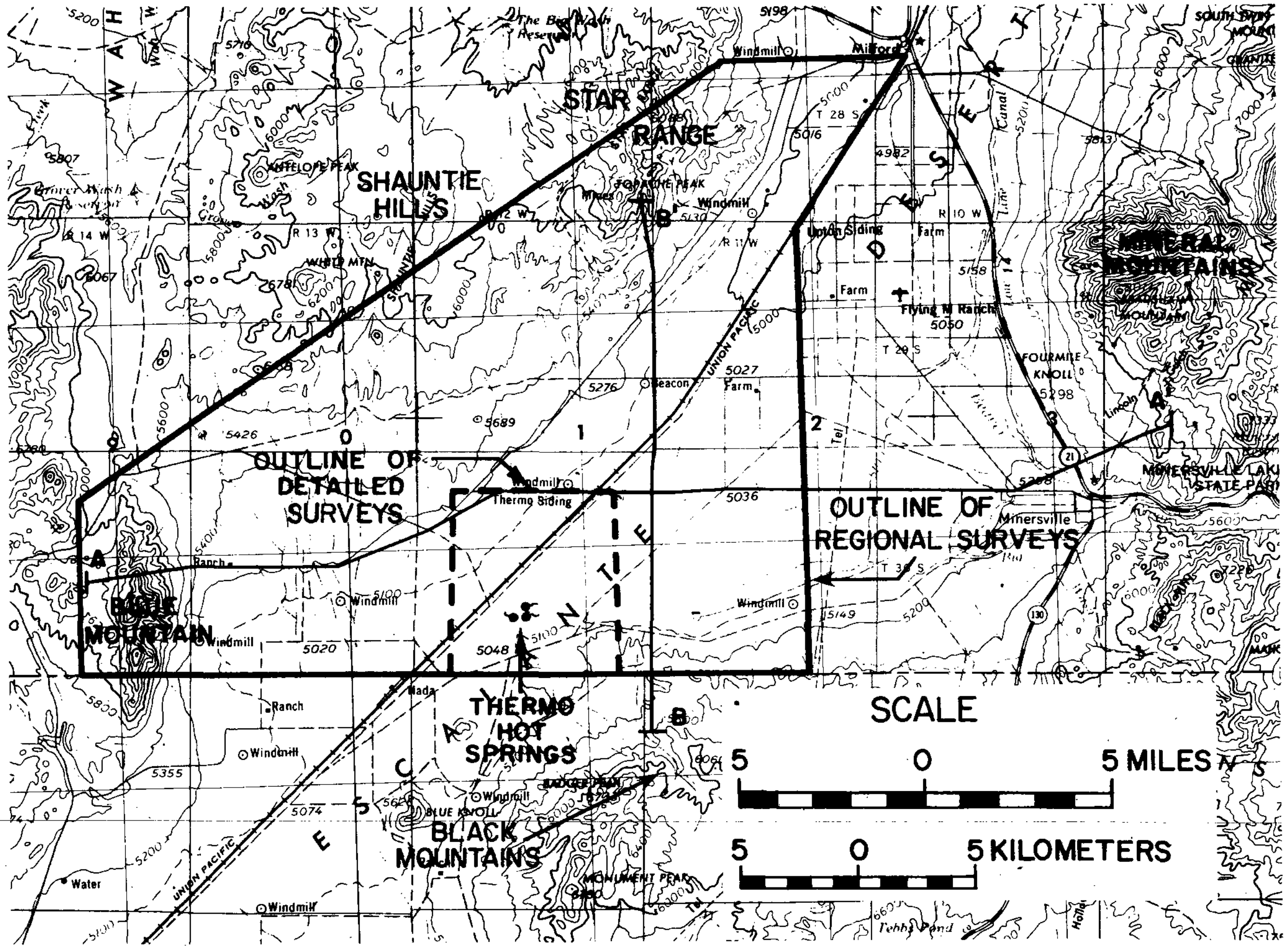

Figure 2. Index map of the surveyed area showing outlines of gravity and magnetic surveys: 1) Regional, 2) Detailed, and 3) Profiles AA' and BB'.

locations of major Basin and Range faults, and to obtain probable depths to bedrock in the alluvium-covered areas. The detailed gravity data were obtained to enhance the regional survey in the hot springs area and to define more precisely the structure associated with the hot springs.

The ground magnetic survey was made for two primary reasons. First, it was felt that the magnetics might be used to discriminate between lithologies in a general sense. In particular, it was hoped that different magnetic "signatures" would be obtained for volcanics, intrusives, and sediments. This would then allow one possibly to outline intrusives and determine projections of the volcanics under the alluvium. Secondly, in the area of the hot springs, the hydrothermal activity associated with the upward perculating hot waters may have altered the magnetite in the volcanics and consequently cause a magnetic low. This would yield helpful information concerning the hot springs and the geothermal area in general. The survey provided a means of testing this hypothesis and possibly providing insight as to the origin or movement of the hot water associated with the hydrothermal system.

Previous Investigations

A number of geological and geophysical studies have been made of portions of the thesis area. The Blue Mountain region was mapped in an investigation by Miller (1958). The Star Range was described and mapped in reports by Baer (1962), Abou-Zied (1968) and Baetcke (1969). Parts of the Black Mountains and the Shauntie Hills were described in a special study by Erickson and Dasch (1963). Brief discussions of the hot springs were presented by Mundorff (1970) and Peterson (1973).

Both gravity and aeromagnetic surveys have previously been conducted in parts of the thesis area. However, these surveys typically comprised large station spacings of a reconnaissance nature and, therefore, do not provide the detail necessary to properly delineate many of the anomalous features of this region.

Mudgett (1963) conducted a regional gravity study which included about 25 stations in the northern portion of the thesis area. His work was restricted to improved roads only.

Montgomery (1973) compiled a simple Bouguer gravity anomaly map for the western half of Utah. In his investigation, he obtained gravity measurements for 13 stations in the western part of the thesis area. Again, the stations were widely spaced.

The work of Peterson (1972) provided broad gravity coverage of the thesis area and regions farther north and east. Although about 80 stations were acquired by Peterson within the area of this investigation, further detail was considered essential to obtain a better understanding of the region.

A gravity study was recently completed by Thangsuphanich (1976) east of the study area and a gravity investigation is presently being conducted by Carter (1977) north of this survey. Both of these surveys are tied to this study and will provide extended regional coverage.

The University of Utah GG 521 classes of 1974 and 1975 acquired gravity and magnetic data in the Thermo Hot Springs region. Portions of these data have been incorporated in this study.

Schmoker (1972) analyzed gravity and aeromagnetics for the northern portion of the area using data obtained from the U. S. Geological Survey aeromagnetic and gravity maps (1966) for the San Francisco Mountains and vicinity. The aeromagnetic survey was flown at an elevation of 2743 m above sea level along east-west flight lines with a typical separation of 1.61 km. The gravity survey consisted of 390 stations over the same area as the aeromagnetics. The total area of these surveys was approximately 2540 km^2.

Additional aeromagnetic data are available from the state map which was compiled by Zietz et al., 1976.

GEOLOGY

The majority of the thesis area lies in the Escalante Desert, a basin filled with Quaternary alluvium and Tertiary volcanics. A number of prominent geologic features are found on the perimeter of the surveyed region. These include the Star Range, Shauntie Hills, Blue Mountain, and the Black Mountains. Located in the south-central portion of the survey are the two mounds which have been designated the Thermo Hot Springs. Each of these areas is further discussed in a later section.

Star Range

The Star Range is considered a typical Basin and Range style mountain range which consists of block-faulted eastward-dipping sedimentary and volcanic rocks that have been intruded by acidic to intermediate plutons (Baer, 1973). These intrusives have been dated at approximately 21 m.y. (Lemmon, Silberman and Kistler, 1973). In the range, approximately 3050 m of sedimentary section is exposed, ranging from Devonian to Jurassic in age. The Devonian units are typically dolomites and shale whereas the Mississippian and Pennsylvanian-Permian rocks are limestone. The Permian portion of the section is composed of limestone, gypsum, and dolomite.

The Mesozoic lithologies differ from the Paleozoic units. Triassic rocks are shales, siltstones and limestones whereas the Jurassic unit is a sandstone.

Tertiary volcanic rocks are predominant on the western edge of the Star Range and small outcrops can be found in the northeastern portion of the range due west of Milford. The volcanics west of the range are mapped as the Isom Formation which is mostly andesite to latite ignimbrites (Hintze, 1963). The two minor outcrops to the northeast have been designated undifferentiated Tertiary volcanics (Baer, 1973).

Tertiary intrusives are found scattered throughout the range (see Fig. 3 for locations). The composition of these intrusives varies from granite to granodiorite. Mineralization is associated with these intrusives and has accounted for intermittent mining in the range.

Both normal and thrust faulting can be found in the range. The range is considered to be part of an upper plate which was thrust in an east and southeast direction (Baer, 1973). This thrust faulting is dated as Jurassic or later, as Paleozoic rocks are found thrust over Jurassic sandstone.

The thrust faulting was followed by a period of normal faulting. The normal faulting exhibits two primary directions which are north-south and east-west and the east-west faulting post dates the north-south faulting.

<u>Shauntie Hills</u>

The Shauntie Hills are located southwest of the Star Range in the north-central portion of the thesis area. These hills primarily consist of Tertiary volcanics with minor outcrops of Paleozoic and

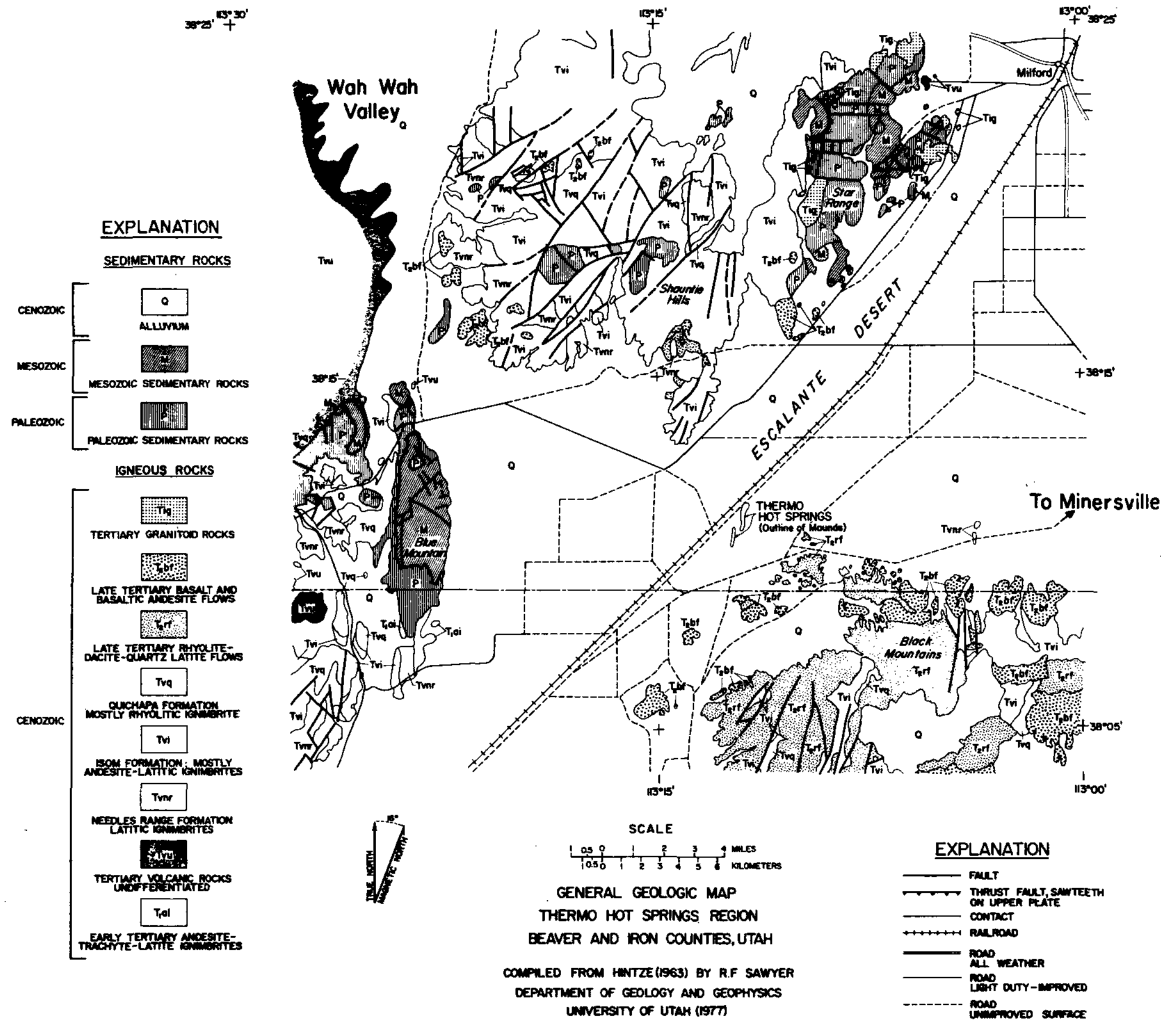
EXPLANATION
SEDIMENTARY ROCKS
CENOZOIC
Q
ALLUVIUM
MESOZOIC
MESOZOIC SEDIMENTARY ROCKS
PALEOZOIC
PALEOZOIC SEDIMENTARY ROCKS
IGNEOUS ROCKS
Tig
TERTIARY GRANITOID ROCKS
LATE TERTIARY BASALT AND BASALTIC ANDESITE FLOWS
LATE TERTIARY RHYOLITE-DACITE-QUARTZ LATITE FLOWS
Tvq
QUICHAPA FORMATION MOSTLY RHYOLITIC IGNIMBRITE
Tvi
ISOM FORMATION: MOSTLY ANDESITE-LATITIC IGNIMBRITES
Tvnr
NEEDLES RANGE FORMATION LATITIC IGNIMBRITES
Tvu
TERTIARY VOLCANIC ROCKS UNDIFFERENTIATED
EARLY TERTIARY ANDESITE-TRACHYTE-LATITE IGNIMBRITES
CENOZOIC
Wah Wah Valley
Milford
Star Range
Shauntie Hills
Blue Mountain
ESCALANTE DESERT
THERMO HOT SPRINGS (Outline of Mounds)
To Minersville
Black Mountains
113°30'
113°15'
113°00'
38°25'
38°15'
38°05'
TRUE NORTH
MAGNETIC NORTH
SCALE
MILES
KILOMETERS
GENERAL GEOLOGIC MAP
THERMO HOT SPRINGS REGION
BEAVER AND IRON COUNTIES, UTAH
COMPILED FROM HINTZE (1963) BY R.F SAWYER
DEPARTMENT OF GEOLOGY AND GEOPHYSICS
UNIVERSITY OF UTAH (1977)
EXPLANATION
FAULT
THRUST FAULT, SAWTEETH ON UPPER PLATE
CONTACT
RAILROAD
ROAD ALL WEATHER
ROAD LIGHT DUTY-IMPROVED
ROAD UNIMPROVED SURFACE

Figure 3.

Mesozoic sediments.

The predominant volcanic unit in the survey area is the Isom Formation which primarily consists of andesite-latite ignimbrites. Scattered outcrops adjacent to the alluvial fill of the Escalante Desert have been identified as late Tertiary basalt and basaltic andesite flows, late Tertiary rhyolite-dacite-quartz latite flows, and the Needles Range Formation which is a Tertiary latite ignimbrite. Locations of these exposures are shown on Figure 3.

The Needles Range Formation is the oldest volcanic unit of the group and is overlain by the Isom Formation in the Milford area (Erickson, 1973). Both the rhyolitic and basaltic units are known to be younger than the two previously mentioned formations and the basaltic units are the youngest volcanics in this area (Erickson, 1973).

For the portion of the Shauntie Hills located in the thesis area, the dominant structural direction exhibited by a normal faulting appears to be north-northeast. This is illustrated by the mapped faults shown on Figure 3.

Blue Mountain

Blue Mountain is located in the southeastern portion of the Wah Wah Mountains and is situated at the extreme western margin of the thesis area. It is composed of both Paleozoic and Mesozoic sediments.

The Paleozoic exposures have been designated Cambrian undifferentiated and are principally composed of dolomite and limestone (Miller, 1958). These rocks are exposed on both the northern and southern ends of Blue Mountain with additional continuous exposure along the western edge of the mountain.

The Mesozoic sediments comprise the bulk of exposed sediments in the Blue Mountain area. They range from Lower Triassic to Upper Jurassic in age. The Triassic rocks are typically sandstones, siltstones, and shales whereas the Jurassic lithologies are principally sandstones and siltstones.

The predominant structural feature of this area is the thrusting of the Paleozoic sediments over the Mesozoic units. This thrusting is post Upper Jurassic as the Cambrian units overlie Jurassic sandstones (Miller, 1958). After the period of thrusting, Miller postulates doming with associated north-south and east-west normal faulting. His work indicates only minor normal faulting on the eastern edge of Blue Mountain but also predicts the possible existence of a pediment with more dominant normal faulting further east under alluvial cover.

Black Mountains

Only the northwestern portion of the Black Mountains is included in the survey area and is located in the southeast portion of that area. As in the Shauntie Hills, this region is composed of Tertiary volcanics. Three of the four units mentioned in the Shauntie Hills area can be found in this region. These include the late Tertiary basaltic units, the late Tertiary rhyolitic units, and the Isom Formation. The Isom Formation appears as only a single exposure adjacent to the alluvial fill on the northern boundary of the mountains (see Fig. 3 for location). The basaltic and rhyolitic units show approximately even distribution in the survey region, but the rhyolites become dominant to the south. The same relative age correlation exists for these two units as was previously mentioned.

Mapped normal faulting in this portion of the Black Mountains appears to indicate a preferential structural direction. As in the Shauntie Hills, this direction is north-northeast.

Thermo Hot Springs

The Thermo Hot Springs are located in the south central portion of the thesis area approximately 26 km west of Minersville. The springs system consists of twenty small springs that issue from the sides and tops of two elongate mounds (Peterson, 1973). These two mounds are roughly 6 m high, 75 m wide, and have a combined length of 2.4 km. The mounds are en echelon with the northern mound offset about 91 m to the east of the southern mound. The composition of these mounds is primarily loose sands combined with silica and carbonate cemented sands.

Studies of these springs have indicated temperatures of 77°C and discharge estimates of 750 l/min (Mundorff, 1970). Dissolved solids content has been determined to be about 1500 ppm (Mundorff, 1970).

The springs are probably fault controlled. Previous gravity studies by Peterson and the University of Utah classes implied a north-south-trending gravity feature adjacent to the springs.

INSTRUMENTS AND DATA ACQUISITION

Instrumentation

All ground magnetic data were obtained using a Geometrics Model G816 magnetometer owned by the University of Utah. This is a proton precession total field magnetometer which has an accuracy of ± 1 gamma. All gravity stations were read using a LaCoste and Romberg Model G geodetic gravity meter No. 264 owned by the University of Utah. This instrument has a precision capability of 0.001 milligal (mgal).

Gravity Data Acquisition

The gravity data acquisition consisted of two phases, a regional and a detailed. For the regional gravity work, 273 new gravity stations were taken. The stations were located on published or preliminary 7-1/2-minute U.S.G.S. topographic quadrangle maps. These stations were typically taken along roads, jeep trails, bench marks, section corners, and spot elevations. The elevations for these stations were obtained directly from the maps. For stations where the specific elevations were not indicated, the elevations were determined from the contours. Because the contour intervals were small, typically 6.1 m, and most of the area relatively flat, this technique provided greater accuracy than the use of altimeters.

All of the regional gravity stations were tied to the Milford gravity base station in the Utah Gravity Base Station Network (Cook et al., 1971). The initial and final readings of each day were taken at this base. In addition, three temporary field bases were established in the thesis area. These three temporary bases were tied both to each other and also to the Milford base. The ties were made using a series of loops in the following sequence: A B C D B C D A where A is the Milford base and B, C and D are the temporary field bases.

A "looping" technique was used to acquire all data for the regular gravity stations. The readings were all looped to the field bases within a time period of 4 hours or less to minimize effects of tidal variation and check for instrument tares.

In addition to the previously mentioned stations, 104 regional stations were incorporated from the University of Utah GG 521 classes of 1974 and 1975. It should be noted that for their surveys both of these classes used one of the same field bases, RS-1, as the author and followed essentially the same acquisition technique as just described. The combined data sets, which total 377 stations, constitute the regional gravity information for this report.

The second phase of the field work was the acquisition of detailed gravity data, which was restricted to the immediate area of the hot springs (see Fig. 2). A total of 225 detailed gravity stations were obtained along 9 east-west profiles. The length of the profiles varied from 610 m to 3.22 km (see Fig. 4). The station spacing was either 30.5 m or 161 m. Most of the detailed gravity stations, taken over and adjacent to the hot springs mounds were spaced 30.5 m apart. A total of approximately 19 km of profile data

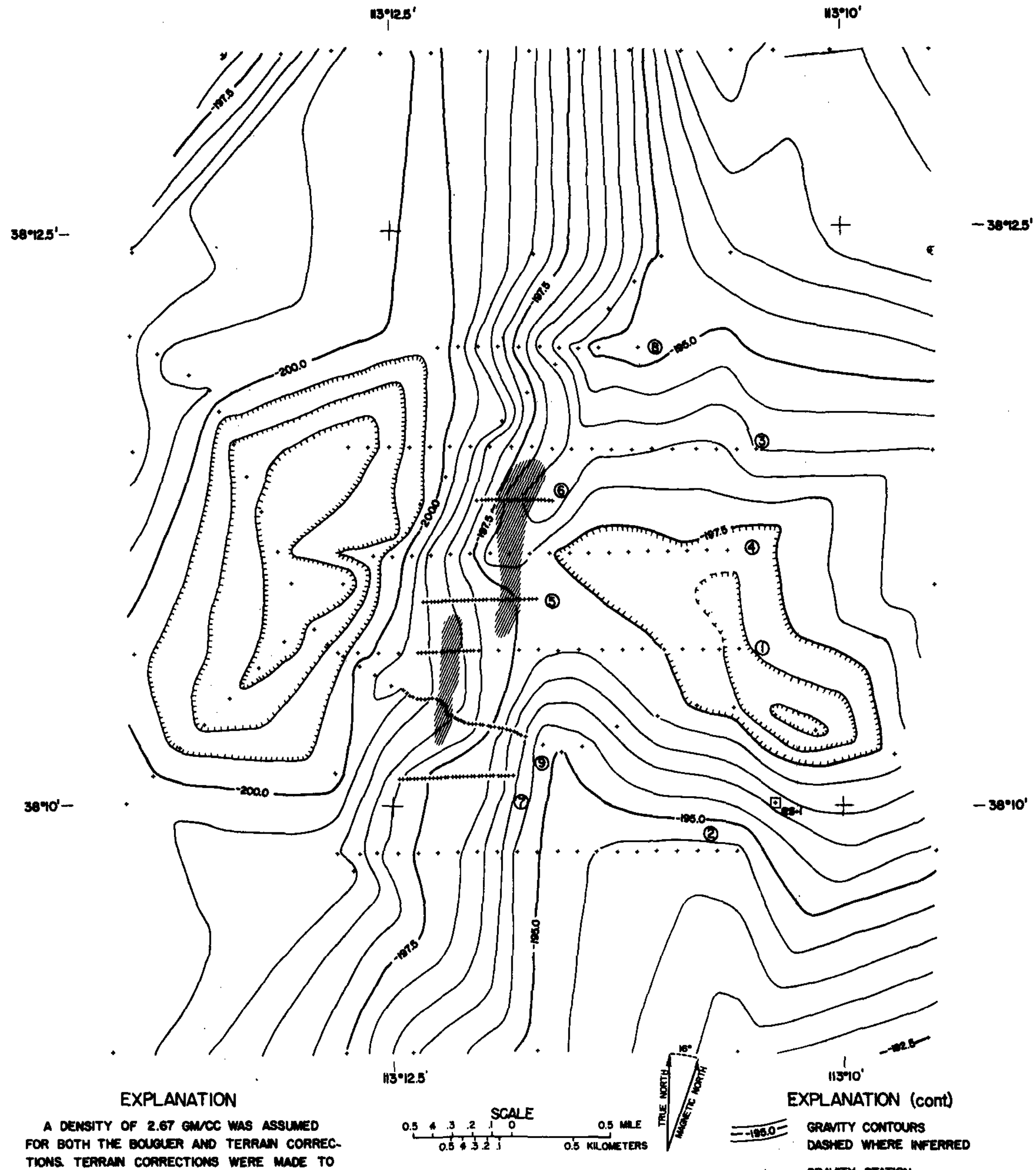

EXPLANATION

A DENSITY OF 2.67 GM/CC WAS ASSUMED FOR BOTH THE BOUGUER AND TERRAIN CORRECTIONS. TERRAIN CORRECTIONS WERE MADE TO A DISTANCE OF 18.8 KM USING A U.S.C. & G.S ZONE CHART.

GRAVITY DATA SOURCES: R.F. SAWYER AND UNIVERSITY OF UTAH GG 521 CLASSES OF 1974 AND 1975.

GRAVITY REDUCTION AND COMPILATION BY R.F. SAWYER, ADVISED BY K.L. COOK, DEPARTMENT OF GEOLOGY AND GEOPHYSICS, UNIVERSITY OF UTAH.

DETAILED TERRAIN-CORRECTED
BOUGUER GRAVITY ANOMALY MAP
THERMO HOT SPRINGS REGION,
BEAVER COUNTY, UTAH
1977

CONTOUR INTERVAL 0.5 MILLIGAL

EXPLANATION (cont)

- -195.0 GRAVITY CONTOURS DASHED WHERE INFERRED
- + GRAVITY STATION
- ⊞ RS-1 GRAVITY BASE STATION
- ① PROFILE NUMBER
- (hatched) HOT SPRINGS MOUNDS

Figure 4.

were taken.

For the detailed gravity stations along the profiles, the elevations of the gravity stations were obtained using a Kauffel and Esser Wye level. The elevations were tied to the known elevations of several different section corners. All elevation readings were made to the nearest 0.003 m. Typically, the difference between the author's measurements and the elevations given on the U.S.G.S. 7-1/2-minute quadrangle maps was less than 0.61 m. The worst case encountered was a difference of 1.08 m which would introduce an error of approximately 0.01 mgal per station along the affected line if the error was evenly distributed, or an error of 0.2 mgal if the elevation error was made at one station. Actually, the author estimates an accuracy of about 0.15 m per station for the detailed survey. This would introduce a gravity uncertainty of approximately 0.03 mgal per station.

For horizontal control along these profiles, directions were obtained by compass and horizontal distances were taped with a 100-m cloth tape.

For the detailed gravity stations, a "looping" technique was again employed for all readings. Field base, RS-1, was used for reference as it had been tied to the Milford base by averaging over 20 ties between these two stations. Individual loops were made within the profiles and these loops were then tied to field base, RS-1. The time of the loops was decreased to an average of approximately 2 hr for the detailed profile surveys, in comparison to 4 hr for the regional gravity survey. This decrease in loop time was established to increase the accuracy of the data.

Magnetic Data Acquisition

As was so for the gravity data, the magnetic data acquisition consisted of regional and detailed phases. For the regional magnetic data, readings were taken at the same 273 station locations and at the same time as the gravity stations. For the magnetic regional survey the same three temporary field bases were used with all bases tied to the field base, RS-1, located at a road intersection near the hot springs (see Fig. 5). This master base was chosen for reference because it is the same base used by the University of Utah GG 521 class of 1975 whose magnetic data were incorporated into this study.

The magnetic data were taken using the same looping sequence as the gravity data. Depending on the variation of the individual magnetometer readings, either three or five independent readings were made and averaged to obtain a value for the station. Where readings were somewhat erratic, five readings were recorded at a centerpoint (i.e., the station) and at each of the major cardinal geographic directions at a distance of 1.83 m from the centerpoint. For some stable readings, the centerpoint, east and west were recorded.

The detail magnetic data were acquired along the same profiles as as the detailed gravity stations. The same procedure was followed for the detailed work as is outlined for the detailed gravity stations. The total number of magnetic stations is 185. This

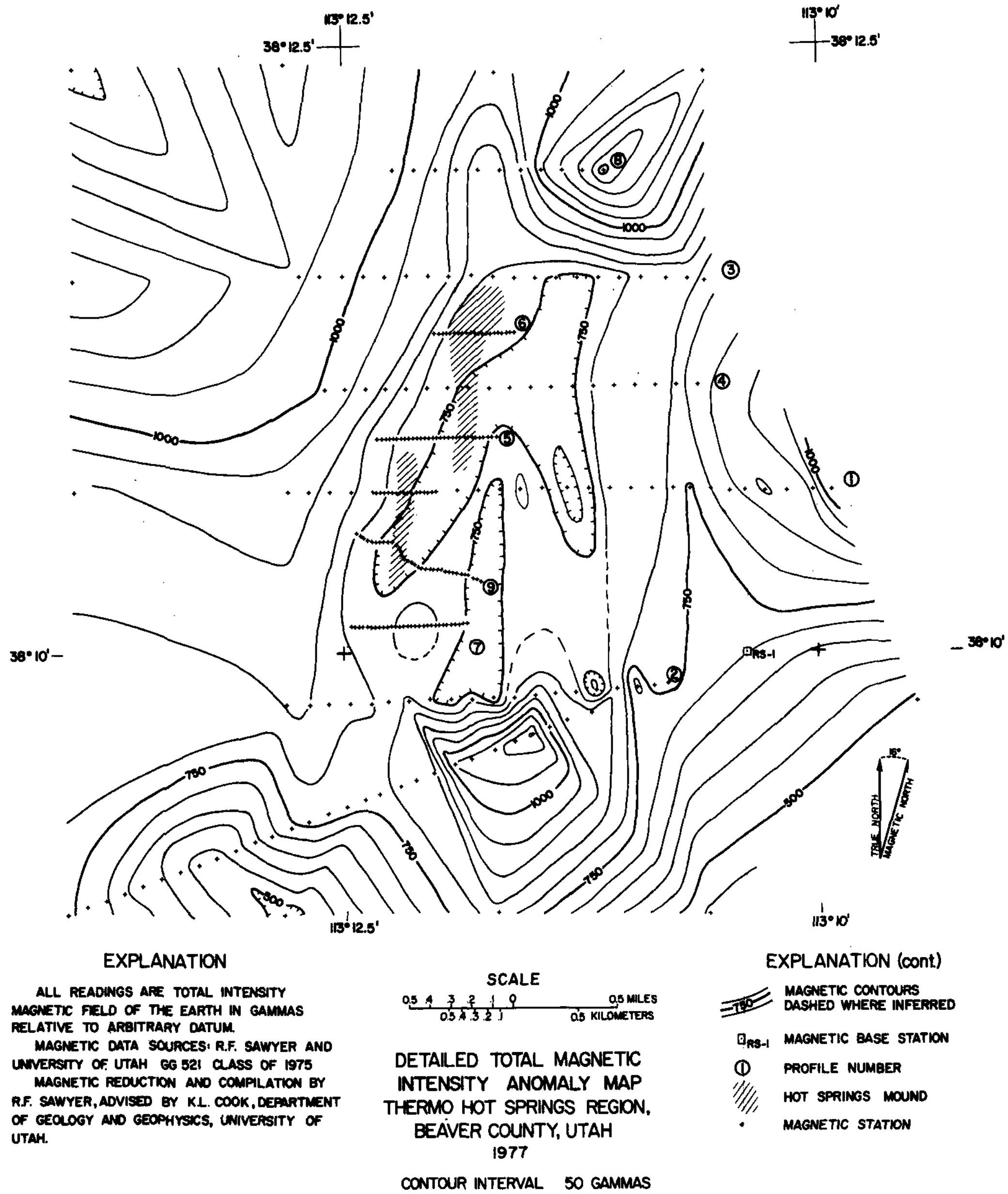
113° 12.5'
38° 12.5'
113° 10'
38° 12.5'
38° 10'
38° 10'
113° 12.5'
113° 10'
1000
750
500
RS-1
TRUE NORTH
MAGNETIC NORTH
16°
EXPLANATION
ALL READINGS ARE TOTAL INTENSITY MAGNETIC FIELD OF THE EARTH IN GAMMAS RELATIVE TO ARBITRARY DATUM.
MAGNETIC DATA SOURCES: R.F. SAWYER AND UNIVERSITY OF UTAH GG 521 CLASS OF 1975
MAGNETIC REDUCTION AND COMPILATION BY R.F. SAWYER, ADVISED BY K.L. COOK, DEPARTMENT OF GEOLOGY AND GEOPHYSICS, UNIVERSITY OF UTAH.
SCALE
0.5 MILES
0.5 KILOMETERS
DETAILED TOTAL MAGNETIC INTENSITY ANOMALY MAP
THERMO HOT SPRINGS REGION, BEAVER COUNTY, UTAH
1977
CONTOUR INTERVAL 50 GAMMAS
EXPLANATION (cont.)
MAGNETIC CONTOURS DASHED WHERE INFERRED
MAGNETIC BASE STATION
PROFILE NUMBER
HOT SPRINGS MOUND
MAGNETIC STATION

Figure 5.

number of magnetic stations is less than the detailed gravity stations because some profile data were incorporated from the University of Utah class work previously mentioned.

Physical Properties Data Acquisition

A total of 35 rock samples were taken in the thesis area. All samples were selected from outcrops (i.e., not float) and therefore should be representative of the selected area. Of these, 31 samples were measured for density and magnetic susceptibility.

Density measurements were made in the laboratory using a single pan balance with readings measured to the nearest gram and densities computed to the nearest 0.01 gm/cm^3. The same samples were used for magnetic susceptibility measurements. All samples were crushed to pea size, and inserted (in a plastic tube) into a Geophysical Specialties Co. Model MS-2 magnetic susceptibility bridge to obtain the readings. A volume correction was required for all magnetic susceptibility measurements because crushed samples were used.

DATA REDUCTION

Gravity Data Reduction

All gravity stations were reduced using a computer program which had previously been written specifically for reduction of data acquired with the LaCoste and Romberg gravity meter no. 264. The program was run on the UNIVAC 1108 computer at the University of Utah. Instrument readings were corrected for drift on the assumption that the drift was linear between the first and last readings within a loop.

For the theoretical gravity value calculation, the International Gravity Formula (Swick, 1942) was employed. The program uses a free-air correction value of 0.30861 mgal/m and a density of 2.67 gm/cm^3 was assumed for the Bouguer correction. This density value was chosen because: 1) it is the average density for crustal rock above sea level (Nettleton, 1940, p. 101); 2) it is in good agreement with laboratory measurements for the density of the surrounding bedrock of Paleozoic sedimentary units; and 3) investigations in surrounding areas assumed this value, thereby allowing the author to tie his results to previous work. On the basis of these assumptions, the total elevation correction used was 0.19683 mgal/m and the datum was chosen at sea level.

For the regional stations, all reductions were made in reference to the Milford base station which is part of the Utah Gravity Base

Station Network and for which the observed gravity value was assigned 979539.86 mgal (Cook et al., 1971). The detailed profile stations were reduced using master field base RS-1, located near the hot springs, for reference. On the basis of the averaging of 20 ties made between the master field station RS-1 and the Milford base, the observed gravity value for RS-1 was assigned as 979517.67 mgal. This procedure gave a greater accuracy to the profile stations.

The terrain corrections were calculated through zone K (18.8 km) with U.S. Coast and Geodetic Survey terrain correction charts (Swick, 1942). Again, a density of 2.67 gm/cc was assumed for the rock density. As the majority of the thesis area is located in areas of minor relief, only a judicious number of stations (about 100) were chosen to be terrain corrected. The largest terrain correction value obtained was 4.02 mgal. The results of these corrections were plotted on an overlay and the terrain corrections for the remaining stations were then interpolated. The end result of the gravity reduction process was terrain-corrected Bouguer gravity anomaly values.

Magnetic Data Reduction

As with the gravity data, all magnetic data were reduced using a computer program and run on the UNIVAC 1108 at the University of Utah computer center. Drift curves were computed by hand for each day of the survey and this information was read into the program at 2-hr intervals. Using this input, the magnetic data were drift corrected. The program for this magnetic data reduction was written by Dr. Ralph T. Shuey.

All reductions were made to an assumed value of 697 gammas at master field base RS-1, near the hot springs. The other field bases were tied to RS-1 by a series of loops in order that all stations could be reduced with respect to the same datum. This master field base station was chosen because it is the same reference used by the University of Utah GG 521 class of 1975 and would facilitate incorporation of a portion of that data.

DATA PROCESSING

To facilitate interpretation, a number of processing steps were taken in both the frequency and space domains. The following discussion provides a brief description of how the residual maps and models, used for interpretation, were compiled.

To enable processing of both the regional gravity and regional magnetic maps, it was necessary to establish a grid of digitized values. After the station data were reduced, the reduced values were plotted at their appropriate locations using a Calcomp plotter and then hand contoured. A 39 by 39 grid was then digitized from the hand-contoured data. A grid spacing of 0.79 km was chosen so as to interface with previous grids established by Crebs (1976) and Thangsuphanich (1976).

As the area of this study did not constitute a square region, it was necessary to incorporate U.S.G.S. gravity data (Peterson, 1972) to complete the gravity grid. A third-order polynomial extrapolation was employed to fill the magnetic grid. It should be noted that these fictitious magnetic data were only used to allow processing with existing software and were discarded after processing. This accounts for the irregular boundary of the processed magnetic maps. These maps represent only the real data from this survey.

The polynomial fitting of the regional gravity data was accomplished by inputting the gridded values into the existing software of Dr. J. R Montgomery. His programs calculate a least-square polynomial surface of desired order which fits the data set. A third-order polynomial residual map was computed for comparison with the high-pass filtered and second vertical derivative maps. This order was selected based on a plot of the root-mean-square error versus the order the polynomial (Appendix 2). It was the opinion of both Dr. J. R Montgomery (1977, oral communication) and the author that this order would best approximate the regional gravity surface for the surveyed area.

The remainder of the regional processing was completed using the software of Dr. R. T. Shuey and T. J. Crebs. This processing was accomplished in the frequency domain. Several steps were necessary to prepare the data set for the frequency filtering. In order to transform the data from the space to the frequency domain, a two-dimensional Fast Fourier Transform program was employed which requires that the matrix size be input as a power of 2. Therefore, the 39 by 39 gridded data were padded with zeros to a 64 by 64 data set. Next, to remove a constant value and regional trend, a first-order polynomial, which was computed using the previously mentioned software, was subtracted from the data. Finally, to eliminate edge effects, a 5-point cosine bell taper was applied to the borders of the real data. Data were tapered to zero along all borders.

The next step was to transform the data and to calculate the appropriate filter factors to accomplish the desired operations.

For the second vertical derivative calculation, the data set was first low-pass filtered. This operation was performed to eliminate excessive amplification of high-frequency components in the second derivative filtering. A cut-off frequency of 0.33 cycles/grid interval (corresponding to a wavelength of 2.4 km) was selected for this low-pass filtering. The second-derivative filtering was then performed by multiplying the transformed, low-pass-filtered data by $4\pi^2 (f_x^2 + f_y^2)$ where f_x and f_y are the frequencies in the x and y directions, respectively.

A high-pass-filtered regional gravity anomaly map was obtained using the low-pass filter and subtracting the filtered data set from the original transformed digitized values. The filter factor which multiplies the transformed values was calculated as follows:

$$RR = \begin{cases} 1, & (f_x^2 + f_y^2)^{\frac{1}{2}} < f_c \\ 0, & (f_x^2 + f_y^2)^{\frac{1}{2}} > f_c \end{cases}$$

where RR is the filter factor and f_c is the cut-off frequency. The cut-off frequency used in this study was 0.10 cycles/grid interval (corresponding to a wavelength of 7.9 km).

The final filtered regional gravity anomaly maps processed in this study were east-west and north-south strike-filtered maps. These filters are a form of band-pass filters which operate in the frequency domain. To pass a certain direction, one simply specifies a set of azimuths and a taper width to be applied within the aforementioned azimuths. The filter then calculates a filter factor to be applied to the transformed data. For data outside the specified azimuths, the filter factor, RR, is set equal to zero. For data inside the azimuths but within the taper windows, a cosine tapered value between 0 and 1 is obtained for the filter factor. Finally, for data within the azimuths and not within the taper windows, the filter factor is set equal to one. Because a given direction in the space domain is perpendicular to its direction in the frequency domain, the following parameters were specified for the strike-filtering of this study:

East-West Strike-Filter

Azimuths: 225° and 315°
Taper Width: 30°

North-South Strike-Filter

Azimuths: 135° and 225°
Taper Width: 30°

(where angles are measured counterclockwise from the right).

The regional total magnetic intensity map was filtered using the same frequency-domain software described for the regional gravity processing. North-south and east-west strike-filtered maps were obtained for the magnetics using the same parameters specified in the gravity processing.

A low-pass filtered total magnetic intensity anomaly map was created using the previously mentioned low-pass filter and a cut-off frequency of 0.1644 cycles/grid interval (corresponding to a wavelength of 4.8 km).

The final processed regional map of this study is a pseudo-gravity anomaly map which was obtained from the regional total magnetic intensity data. This operation was again performed in the frequency domain but required two filtering routines not used for the gravity data: 1) a routine to calculate the reduction to the pole and 2) a routine to obtain the vertical integral of the magnetic field. The vertical integral as designated by Dr. R. T. Shuey is actually a filter factor which is applied to transformed data which have been reduced to the pole. This factor is calculated as follows:

$$RR = \frac{GRID}{2\pi(f_x^{\,2} + f_y^{\,2})^{\frac{1}{2}}}$$

where RR is the filter factor, GRID is the grid interval in km and f_x and f_y are in units of cycles/km.

The reduction to the pole routine performs the calculation of the following operator:

$$\left[\mathrm{Sin}\ I + \left\{\frac{i\ \cos I(f_x \cos D + f_y \sin D)}{(f_x^{\,2} + f_y^{\,2})^{\frac{1}{2}}}\right\}\right]^{-2}$$

where I and D are the inclination and the declination, respectively, of the magnetic field.

To obtain the pseudogravity field, one must then proceed as follows:

1) Calculate reduction to the pole for the transformed data.

2) Calculate "vertical integral" of data which have been reduced to the pole.

3) Multiply by a constant, $\frac{\gamma\rho}{M}$, where γ is the gravitational constant in cgs units, ρ is the assumed density in gm/cm^3 and M is the intensity of magnetization, which is equal to KH, where H is in oersted and K is in cgs units.

For this study, ρ was assumed to be 0.5 gm/cm^3 and the magnetic susceptibility, K, was assumed to be 0.002 cgs.

For the modeling of profile data, the software of J. H. Snow (1977) was employed. The following section is a brief description of his software.

For the calculation of the forward problem, the gravity program uses the two-dimensional algorithm (Talwani et al., 1959) and the magnetic program employs the two and one-half dimensional algorithm (Shuey and Pasquale, 1973). After calculating the forward problem for the initial guess, the program conducts a one-dimensional direct search over user specified parameters (certain vertices, densities or magnetic susceptibilities) to minimize the sum of the square of the differences between the observed and computed anomalies. The user specifies the order of search, direction of search (either vertical or horizontal), step size and tolerance for the search.

After completing the direct search for a profile, the model can be further refined using inversion techniques. The model determined from the direct search is input into the inversion program as its initial model. Using this model, a linearization method is employed to adjust all parameters simultaneously and obtain a final model. The techniques employed in Snow's (1977) inversion program are that the forward problem is expressed as a Taylor series expansion and this expansion is then used to generate N equations in M unknowns, where N is the number of stations and M is the number of parameters. These N equations are then solved using matrix inversion methods.

For the profiles in this study, the inversion program was only utilized on several cases as it was found that the search program would typically resolve the model with sufficient accuracy that inversion was not necessary.

A final note is necessary regarding the magnetic profile data. To suppress surface effects on the ground magnetic data, the readings were upward continued a distance proportional to the station spacing. For data spaced at 161 m, the upward continuation was 161 m and for data spaced at 30.5 m, the upward continuation was 152 m.

The upward continuation was performed in the space domain using an algorithm developed by Henderson and Zeitz (1949). The algorithm involves the convolution of the observed data with a set of coefficients calculated by the program to obtain the upward continued results.

INTERPRETATION OF DATA

Regional Gravity Data

As previously mentioned, to facilitate interpretation of the data, a number of processing and modeling techniques were used. The base map for the regional gravity interpretation was the terrain-corrected Bouguer gravity anomaly map. This map is shown as Figure 6 with a contour interval of 1 mgal. From this map, the high-pass, polynomial residual, second vertical derivative and two strike-filtered maps were created. In addition, two regional profiles were modeled. The complete set of the aforementioned maps and profiles constitutes the basis for this interpretation.

Regional gravity map and regional profiles.--The terrain-corrected Bouguer gravity anomaly map delineates a number of interesting features. Probably the most conspicuous of these features is a large north-south trend with a total relief of 5 mgal, which extends throughout the entire central portion of the survey area. Geophysical and geological evidence indicates that this trend corresponds to a large Basin and Range fault with downthrow to the west. Schmoker (1972), in his interpretation of regional gravity and aeromagnetics north of the survey area, defined the northern extension of this same gradient as a fault bounding the eastern portion of the Big Wash graben. Furthermore, he modeled this graben and obtained a depth estimate of approximately 366 m of

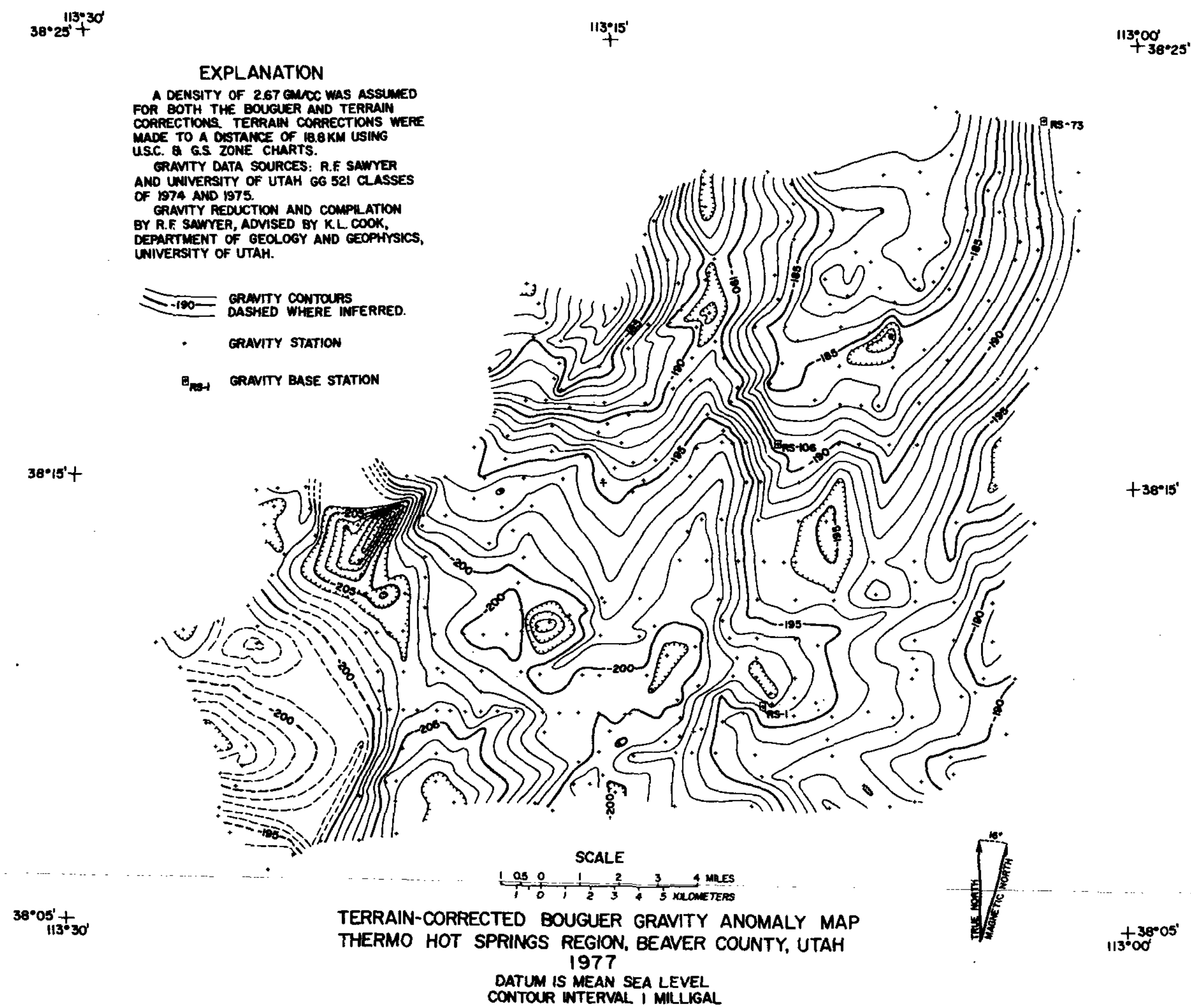
113°30'
38°25'
113°15'
113°00'
38°25'
EXPLANATION
A DENSITY OF 2.67 GM/CC WAS ASSUMED FOR BOTH THE BOUGUER AND TERRAIN CORRECTIONS. TERRAIN CORRECTIONS WERE MADE TO A DISTANCE OF 18.8 KM USING U.S.C. & G.S. ZONE CHARTS.
GRAVITY DATA SOURCES: R.F. SAWYER AND UNIVERSITY OF UTAH GG 521 CLASSES OF 1974 AND 1975.
GRAVITY REDUCTION AND COMPILATION BY R.F. SAWYER, ADVISED BY K.L. COOK, DEPARTMENT OF GEOLOGY AND GEOPHYSICS, UNIVERSITY OF UTAH.
-190- GRAVITY CONTOURS DASHED WHERE INFERRED.
GRAVITY STATION
B RS-1 GRAVITY BASE STATION
RS-73
RS-106
RS-1
38°15'
38°15'
-185
-190
-195
-200
-205
SCALE
1 0.5 0 1 2 3 4 MILES
1 0 1 2 3 4 5 KILOMETERS
TRUE NORTH
MAGNETIC NORTH
16°
38°05'
113°30'
38°05'
113°00'
TERRAIN-CORRECTED BOUGUER GRAVITY ANOMALY MAP
THERMO HOT SPRINGS REGION, BEAVER COUNTY, UTAH
1977
DATUM IS MEAN SEA LEVEL
CONTOUR INTERVAL 1 MILLIGAL

Figure 6.

valley fill for the portion of the graben just west of the Star Range. In the present study, a throw of approximately 200 to 300 m is indicated in the area of the hot springs and a throw of approximately 200 m is indicated where regional profile A-A' (Fig. 7) tranverses this fault.

Baer (1962) further supports this interpretation in his geologic study of the Star Range. He mentions that the range is bounded by high angle (75-80°) faults on the west. This correlates well with the location of the gravity gradient.

A second conspicuous trend is a large east-west feature that intersects the north-south fault in the north central portion of the survey region. This could be interpreted as a large fault with downthrow on the south. Regional profile B-B' (Fig. 8) yields an estimated throw of about 200 m for this fault. Geologically, this probable fault may represent the southern termination of the Star Range and possibly the San Francisco Mountains, as Schmoker's (1972) report implies the extension of the latter range under the Shauntie Hills.

A gravity high in the northeast corner of the thesis area correlates well with the Paleozoic and Mesozoic strata of the Star Range. The gravity data thus outline the range as a horst block which has been previously interpreted by several authors in their geologic studies of this area (Baer, 1973).

East of the Star Range, a north-northeast gravity trend is apparent. This trend defines a Basin and Range fault with downthrow to the west. The fault constitutes the eastern boundary for the Star

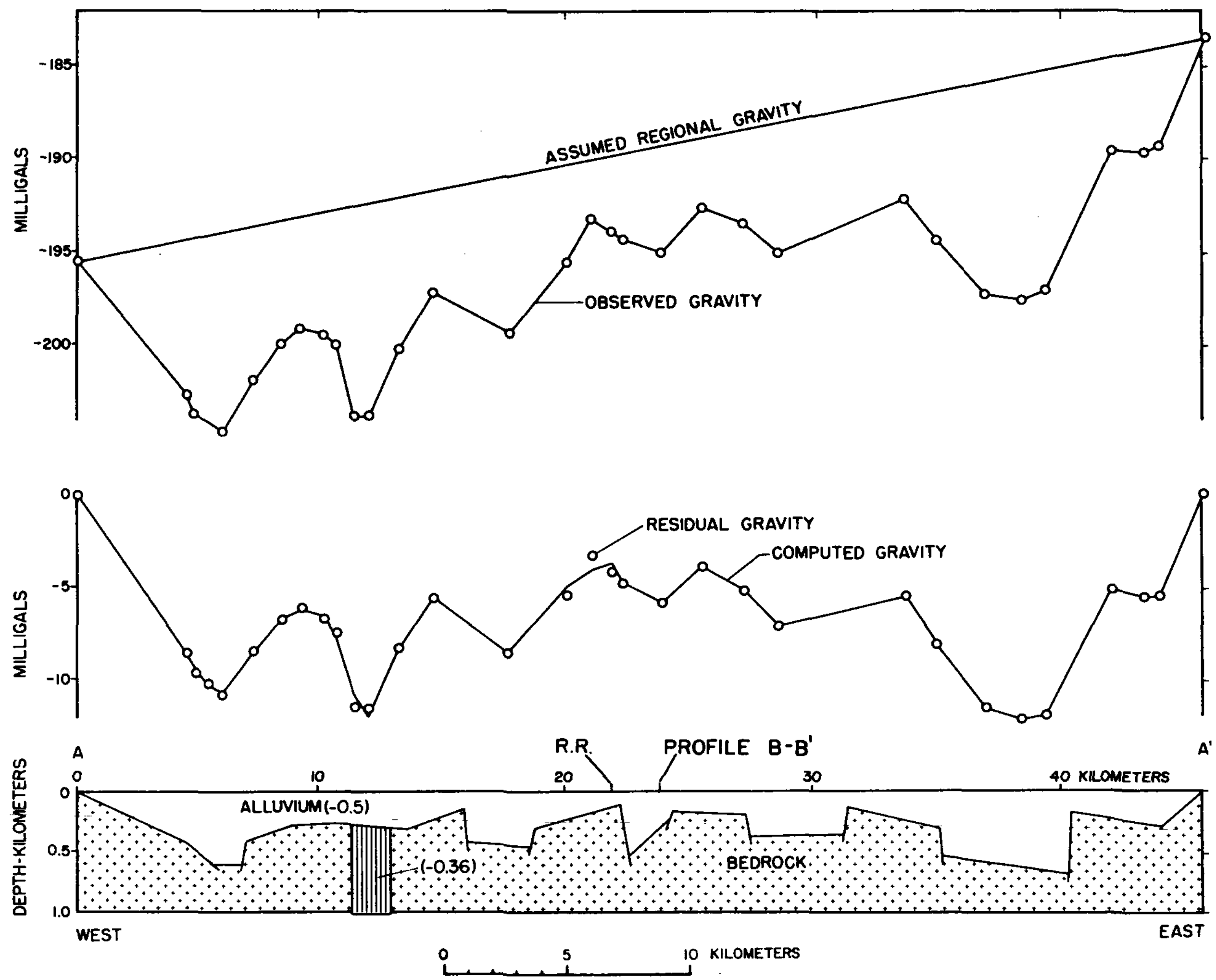

Figure 7. Interpretive two-dimensional model for gravity profile A-A'. Numbers in cross section indicates the assumed density contrast in gm/cm^3 in relation to bedrock.

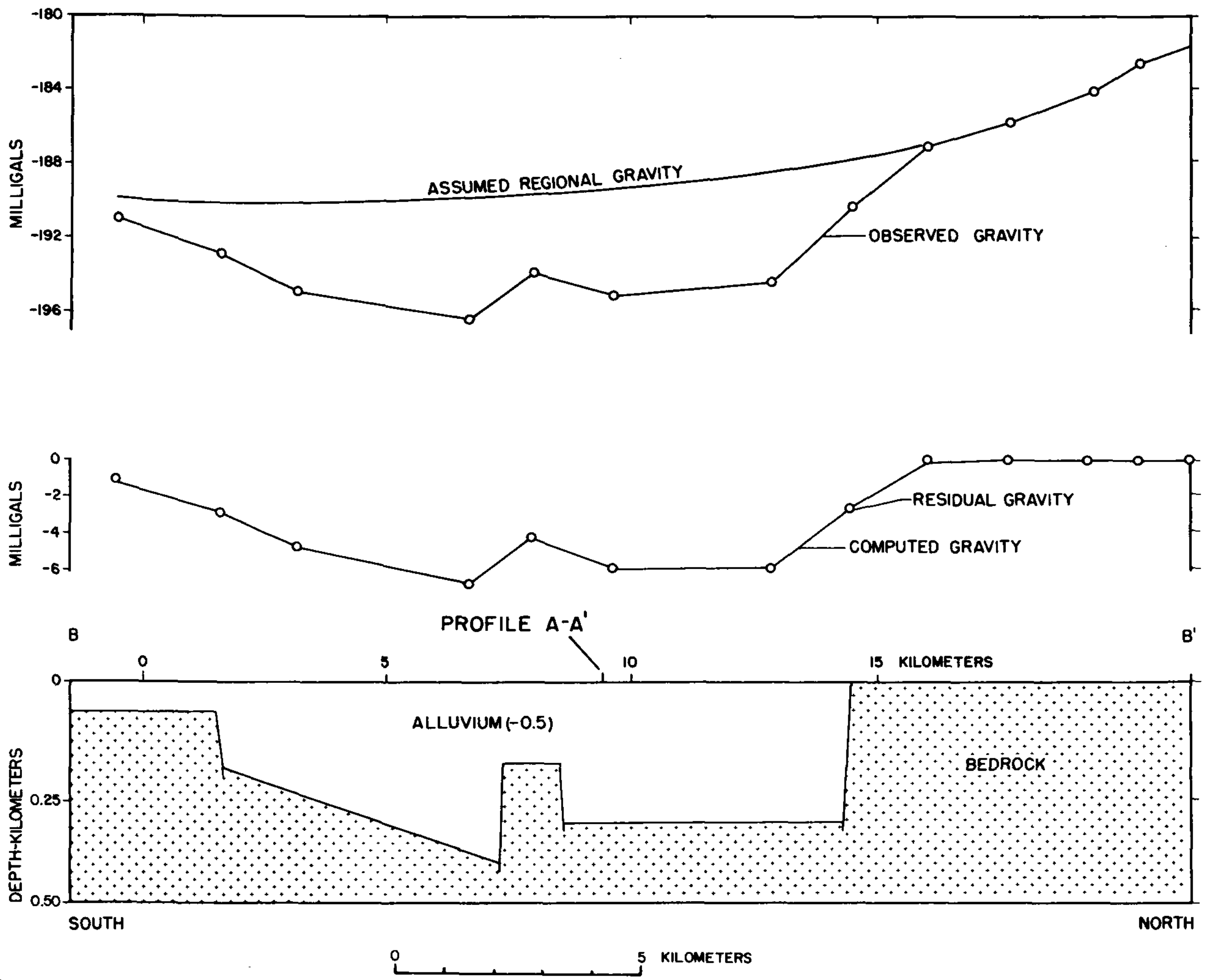

Figure 8. Interpretive two-dimensional model for gravity profile B-B'. Number in cross section indicates the assumed density contrast in gm/cm^3 in relation to bedrock.

Range and the west side of the Milford graben. Schmoker (1972) has estimated the throw of this fault as 762 m east of the Star Range.

West of the Star Range, in the northwest corner of the survey, exists another gravity high. This high probably constitutes another horst block. It correlates well with local outcrops of Paleozoic sediments. This could possibly represent a small isolated horst block or, as previously mentioned, a southern extension of the San Francisco Mountains.

Just east of this high exists another north-south trend. This trend delineates the western edge of the Big Wash graben and bounds the probable horst to the west.

In the west central portion of the survey area, a large gravity low with 5 mgal closure is outlined. This anomalous feature probably represents the southernmost end of the Wah Wah Valley graben which is an elongate graben that extends approximately 80 km to the north.

To the southeast of this low, in the Escalante Desert, a small but distinct circular gravity low, as defined by several stations, is outlined. Profile A-A' (Fig. 2) traverses this feature and a low-density dike was used to approximate the observed data. An estimate of about 2.3 gm/cc was obtained for the density of the dike from the profile model. The shape of the anomaly implies a low-density body, possibly an intrusive. Rowley (1975) notes the existence of an east-west belt of small isolated rhyolite plugs in this region. It is therefore probable that this feature represents such a plug. It should also be noted that this low is located along a possible extension of an east-west fault and therefore a favorable locale for an intrusive.

An area of prime importance is that of the hot springs. This area will be discussed in detail in subsequent sections of this report but warrants some note at this time. The area is characterized by a semi-circular gravity low intersecting a large north-south fault. A preliminary interpretation is that two east-west faults intersect a major Basin and Range fault at the hot springs and approximately 3.2 km north of the springs.

Approximately 8 km northeast of the hot springs there exists an elongate gravity low. This feature could be interpreted as possibly a downdropped block or a result of downwarping of the underlying bedrock. Based on the interpretation of faulting surrounding this low, the downdropped block is considered a preferable interpretation. Depth estimates to bedrock from profiles A-A' and B-B' are approximately 365 m in this region.

The final feature to be noted on the terrain-corrected Bouguer anomaly map is a gravity trend in the far western portion of map area just east of Blue Mountain. This trend again, implies the existence of a large Basin and Range fault with downthrow to the east. The fault consists of two segments. The northern portion which trends northwest, is probably an extension of the fault on the western side of the Wah Wah Valley graben. The southern portion, which trends southwest, probably forms the western boundary for a graben south of the survey area. The throw for this fault is estimated as 610 m at the point where profile A-A' traverses this feature. As such, this represents one of the deepest areas of alluvial fill in the study area.

As can be seen in profiles A-A' amd B-B', the calculated depth to bedrock varies within the valley from approximately 610 m in the southwest to about 150 m in east central portion, but more typically ranges from 300 to 450 m. Unfortunately, of the many wells in the area, no lithologic logs indicate bedrock penetration and therefore these estimates are based upon bedrock to bedrock ties at the ends of the profile A-A' and bedrock to profile A-A' ties for profile B-B'.

Residual gravity maps.--In order to more closely evaluate the anomalous features of local interest (i.e., the anomalies of intermediate depth), residual maps were produced. The high-pass, second vertical derivative and third-order polynomial residual maps all represent different approaches to regional removal from the data. Consequently, one would expect comparable information to be ascertained from these residual maps.

The high-pass filtered gravity anomaly map (Fig. 9), the second vertical derivative gravity anomaly map (Fig. 10) and the third-order polynomial residual gravity anomaly map (Fig. 11) were all found to be similar in appearance. For that reason, the interpretation of these maps can be treated together.

Probably the most striking feature of the residual maps is the elongate north-south gravity low of the central area of the survey. As such, these maps clearly emphasize the large north-south fault west of the Star Range but also establish the southern extension of a north-south fault approximately 3.2 km to the west.

HIGH - PASS FILTERED
BOUGUER GRAVITY ANOMALY
MAP OF THE THERMO
HOT SPRINGS REGION,
BEAVER COUNTY, UTAH
1977

CUT-OFF FREQUENCY 0.1260 cycles/km

CONTOUR INTERVAL 1.0 mgal

GRAVITY DATA FILTERED BY R.F. SAWYER
DEPARTMENT OF GEOLOGY AND GEOPHYSICS,
UNIVERSITY OF UTAH.

EXPLANATION

CONTOURS

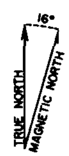

SCALE

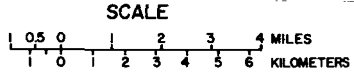

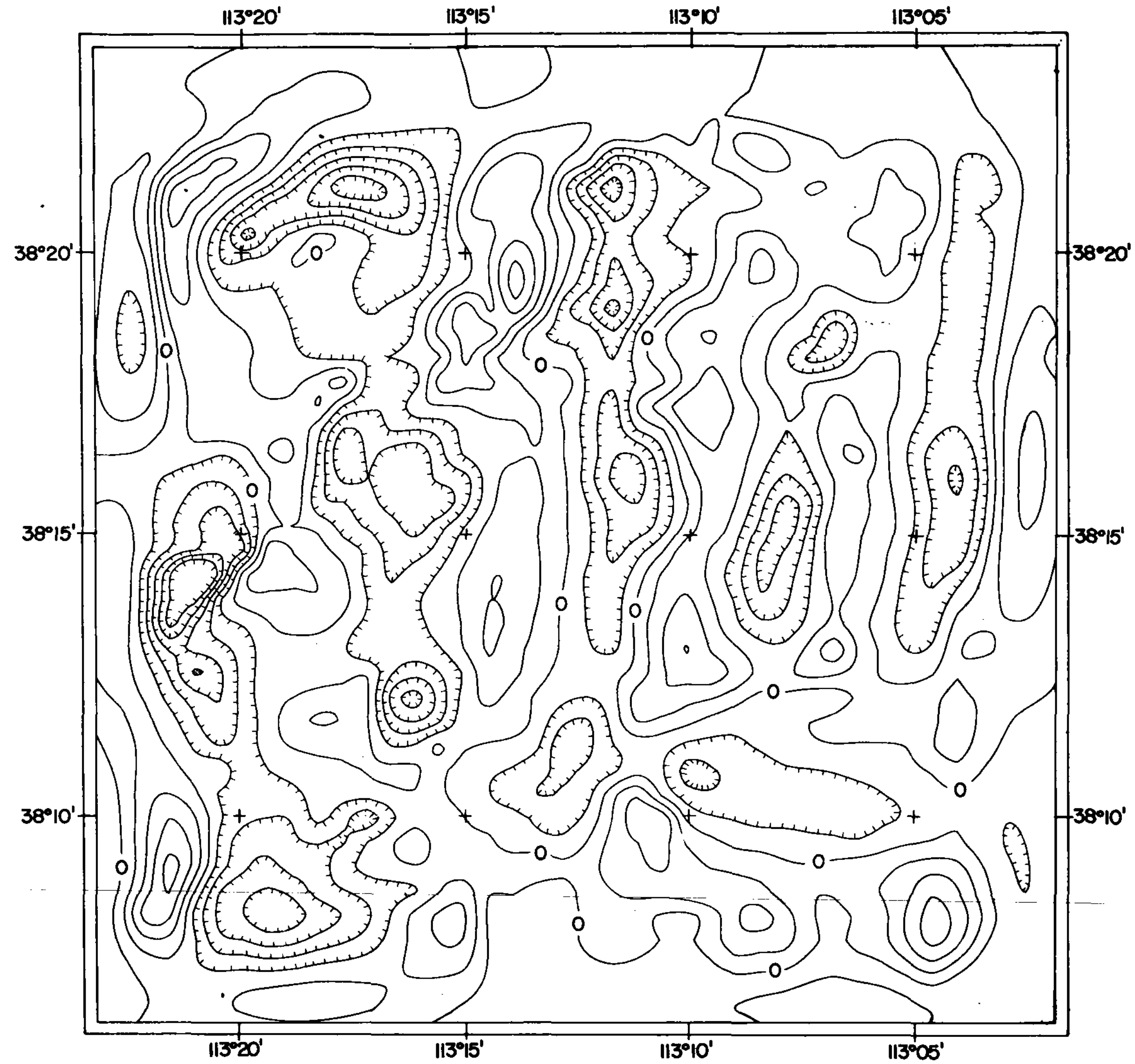

Figure 9.

SECOND VERTICAL DERIVATIVE GRAVITY ANOMALY MAP OF THE THERMO HOT SPRINGS REGION BEAVER COUNTY, UTAH 1977

LOW-PASS FILTER CUT-OFF FREQUENCY 0.4198 cycle/km

CONTOUR INTERVAL 1.0 mgal/km^2

GRAVITY DATA FILTERED BY R.F. SAWYER
DEPARTMENT OF GEOLOGY AND GEOPHYSICS,
UNIVERSITY OF UTAH.

EXPLANATION

CONTOURS

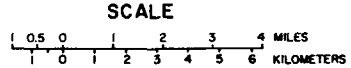

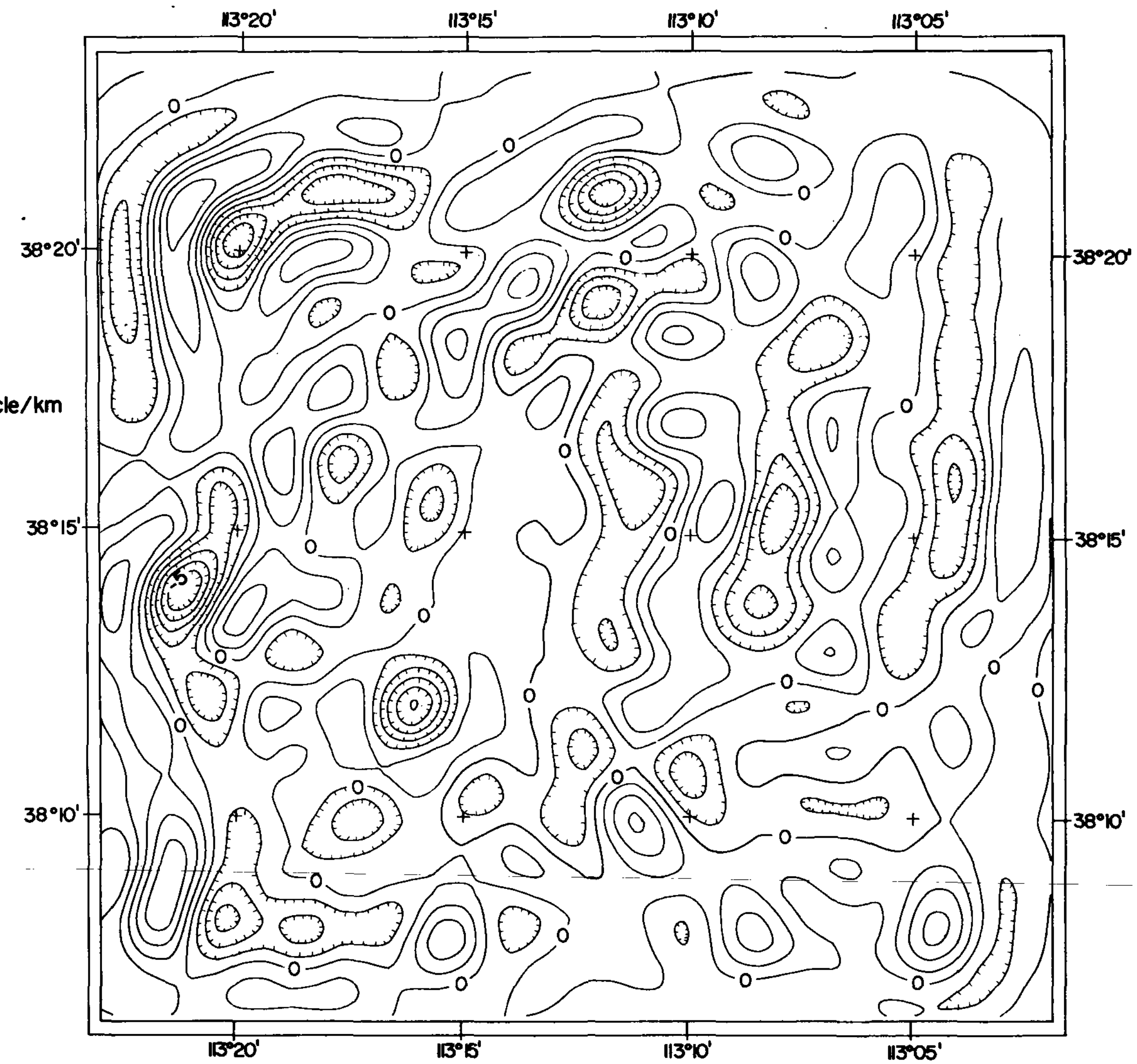

Figure 10.

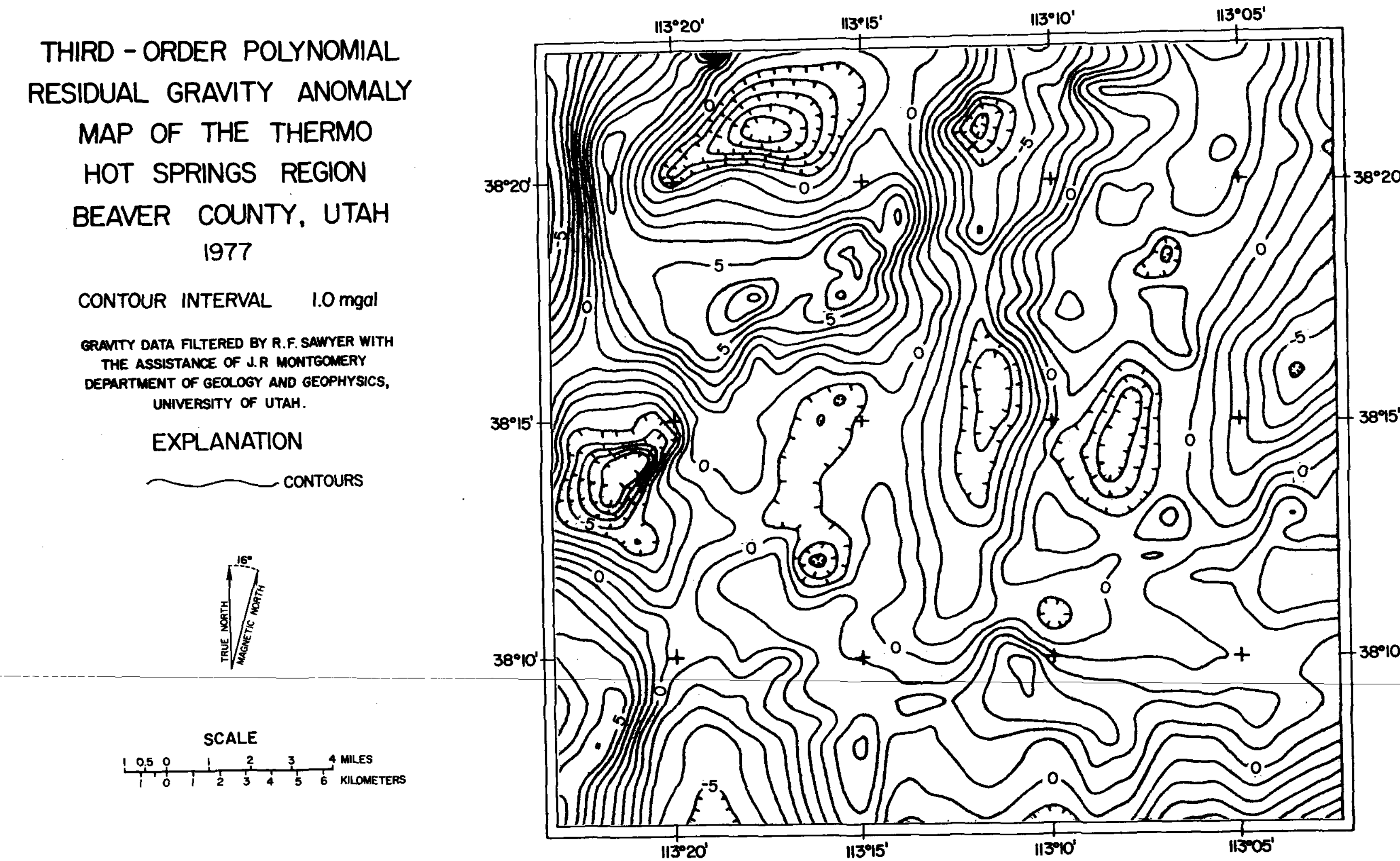
THIRD - ORDER POLYNOMIAL
RESIDUAL GRAVITY ANOMALY
MAP OF THE THERMO
HOT SPRINGS REGION
BEAVER COUNTY, UTAH
1977
CONTOUR INTERVAL 1.0 mgal
GRAVITY DATA FILTERED BY R.F. SAWYER WITH
THE ASSISTANCE OF J.R MONTGOMERY
DEPARTMENT OF GEOLOGY AND GEOPHYSICS,
UNIVERSITY OF UTAH.
EXPLANATION
CONTOURS
16°
TRUE NORTH
MAGNETIC NORTH
SCALE
1 0.5 0 1 2 3 4 MILES
1 0 1 2 3 4 5 6 KILOMETERS
113°20'
113°15'
113°10'
113°05'
38°20'
38°15'
38°10'

Figure 11.

Together, these two large, parallel, north-south Basin and Range faults form a narrow but well-defined graben which appears to be the southern continuation of the Big Wash graben as previously outlined by Schmoker (1972).

All three residual maps indicate that this graben extends to the area of the hot springs and perhaps slightly south. It may possibly be terminated by east-west faulting on its southern end.

In the area of the hot springs, the residual maps accentuate the north-south and east-west features previously pointed out. It is interesting to note that the gravity low east of the hot springs assumes an elongate nature in the high-pass filtered map which would seem to imply lateral extent of the possible east-west faults. The polynomial residual and second vertical derivative maps show this low abbreviated and possibly terminated by north-south structure.

The gravity high associated with the Star Range appears to be truncated to the north in both the high-pass and second vertical derivative maps. This is attributable to edge effects. The second derivative map also attempts to break up the continuity of the anomaly, but the nature of this operator is such that one would expect this response. The polynomial residual and the high-pass filtered maps indicate the true shape of the anomaly which corresponds well with the mapped Paleozoic and Mesozoic geology.

The Shauntie Hills gravity high shows correlation with the Paleozoic outcrops of the area. All three maps seem to indicate that this high does not continue northward which would support the hypothesis of an isolated horst block rather than a continuation of the San Francisco Mountains. The residual maps also indicate an apparent northeast trend in this area of the survey. This trend correlates well with the mapped faults in the Shauntie Hills (see Fig. 3).

East of the Star Range, the Basin and Range fault is delineated as a north-northeast lineament on the residual maps. Proximity to the eastern edge of the map area introduces the possibility of edge effects influencing the expression of this feature. However, good agreement as to location is noted with the terrain-corrected Bouguer anomaly map and therefore the linear expression is considered real. The interesting aspect of this lineament is the southern extension to the east-west fault north of the hot springs. This implies that this north-northeast fault probably continues over the northern two-thirds of the survey area.

In the Black Mountains area, several gravity highs terminated by an east-west low are noted on the second vertical derivative and high-pass filtered maps. It has already been suggested that the northern termination is the result of faulting and the gravity highs are probably the result of high density volcanics underlain by Paleozoic and Mesozoic strata.

The small circular gravity low which is interpreted to be a small intrusive, in the southwest central portion of the survey area, is prevalent on all three residual maps. Furthermore, its alignment with the probable east-west fault is apparent on the high-pass filtered map. Though perhaps less obvious, this alignment is still easily discernible on the second vertical derivative and polynomial residual maps.

Strike-filtered gravity maps.--The aforementioned maps indicated that the prevalent structural directions for the survey region are north-south and east-west. For that reason, strike-filtered maps were processed for those two directions. These maps serve as an interpretive aid which would emphasize previously noted trends and introduce others that may appear more subtly on other maps.

The east-west strike-filtered gravity anomaly map (Fig. 12) indicates four prominent trends in the specified direction. The largest and most dominant of the region is the major east-west feature south of the Shauntie Hills and the Star Range. This map implies continuation of this probable fault outside this area of study. A study to the east (Carter, 1977) appears to verify a possible eastern extension.

A second linear trend is delineated north of the Black Mountains. This correlates with the previously mentioned concept of a frontal fault for that area. Extension to the east is implied and may be substantiated by Carter (1977) but the fault appears to terminate to the west. A possible reason for such a termination is the probable existence of a north-south graben in that area.

A third but less obvious east-west trend is noted immediately north of the Thermo Hot Springs. The map indicates that this fault traverses the entire survey area, as was previously considered.

The fourth east-west linear trend is located in the Shauntie Hills and the Star Range. The feature is predominant in the western

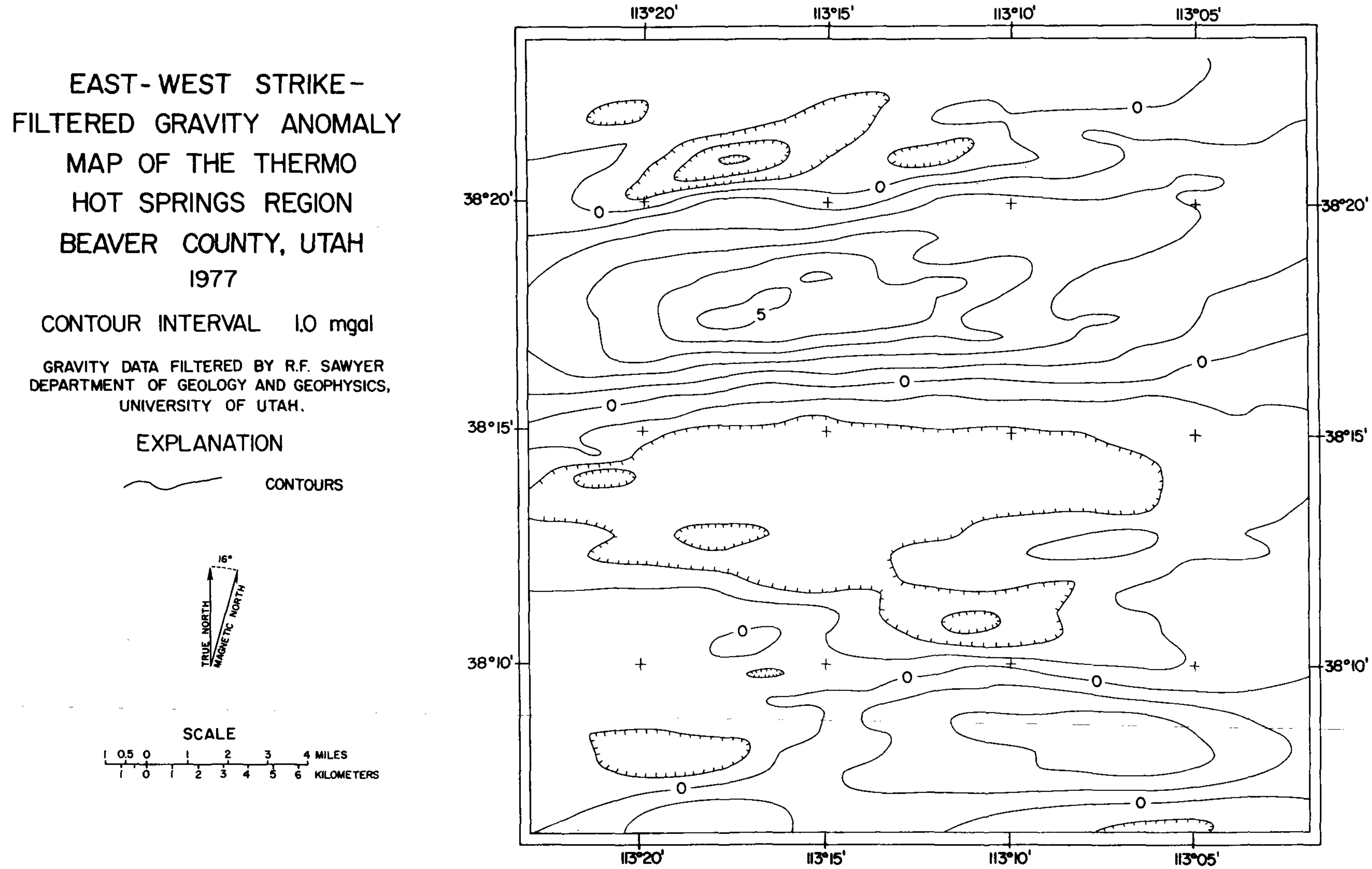
EAST-WEST STRIKE-
FILTERED GRAVITY ANOMALY
MAP OF THE THERMO
HOT SPRINGS REGION
BEAVER COUNTY, UTAH
1977
CONTOUR INTERVAL 1.0 mgal
GRAVITY DATA FILTERED BY R.F. SAWYER
DEPARTMENT OF GEOLOGY AND GEOPHYSICS,
UNIVERSITY OF UTAH.
EXPLANATION
CONTOURS
16°
TRUE NORTH
MAGNETIC NORTH
SCALE
1 0.5 0 1 2 3 4 MILES
1 0 1 2 3 4 5 6 KILOMETERS
113°20'
113°15'
113°10'
113°05'
38°20'
38°15'
38°10'
0
5

Figure 12.

portion of the region. It may represent a fault isolating the Paleozoic rock of the Shauntie Hills and possibly secondary faulting in the Star Range.

The north-south strike-filtered gravity anomaly map (Fig. 13) also indicates four dominant trends. The first two are located in the central portion of the map area and represent the east and west sides of the elongate graben which extends the length of the survey area. This feature has been designated as the Thermo graben. The map indicates the extension of this graben to the north but implies that it may become shallow or terminate at the southernmost end.

A third trend is delineated east of the Star Range. It verifies the extension of the Basin and Range fault south of the region of the east-west faults in the hot springs region.

Finally, a north-south trend is noted east of Blue Mountain. This gradient suggests the extension of the Wah Wah Valley graben through this portion of the survey area and further south.

Regional Magnetic Data

For interpretation of the regional magnetic data, a total magnetic intensity anomaly map (Fig. 14) was employed as a base map. From this map, a low-pass filtered magnetic anomaly map (Fig. 15), an east-west strike-filtered magnetic anomaly map (Fig. 16), a north-south strike-filtered magnetic anomaly map (Fig. 17) and a pseudogravity map (Fig. 18) were constructed. These maps provide the basis for the following interpretation.

NORTH-SOUTH STRIKE-FILTERED GRAVITY ANOMALY MAP OF THE THERMO HOT SPRINGS REGION BEAVER COUNTY, UTAH

1977

CONTOUR INTERVAL 1.0 mgal

GRAVITY DATA FILTERED BY R.F. SAWYER
DEPARTMENT OF GEOLOGY AND GEOPHYSICS,
UNIVERSITY OF UTAH.

EXPLANATION

CONTOURS

16°
TRUE NORTH
MAGNETIC NORTH

SCALE

1 0.5 0 1 2 3 4 MILES
1 0 1 2 3 4 5 6 KILOMETERS

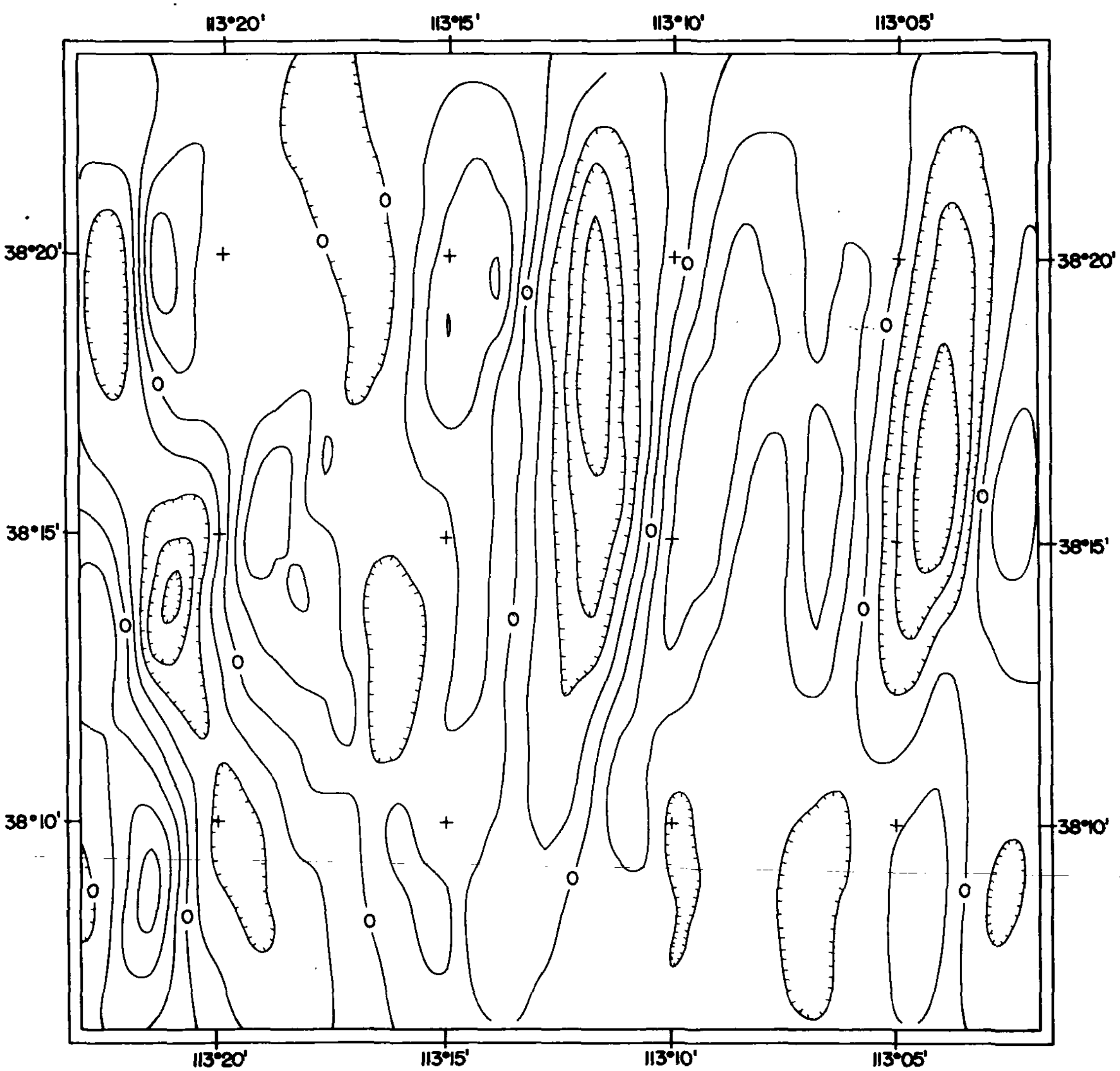

Figure 13.

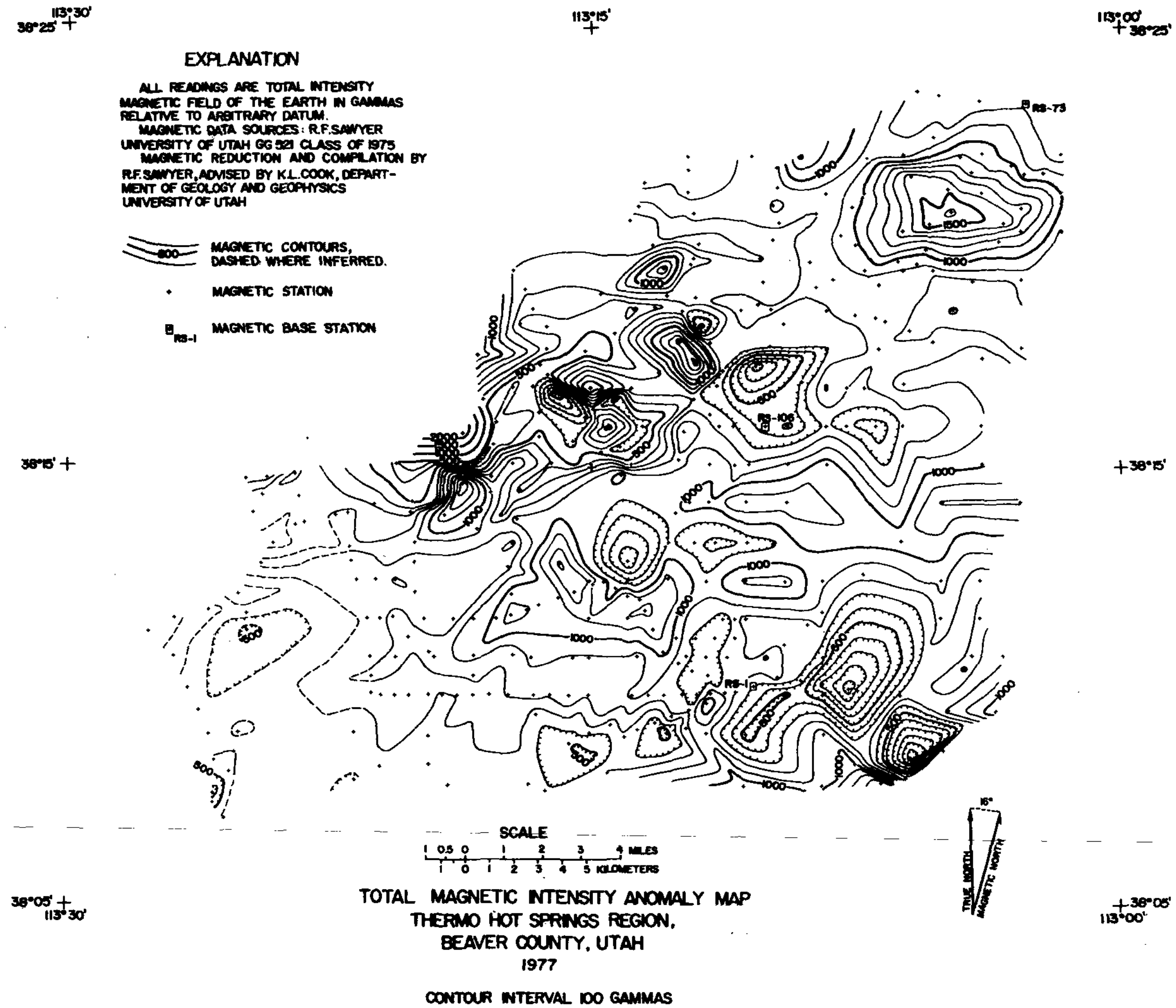

113°30'
38°25'
113°15'
113°00'
38°25'
EXPLANATION
ALL READINGS ARE TOTAL INTENSITY MAGNETIC FIELD OF THE EARTH IN GAMMAS RELATIVE TO ARBITRARY DATUM.
MAGNETIC DATA SOURCES: R.F.SAWYER UNIVERSITY OF UTAH GG 521 CLASS OF 1975
MAGNETIC REDUCTION AND COMPILATION BY R.F.SAWYER, ADVISED BY K.L.COOK, DEPARTMENT OF GEOLOGY AND GEOPHYSICS UNIVERSITY OF UTAH
MAGNETIC CONTOURS, DASHED WHERE INFERRED.
MAGNETIC STATION
MAGNETIC BASE STATION
RS-73
RS-1
1000
1500
38°15'
38°15'
SCALE
MILES
KILOMETERS
TRUE NORTH
MAGNETIC NORTH
38°05'
113°30'
38°05'
113°00'
TOTAL MAGNETIC INTENSITY ANOMALY MAP
THERMO HOT SPRINGS REGION,
BEAVER COUNTY, UTAH
1977
CONTOUR INTERVAL 100 GAMMAS

Figure 14.

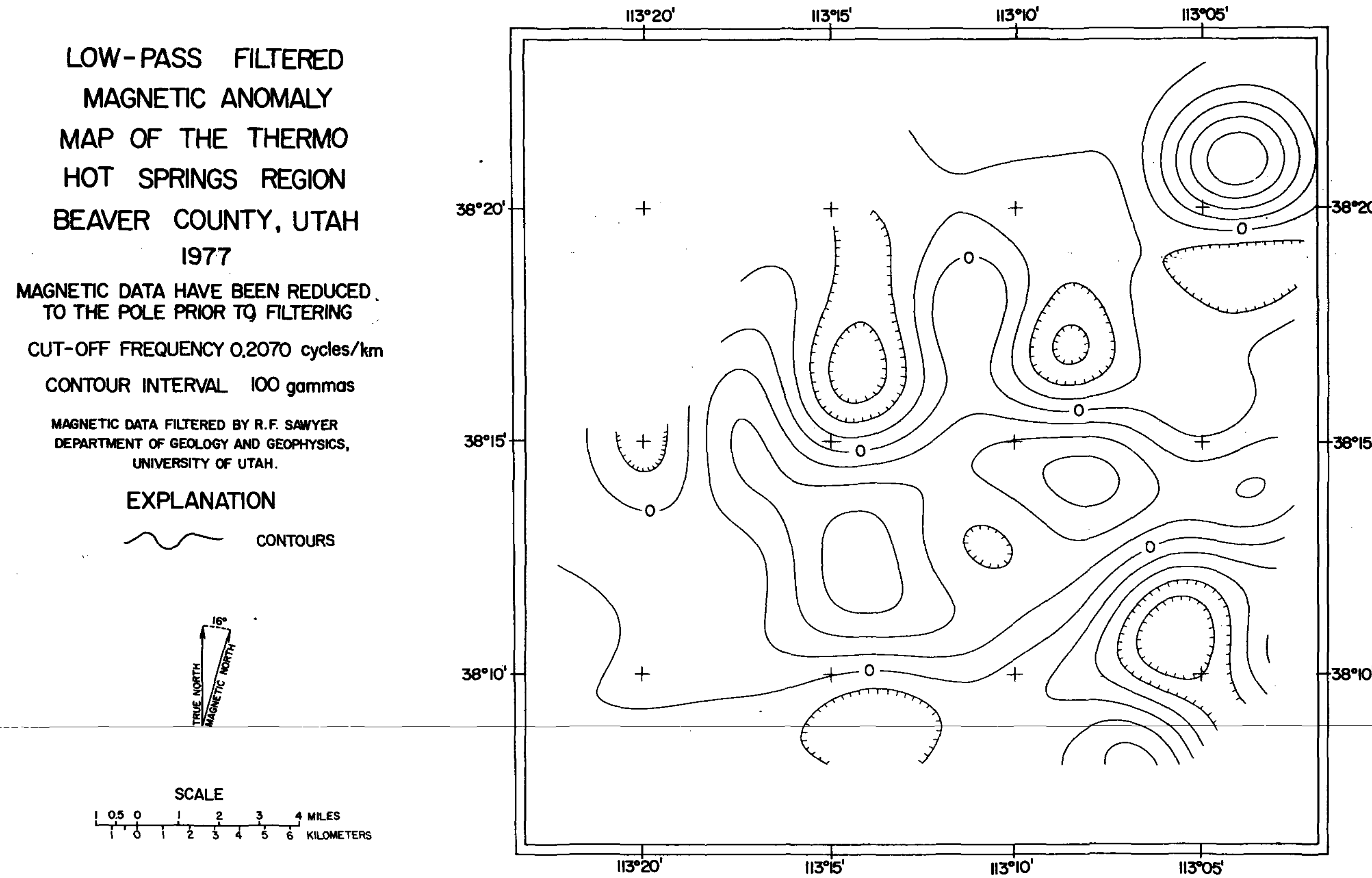
LOW-PASS FILTERED
MAGNETIC ANOMALY
MAP OF THE THERMO
HOT SPRINGS REGION
BEAVER COUNTY, UTAH
1977
MAGNETIC DATA HAVE BEEN REDUCED TO THE POLE PRIOR TO FILTERING
CUT-OFF FREQUENCY 0.2070 cycles/km
CONTOUR INTERVAL 100 gammas
MAGNETIC DATA FILTERED BY R.F. SAWYER
DEPARTMENT OF GEOLOGY AND GEOPHYSICS,
UNIVERSITY OF UTAH.
EXPLANATION
CONTOURS
16°
TRUE NORTH
MAGNETIC NORTH
SCALE
MILES
KILOMETERS
113°20'
113°15'
113°10'
113°05'
38°20'
38°15'
38°10'

Figure 15.

EAST-WEST STRIKE-FILTERED MAGNETIC ANOMALY MAP OF THE THERMO HOT SPRINGS REGION BEAVER COUNTY, UTAH 1977

MAGNETIC DATA HAVE BEEN REDUCED TO THE POLE PRIOR TO FILTERING

CONTOUR INTERVAL 100 GAMMAS

MAGNETIC DATA FILTERED BY R.F. SAWYER
DEPARTMENT OF GEOLOGY AND GEOPHYSICS,
UNIVERSITY OF UTAH.

EXPLANATION

CONTOURS

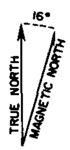

SCALE

0.5 0 1 2 3 4 MILES

1 0 1 2 3 4 5 6 KILOMETERS

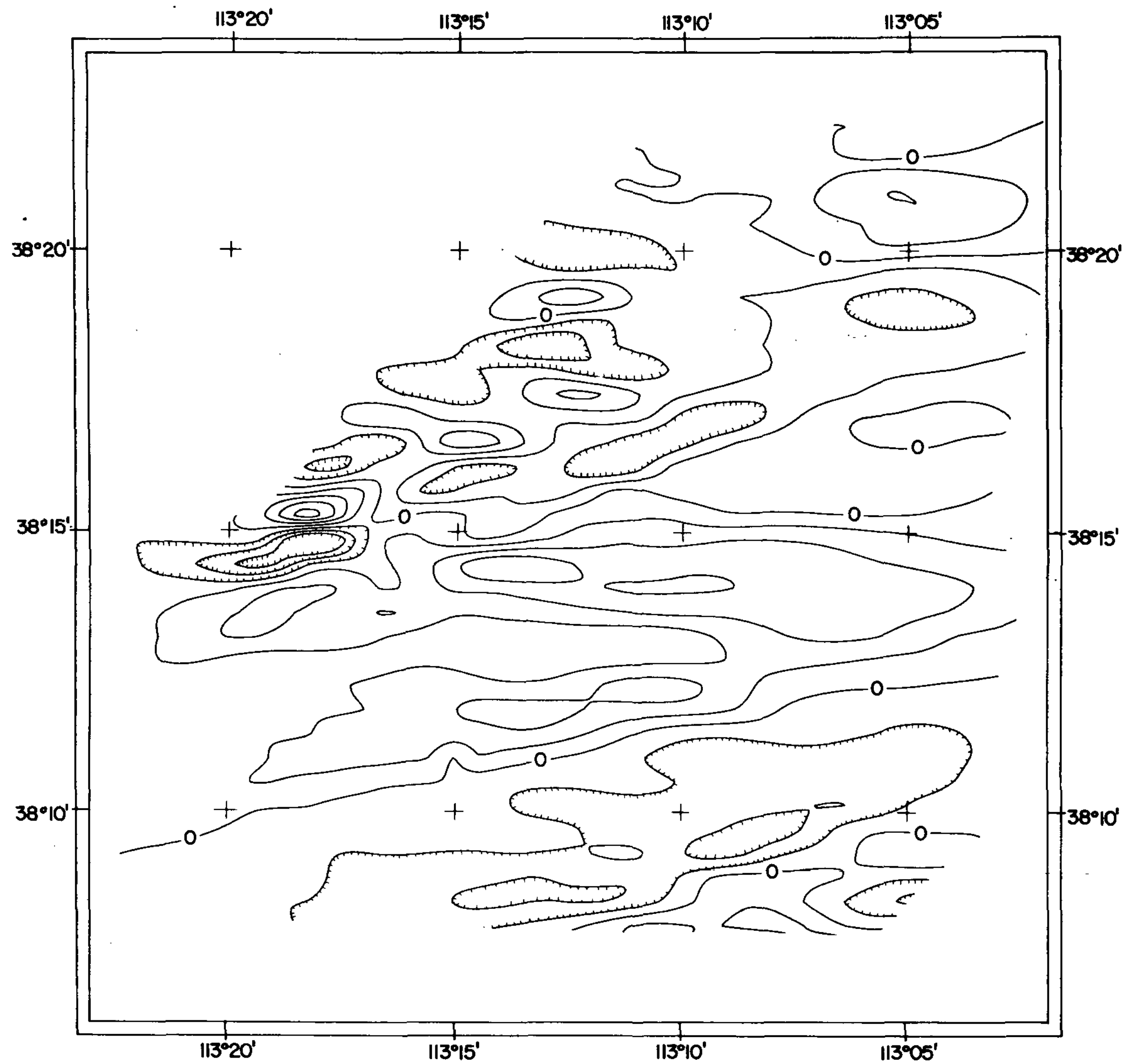

Figure 16.

NORTH-SOUTH STRIKE-FILTERED MAGNETIC ANOMALY MAP OF THE THERMO HOT SPRINGS REGION BEAVER COUNTY, UTAH 1977

MAGNETIC DATA HAVE BEEN REDUCED TO THE POLE PRIOR TO FILTERING

CONTOUR INTERVAL 100 GAMMAS

MAGNETIC DATA FILTERED BY R.F. SAWYER
DEPARTMENT OF GEOLOGY AND GEOPHYSICS
UNIVERSITY OF UTAH.

EXPLANATION

CONTOURS

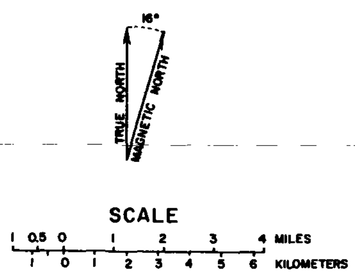

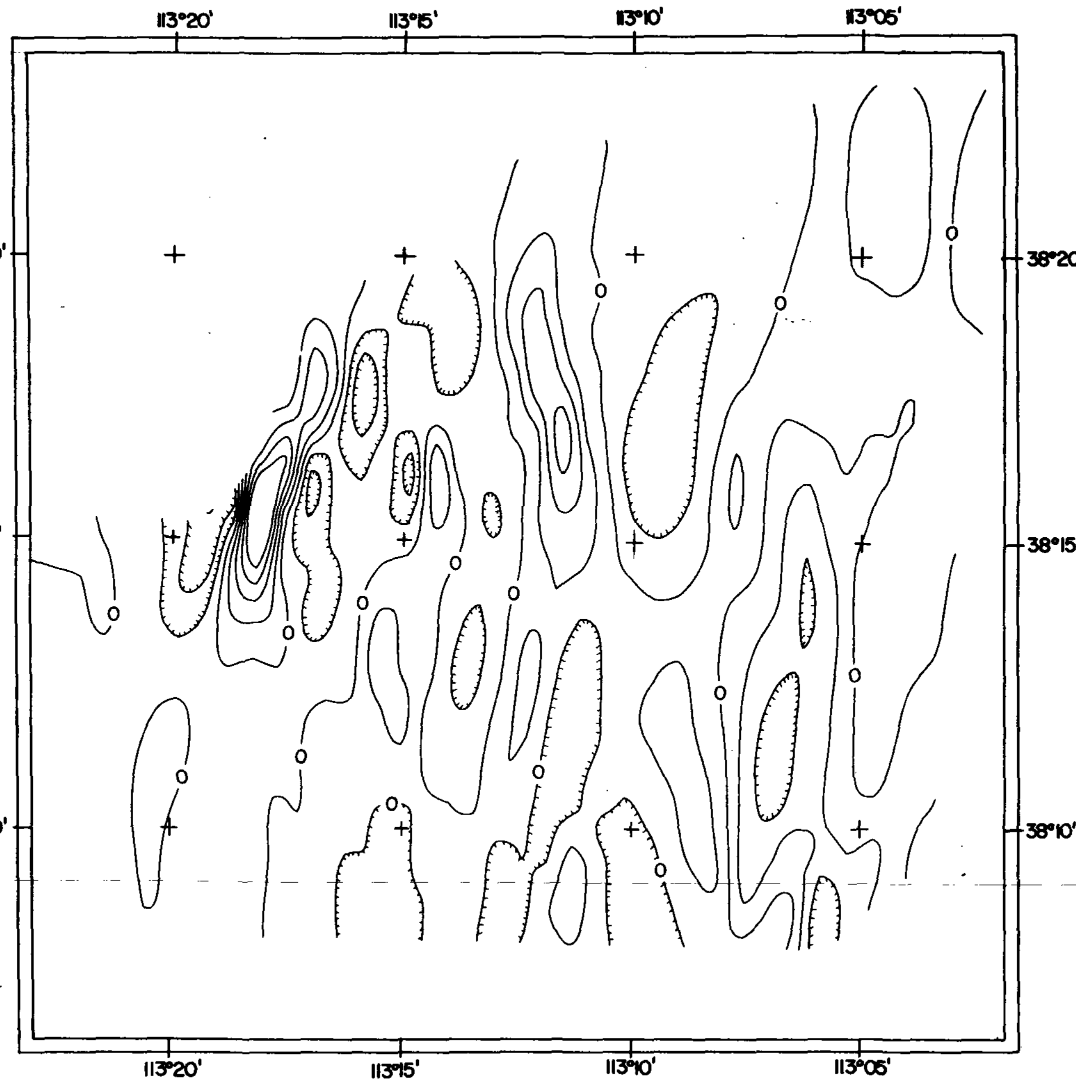

Figure 17.

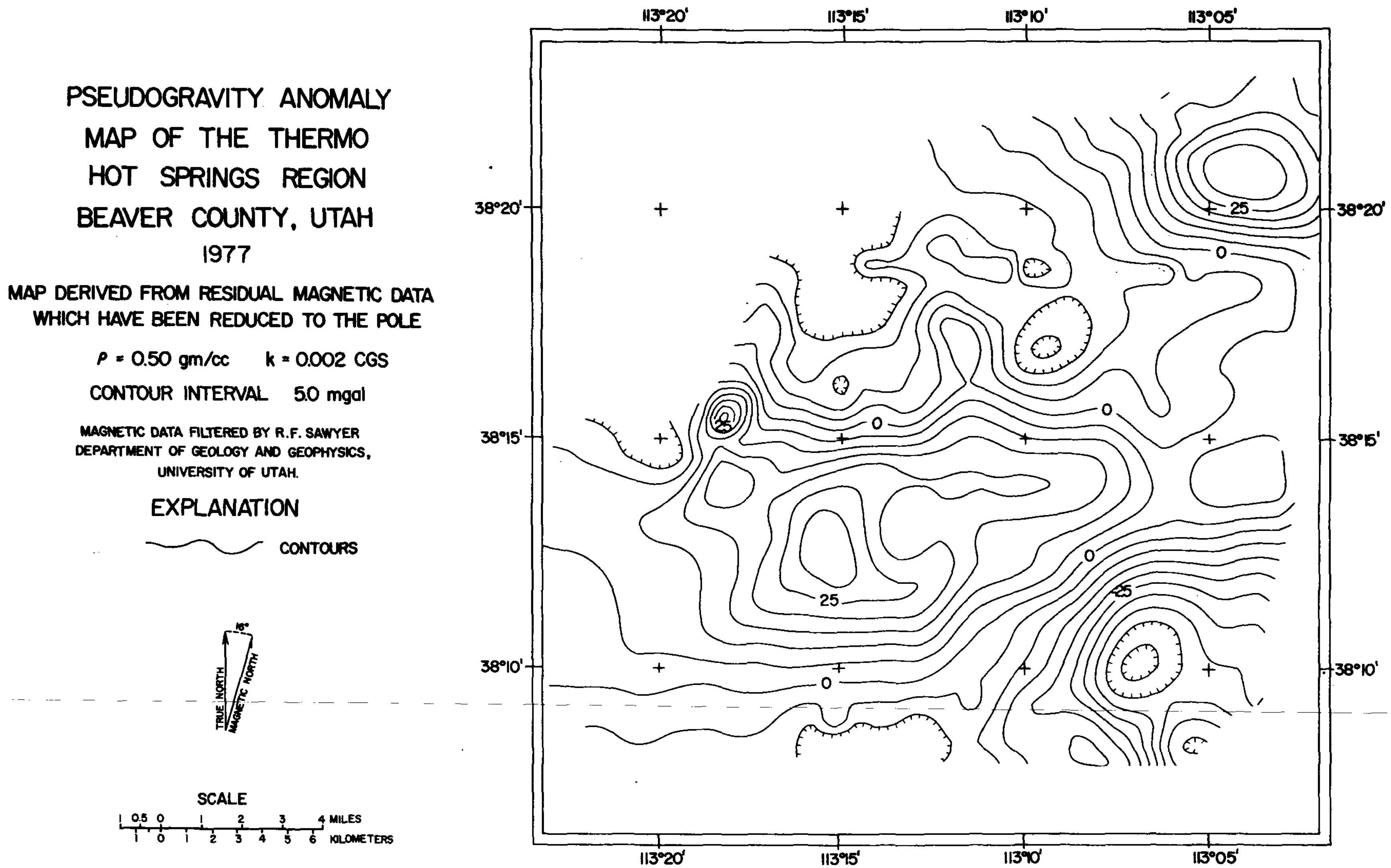
PSEUDOGRAVITY ANOMALY
MAP OF THE THERMO
HOT SPRINGS REGION
BEAVER COUNTY, UTAH
1977
MAP DERIVED FROM RESIDUAL MAGNETIC DATA
WHICH HAVE BEEN REDUCED TO THE POLE
ρ = 0.50 gm/cc k = 0.002 CGS
CONTOUR INTERVAL 5.0 mgal
MAGNETIC DATA FILTERED BY R.F. SAWYER
DEPARTMENT OF GEOLOGY AND GEOPHYSICS,
UNIVERSITY OF UTAH.
EXPLANATION
CONTOURS
16°
TRUE NORTH
MAGNETIC NORTH
SCALE
1 0.5 0 1 2 3 4 MILES
1 0 1 2 3 4 5 6 KILOMETERS
113°20'
113°15'
113°10'
113°05'
38°20'
38°15'
38°10'
25
0
0
0
0
25
25
0
25

Figure 18.

thought that these anomalies might represent a large north-side magnetic low due to volcanics to the south. The Utah state aeromagnetic map (Zietz et al., 1975) indicates that this is not so. Another possibility is that the volcanics of the area have reversed remanent magnetization and possibly extend under the alluvium to the north. Another possible cause for these lows is that the hydrothermal system associated with the Thermo hot springs may cause such a series of lows and their expression may be controlled by local structure.

South of the Shauntie Hills and the Star Range at approximately latitude 38°15'N, a major east-west lineament is noted. This trend probably corresponds to the large east-west fault indicated by gravity for the general locale. The feature is slightly south of the gravity trend, as would be expected at these latitudes. The trend may occur due to a contact between sediments of the Star Range and Shauntie Hills and possibly volcanics underlying the alluvium in the Escalante Valley.

Due south of the east-west trend is an elongate east-west high that traverses the entire study area. Erickson (1973) has indicated that Tertiary volcanics underlie the entire valley, and these volcanics may possibly cause this banded high. Schmoker (1972) suggests the existence of a large batholithic intrusive at depth for this area and the elongate high may represent the southern extent of such a body.

Low-pass filtered magnetic map.--The low-passed filtered magnetic anomaly map (Fig. 15) was processed in an attempt to remove the effects of surface volcanics and noise. This map indicates a number of interesting anomalies as it more clearly delineates some features previously noted on the total magnetic intensity anomaly map.

The large magnetic high, due to the Milford Flat intrusive, is clearly emphasized in the northeast corner of the map area. Its circular shape would seem to imply a slightly elongate vertical cylinder as a possible shape for the causative body.

In the region of the Shauntie Hills and the southern portion of the Star Range are two distinct magnetic lows. These lows probably reflect the presence of Paleozoic and Mesozoic sediments.

The elongate east-west magnetic high of the Escalante Valley is well defined on this map. It should be noted that the high extends north into the Big Wash graben. This would correlate well with the idea of underlying volcanics whose placement is structurally controlled.

East-west lineaments are delineated in the central portions of the map area. Again, these probably reflect structural (i.e., faults) controls.

A large magnetic low is dominant in the southeast portion of the survey area. Rowley (1975) postulates the existence of a rhyolite dome east of the hot springs and perhaps this low reflects such a feature. This low could then have a definite bearing on the placement and existence of the hot springs.

Strike-filtered magnetic maps.--The east-west strike-filtered magnetic anomaly map (Fig. 16) indicates three trends for the map area. These trends correlate well with previously mentioned gravity gradients and thus provide secondary evidence for the location of faults in these regions. Again, the lineations are noted 1) south of the Shauntie Hills and Star Range, 2) north of the Black Mountains, and 3) north of the hot springs in the Escalante Valley.

The north-south strike-filtered magnetic anomaly map (Fig. 17) emphasizes two north-south linear trends that may help substantiate previous interpretation. In the central portion of the survey area an elongate feature corresponding to the gravity graben is clearly outlined. This further supports the existence of two parallel north-south faults for this region.

Southeast of the Star Range, a second linear trend is noted. This trend may also provide evidence for the southern extension of a Basin and Range fault into this area.

Pseudogravity map.--A pseudogravity map (Fig. 18) was generated assuming a density contrast of 0.5 gm/cc and a magnetic susceptibility of 0.002 cgs. This provided a means for testing the assumption that the gravity and magnetic anomalies were caused by the same bodies with uniform density and magnetization. It is noted that this pseudogravity map differs considerably from the gravity map. In fact, there appears to be a reverse correlation in many cases. This may possibly be explained by the occurrence of high-density, low-susceptibility sediments in the Shauntie Hills and Star Range and also by the probable existence of high-susceptibility volcanics under the alluvium in the Escalante Valley.

Three-dimensional modeling.--As a final step to the regional magnetic interpretation, a closer examination was made of the magnetic high in the northeast corner of the survey. As previously mentioned, this anomaly is known to be caused by the Milford Flat intrusive. Therefore, an attempt was made to model the causative body using Talwani 3D modeling techniques. The first step for this modeling was to generate a first-order polynomial residual magnetic anomaly for this feature. This residual anomaly is shown in Figure 19. Next, using a magnetic susceptibility contrast of 0.003 cgs which was determined from sample measurement and previous data (Schmoker, 1972), a number of different models were assumed. The "forward" problem was computed for each model until a reasonable match with the residual anomaly was obtained. The calculated anomaly due to the final model is shown as Figure 20. The three-dimensional model is illustrated as Figure 21. It is characterized by relatively shallow depth and an east-west elongate cylindrical shape as the body continues to depth.

Detailed Gravity Data

Detailed gravity map.--The detailed portion of the survey consisted of nine east-west profiles in the immediate vicinity of the hot springs. A detailed terrain corrected Bouguer gravity anomaly map (Fig. 4) was generated from these nine profiles and stations in close proximity to the springs.

This map clearly delineates the major north-south fault adjacent to the hot springs and indicates the possibility of offsets in that feature. In addition, it also emphasizes the east-west trend north of the hot springs and a second east-west trend which

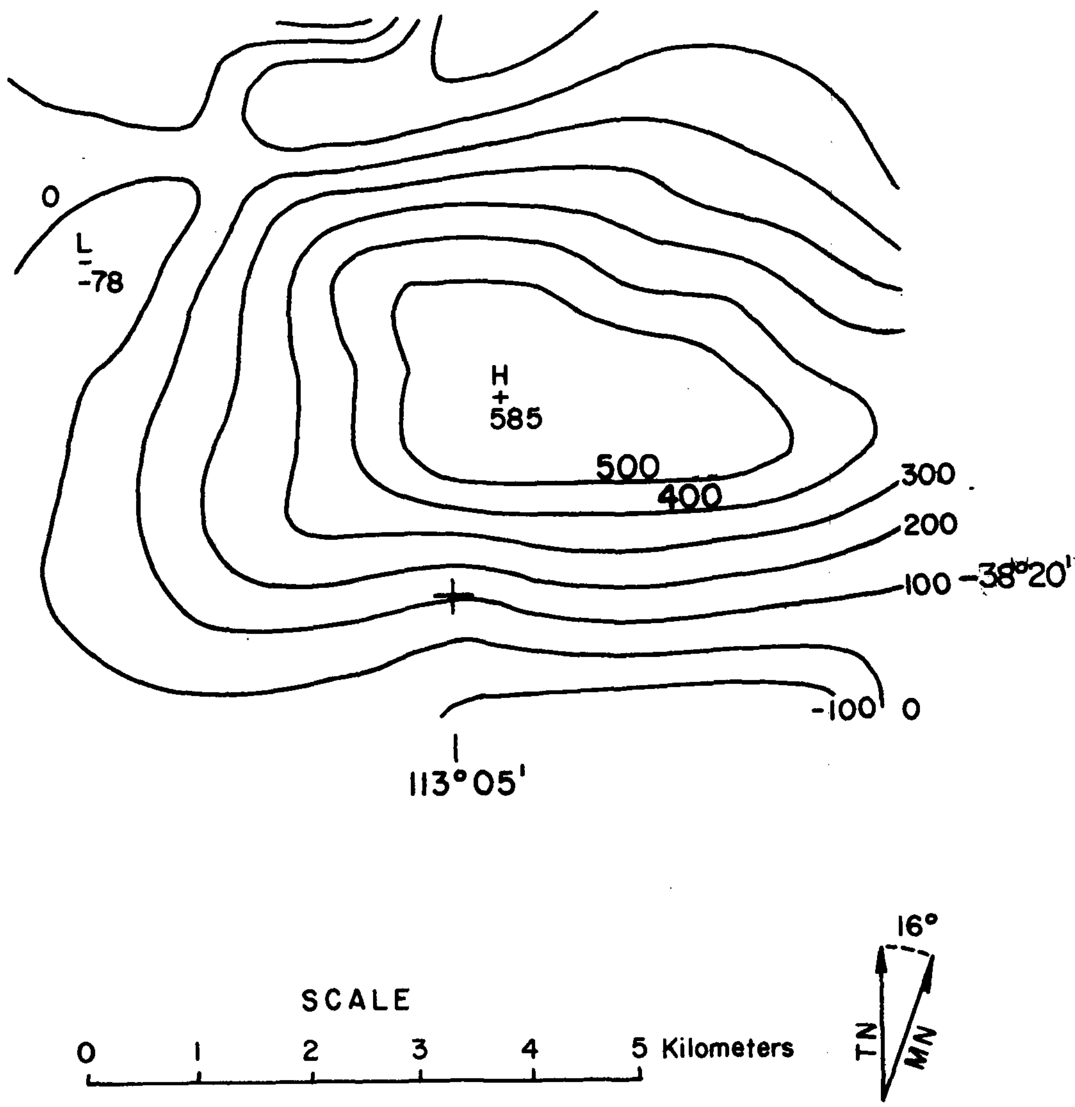

CONTOUR INTERVAL : 100 GAMMAS

Figure 19. First-order polynomial residual magnetic anomaly map of the Milford Flat intrusive.

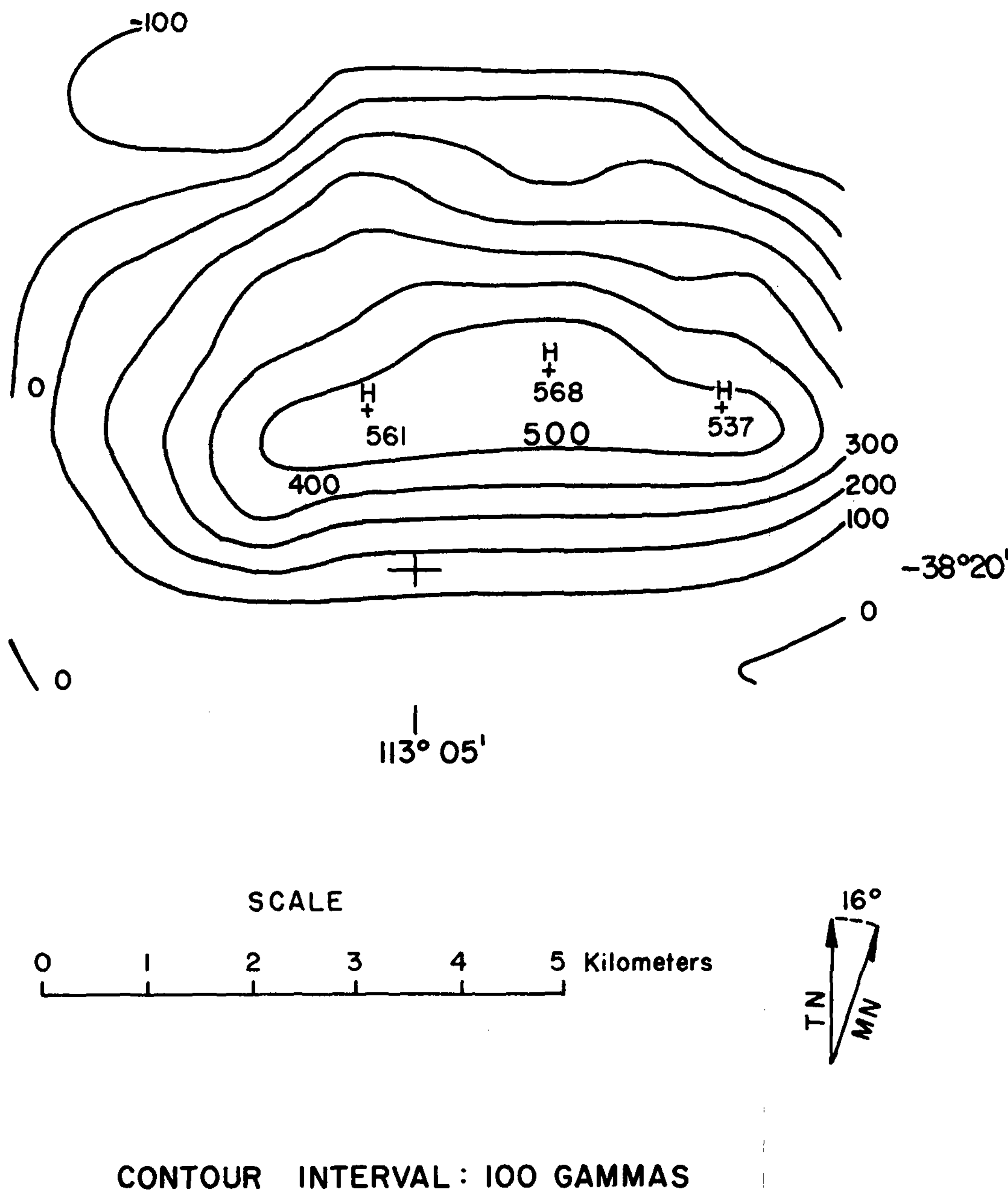

Figure 20. Calculated total magnetic intensity anomaly map for the three-dimensional model of the Milford Flat intrusive shown in Figure 21.

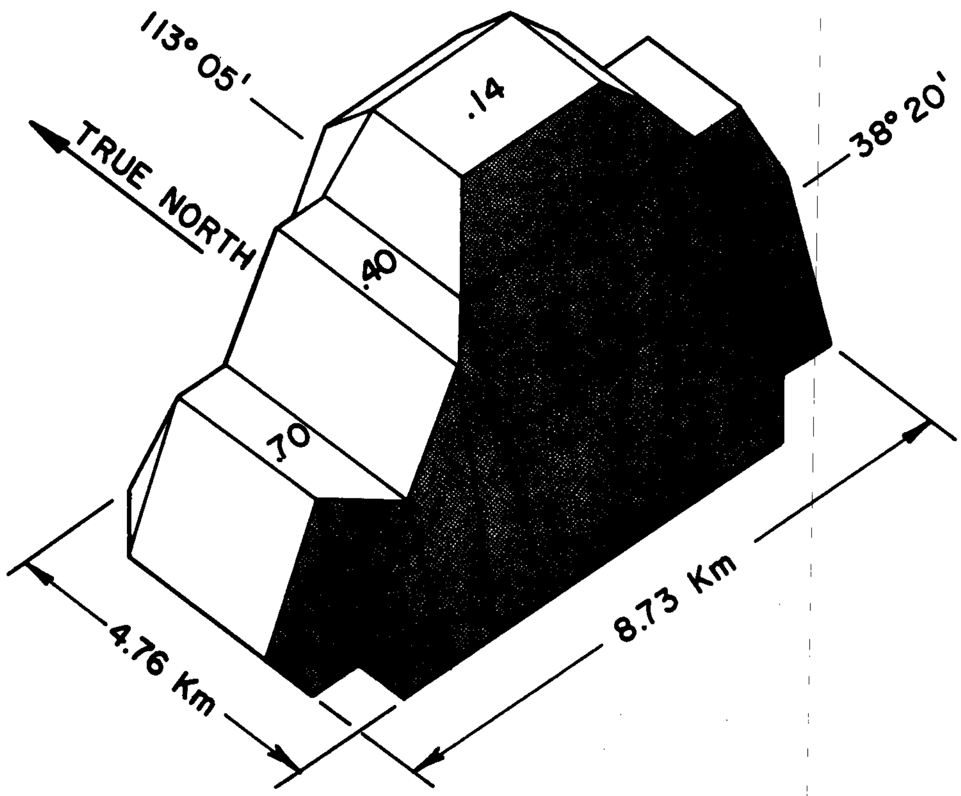

Figure 21. Three-dimensional model of the Milford Flat intrusive that results in the calculated total magnetic intensity anomaly map shown in Figure 20. Depth below surface is indicated in km. Assumed magnetic susceptibility contrast is 0.003 cgs.

appears to cut through the spring mounds.

Two gravity lows, one east of the spring mounds and a second west of these features, are outlined and indicate the relative displacement of the faults in this area. The east-west elongate nature of the eastern low implies lateral extent to a downdropped body east of the hot springs. The north-south elongate character of the low west of the hot springs appears to support the possibility of two parallel north-south faults, as previously proposed, and furthermore the possible extension of the east-west faults is implied by the truncated nature of this low. However, the sparsity of data prevents a more definite statement on the extent of these east-west gradients.

Detailed gravity profiles.--The location of the nine east-west profiles is indicated on Figure 4. All nine profiles were modeled using the Talwani 2D forward algorithm employing a direct search technique (Snow, 1977). A simple two-body model and a density contrast of 0.5 gm/cc were assumed for all profiles. The results of this modeling are shown as Figures 22 through 30. This modeling approach assumes infinite strike length and because of the apparent east-west structures of this region, some question was raised as to the validity of this assumption in the eastern half of the profiles. Talwani 3D modeling was performed to circumvent this problem and general agreement is found to be good between both approaches. Therefore, the results of this 2D modeling will be considered.

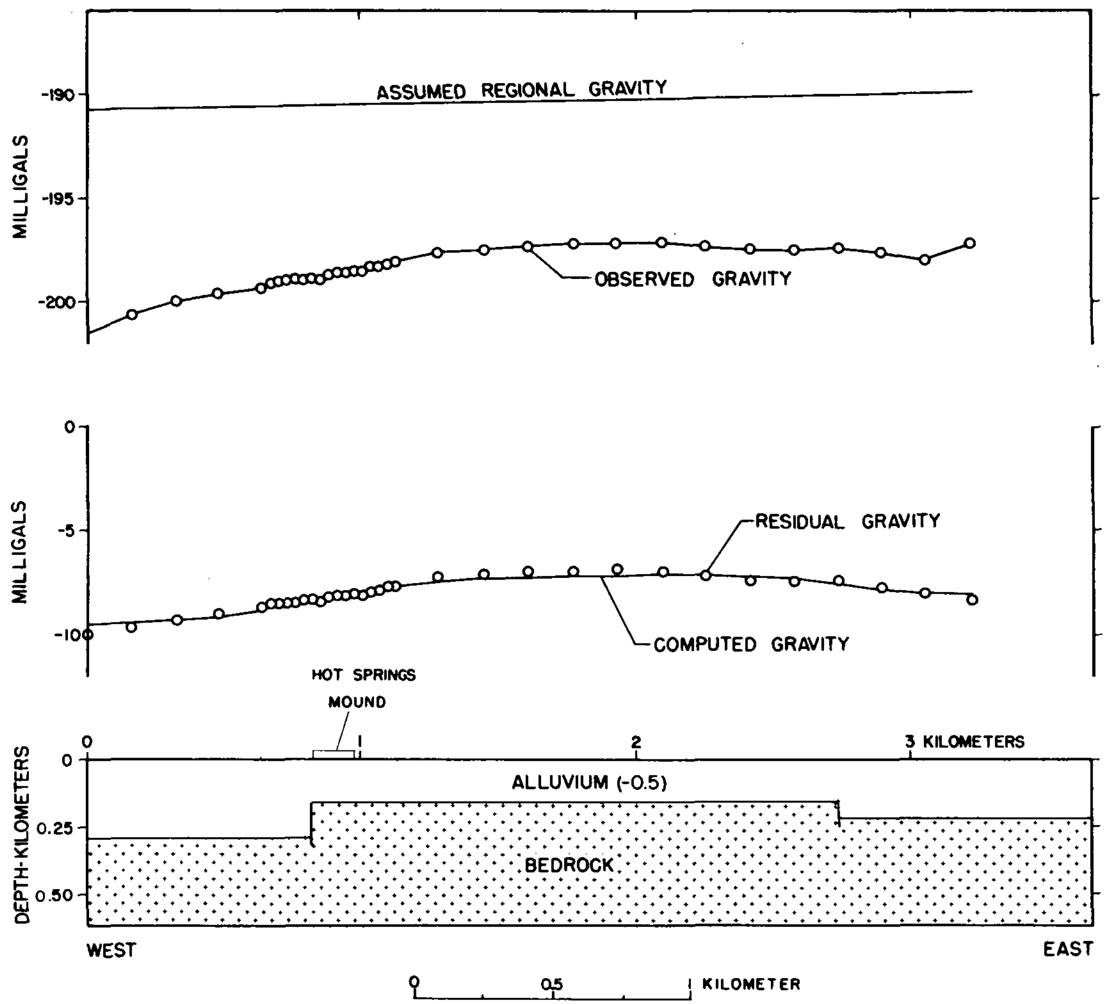

Figure 22. Interpretive two-dimensional model for gravity profile 1. Number in cross section indicates the assumed density contrast in gm/cm^3 in relation to bedrock.

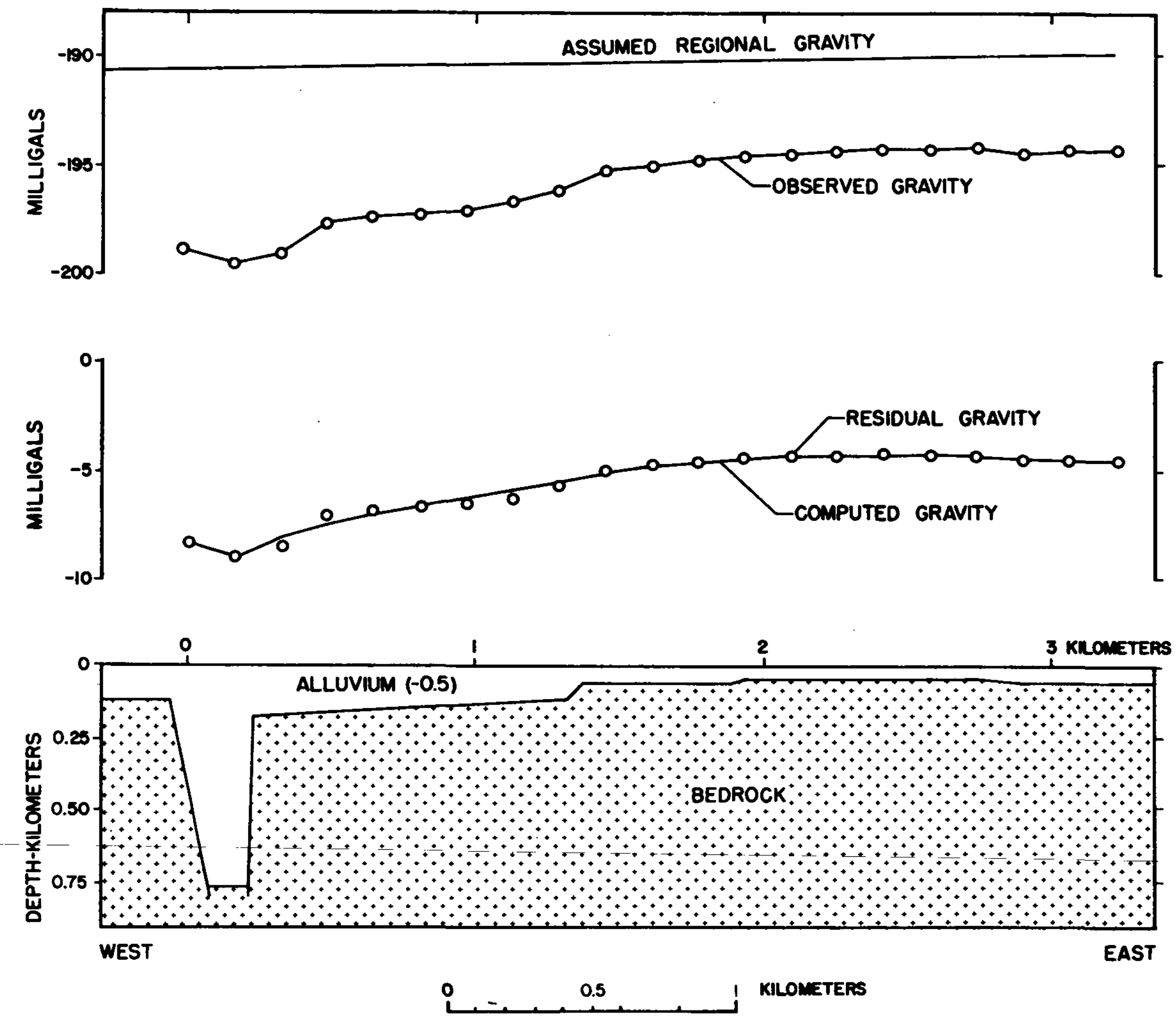

Figure 23. Interpretive two-dimensional model for gravity profile 2. Number in cross section indicates the assumed density contrast in gm/cm^3 in relation to bedrock.

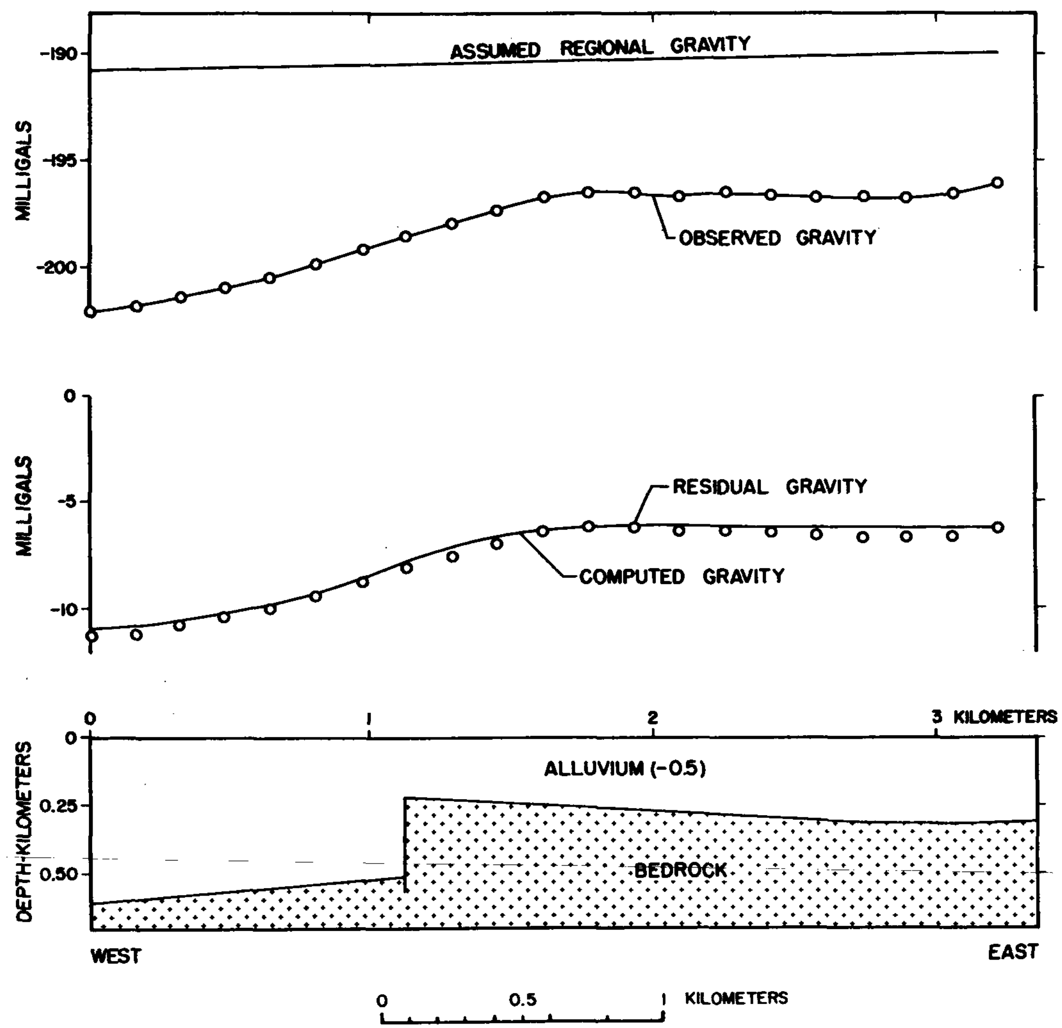

Figure 24. Interpretive two-dimensional model for gravity profile 3. Number in cross section indicates the assumed density contrast in gm/cm^3 in relation to bedrock.

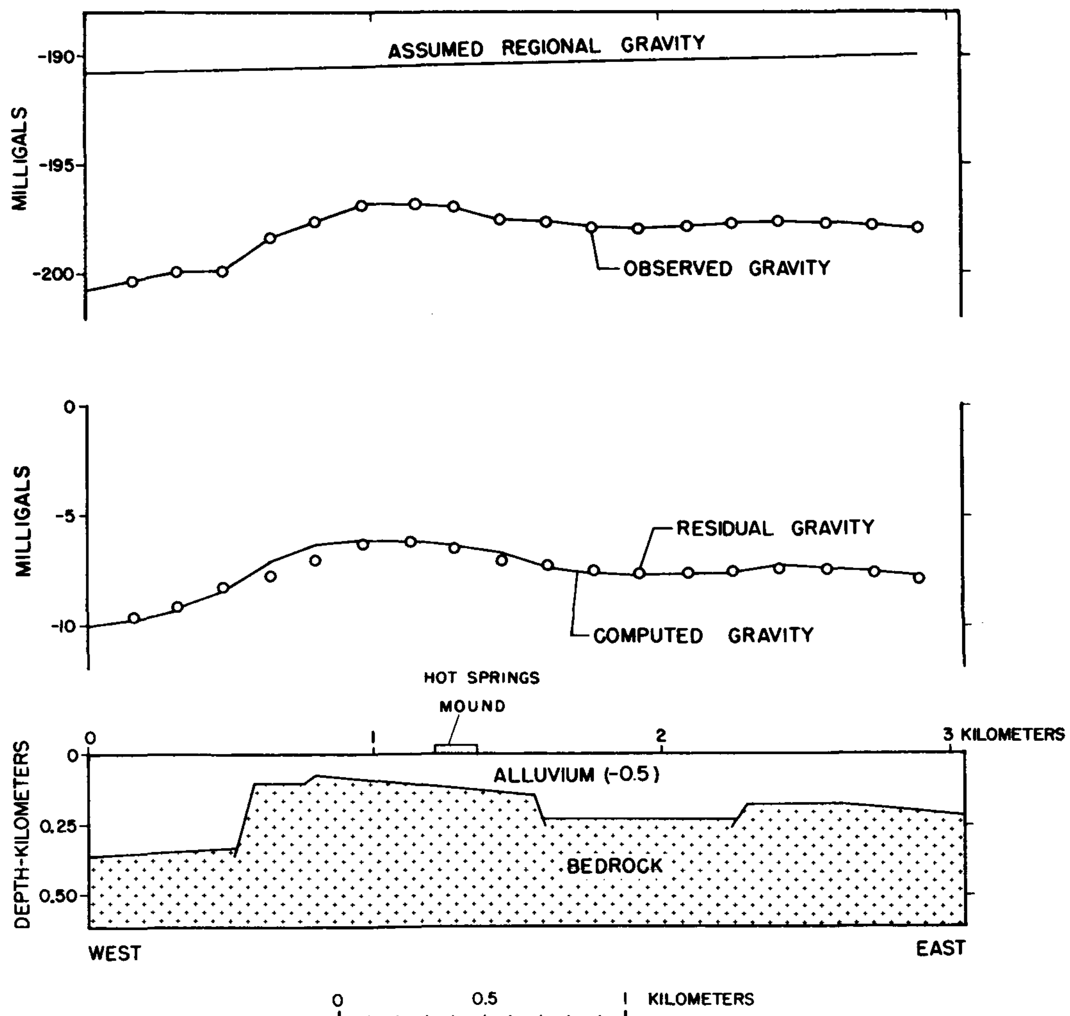

Figure 25. Interpretive two-dimensional model for gravity profile 4. Number in cross section indicates the assumed density contrast in gm/cm^3 in relation to bedrock.

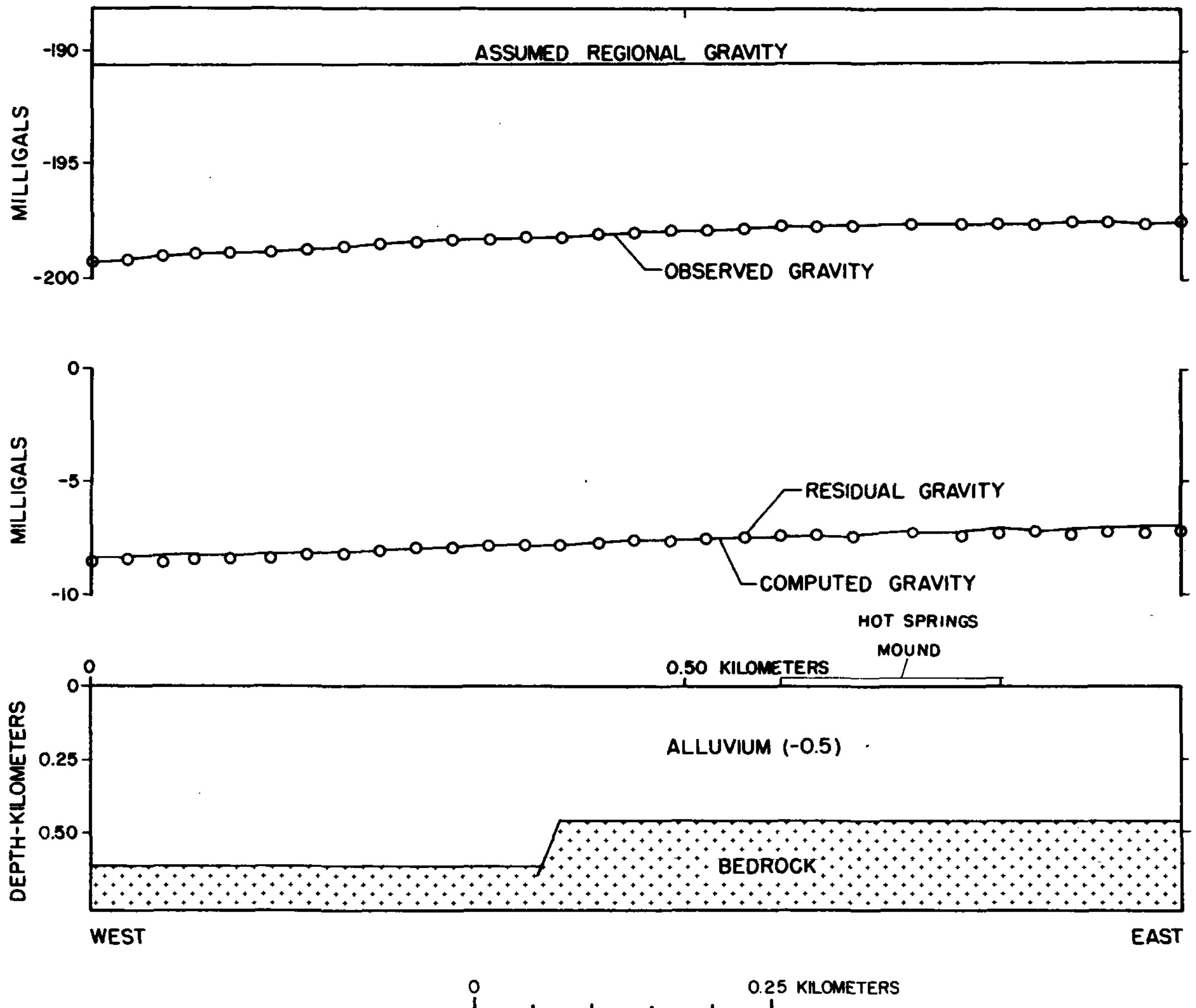

Figure 26. Interpretive two-dimensional model for gravity profile 5. Number in cross section indicates the assumed density contrast in gm/cm^3 in relation to bedrock.

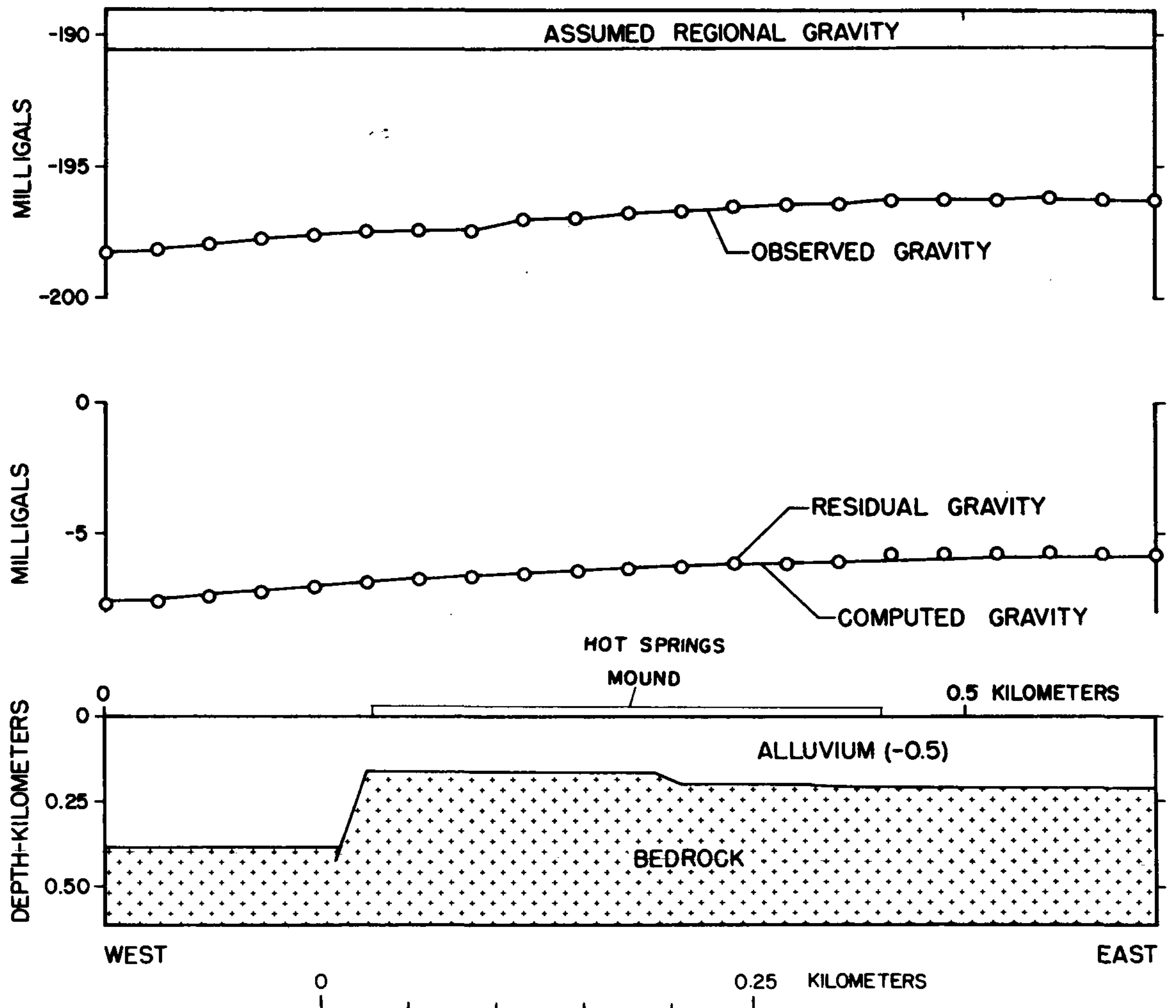

Figure 27. Interpretive two-dimensional model for gravity profile 6. Number in cross section indicates the assumed density contrast in gm/cm^3 in relation to bedrock.

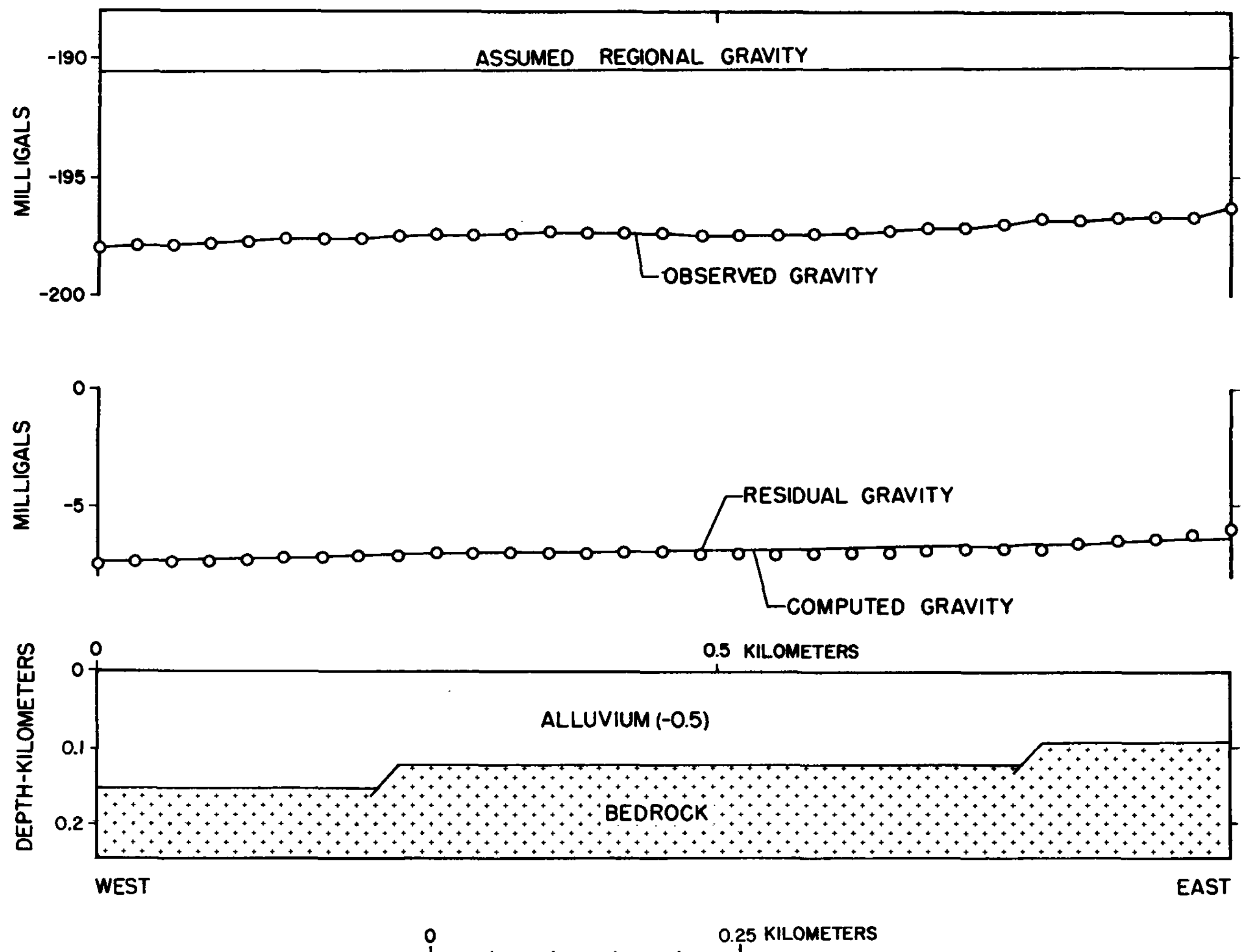

Figure 28. Interpretive two-dimensional model for gravity profile 7. Number in cross section indicates the assumed density contrast in gm/cm^3 in relation to bedrock.

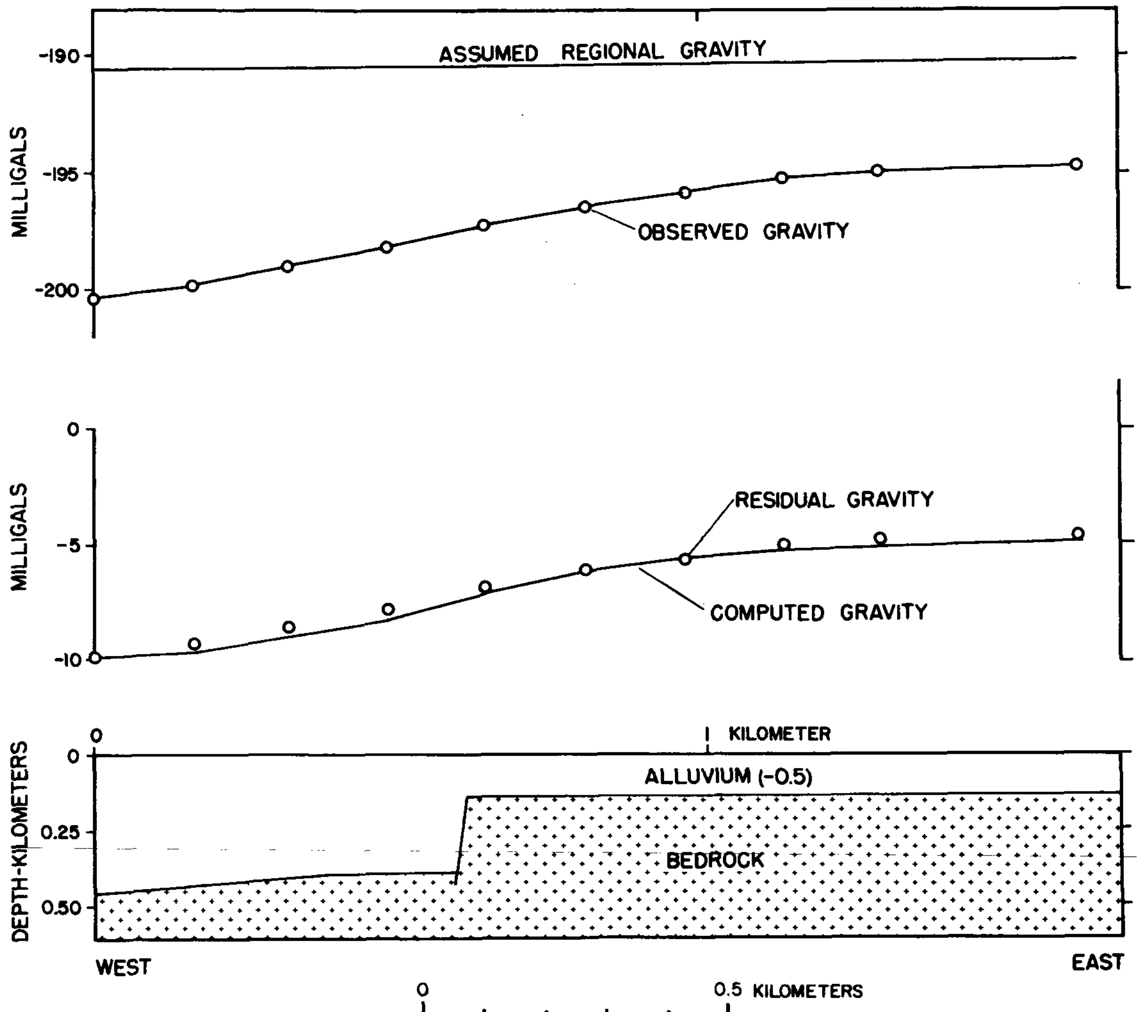

Figure 29. Interpretive two-dimensional model for gravity profile 8. Number in cross section indicates the assumed density contrast in gm/cm^3 in relation to bedrock.

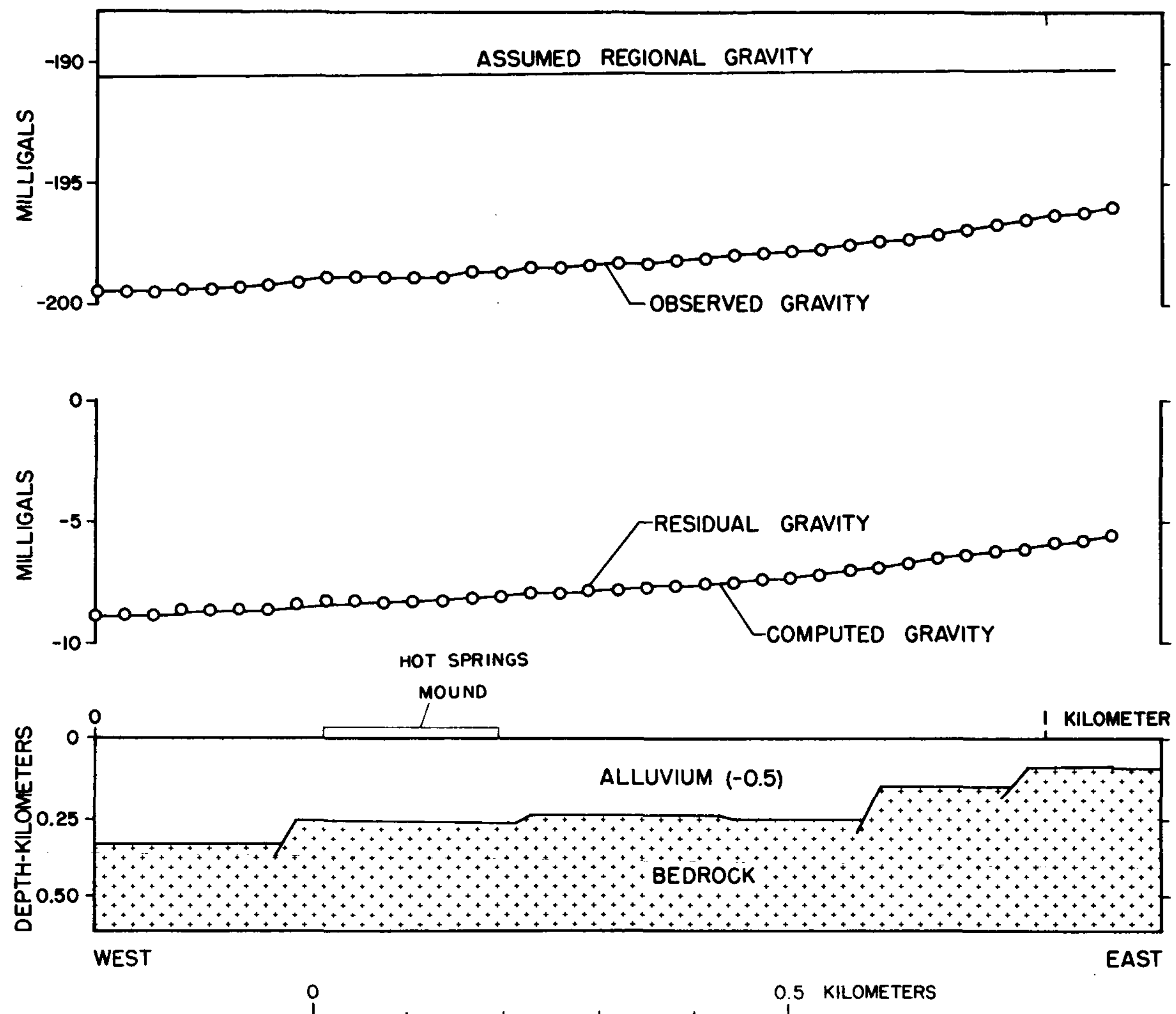

Figure 30. Interpretive two-dimensional model for gravity profile 9. Number in cross section indicates the assumed density contrast in gm/cm^3 in relation to bedrock.

The major north-south fault is apparent on all profiles except profile 7. Depth estimates to bedrock west of this fault vary among profiles but an average figure of approximately 450 m is obtained. Examples of some of the calculated depths for this feature are as follows:

Profile 1 - ∿ 305 m
Profile 3 - ∿ 520 m
Profile 4 - ∿ 365 m
Profile 8 - ∿ 430 m

The location of this same fault seems to be characterized by a series of minor offsets in the immediate area of the hot springs. In the vicinity of the southern hot-spring mound, the fault is modeled adjacent to the mound. It then appears to be offset to the east such that the fault is then adjacent to the northern half of the northern mound and proceeds in a north-northeast direction from that area. South of the southern mound, there appears to be an offset to the west. This is implied by the fact that profile 7 does not detect this fault, and it is located in the westernmost portion of profile 2.

East of the hot springs, an average figure of 245 m is obtained for depth to bedrock. This figure should be considered approximate because of the assumption of two dimensionality.

Three-dimensional modeling.--As mentioned, Talwani 3D modeling of the hot springs region was completed. A first-order polynomial residual shown as Figure 31 served as the anomaly to be modeled. A density contrast of 0.5 gm/cc was assumed and preliminary model was constructed using the results of the 2D modeling for rough depth estimates. A number of "forward" calculations were completed until

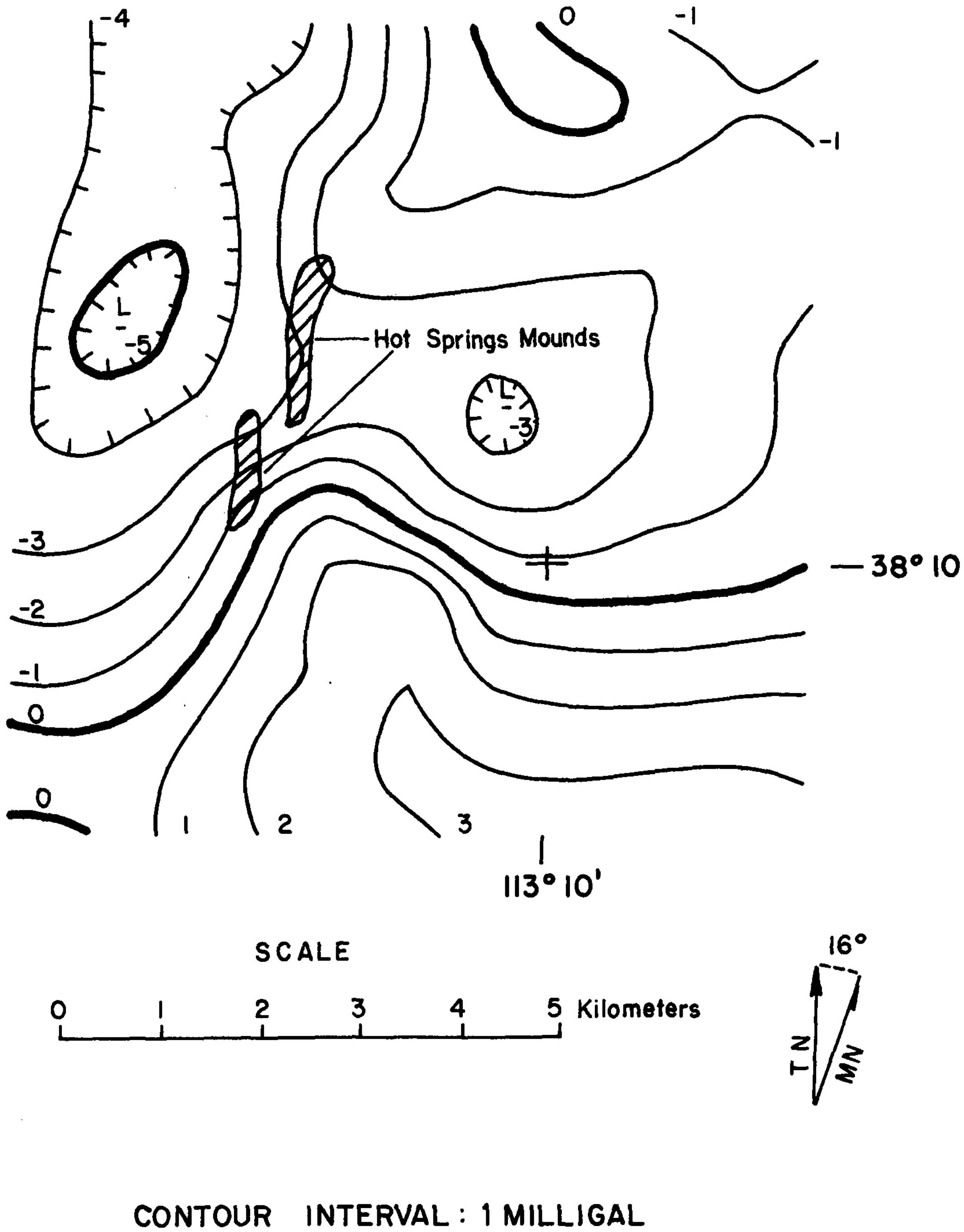

Figure 31. First-order polynomial residual gravity anomaly map of the Thermo Hot Springs area.

a reasonable approximation of the anomaly was obtained. The calculated gravity anomaly for the final model is shown as Figure 32. The 3D model is illustrated as Figure 33.

A number of interesting features are noted for this model. The locations of the 2 east-west and 2 north-south faults are clearly delineated. The hot springs are located at the intersection of the southern east-west and eastern north-south faults.

An estimated depth of 457 m is obtained for the graben west of the springs. This figure shows good agreement with the 2D modeling and is within several hundred feet of Schmoker's estimate of the graben depth in the vicinity of the Star Range.

The model also implies the continuation of the southern east-west fault in a westerly direction. In general, the model shows good agreement with interpretations implied from both the regional and detail studies.

Detailed Magnetic Data

Detailed magnetic map.--The detailed total field magnetic anomaly map (Fig. 5) was compiled from the nine east-west magnetic profiles and a number of nearby stations. The dominant feature of this map is a low with a closure of nearly 100 gammas that is centered in the area of the hot springs. This feature appears to be fault controlled to the west and to the north. In both these areas, it will be noted that the magnetic trends correlate well with the faults indicated by the gravity data.

Further evidence of structural control is implied from the offset of the low in the area of the northern mound. As previously mentioned,

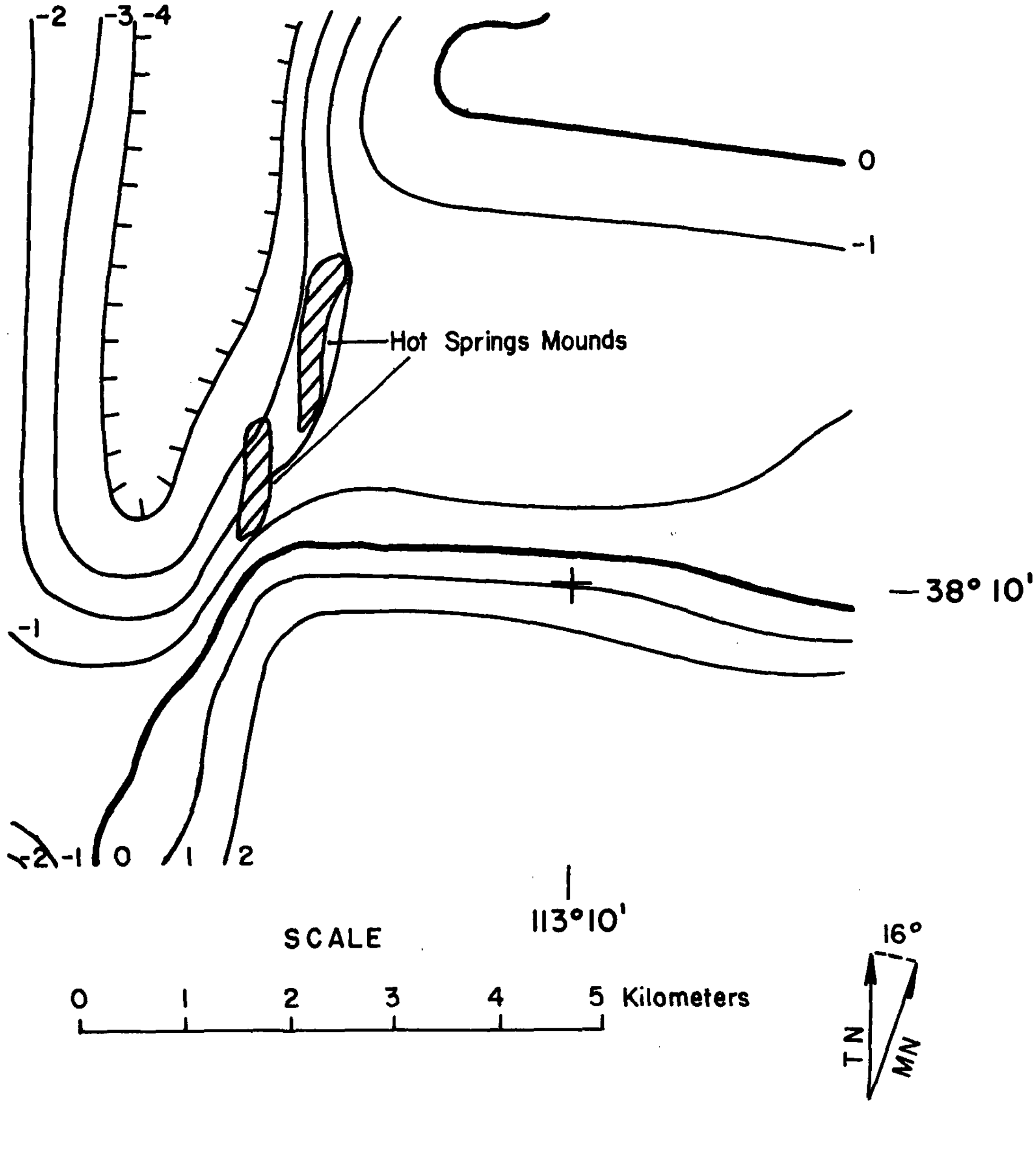

Figure 32. Calculated gravity anomaly map for the three-dimensional model of the Thermo Hot Springs area shown in Figure 33.

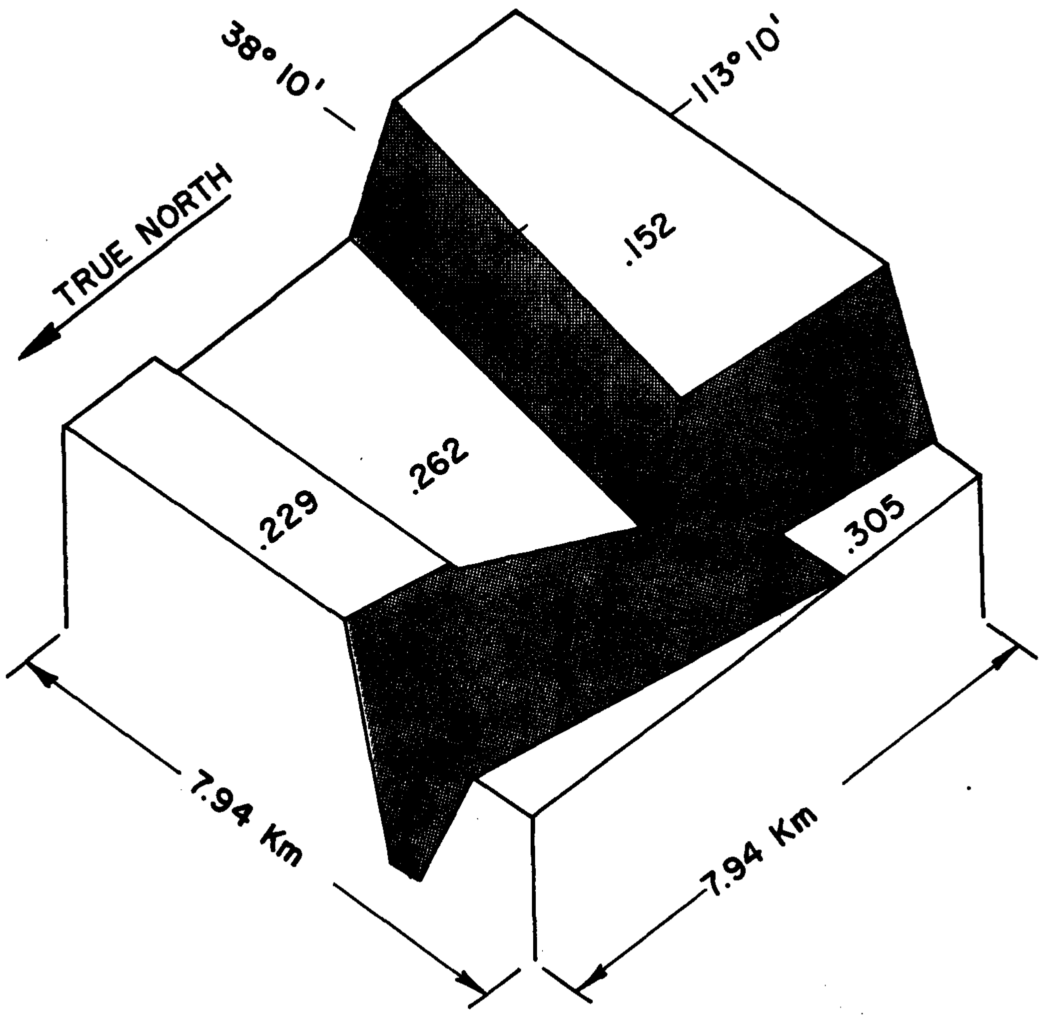

Figure 33. Three-dimensional model of the Thermo Hot Springs area that results in the calculated gravity anomaly map shown in Figure 32. Depth below surface is indicated in km. Assumed density contrast is 0.5 gm/cc.

gravity data inferred such an offset in the north-south fault. Again, the correlation of the magnetics and gravity is considered good.

The magnetic low could possibly be due to alteration of magnetite due to upward perculating hot waters which show surface expression at the hot springs. The magnetic low is apparently a localized feature approximately 2.5 km by 3.2 km which would reflect surface and near-surface alteration with the hot springs occurring at a fault intersection.

Detailed magnetic profiles.--The nine east-west magnetic profiles were modeled using the 2-1/2D forward algorithm (Shuey et al., 1973) and direct search techniques (Snow, 1977). All profiles were upward continued a distance of either 152 or 161 m, depending on the station spacing. For stations spaced at 30.5 m, the continuation was 152 m while stations spaced at 161 m were upward continued that same distance. The results of the modeling of this upward continued data are shown in Figures 34 through 42.

Lack of geological information pertaining to mapped alteration and lithologies at depth prevented the use of such constraints in the modeling. However, the immediate area of the hot springs is known to consist of alluvium which is probably underlain by volcanics. Therefore, using a low magnetic susceptibility for alluvium ($\sim$.0005 cgs), a lower susceptibility for the volcanics ($\sim$.0025-.0030 cgs) possible models were generated. The additional constraint of the results of the gravity profile modeling was imposed on each profile in the location of contacts and alteration zones. It was further assumed that both the alluvium and the possible volcanics in the area of the

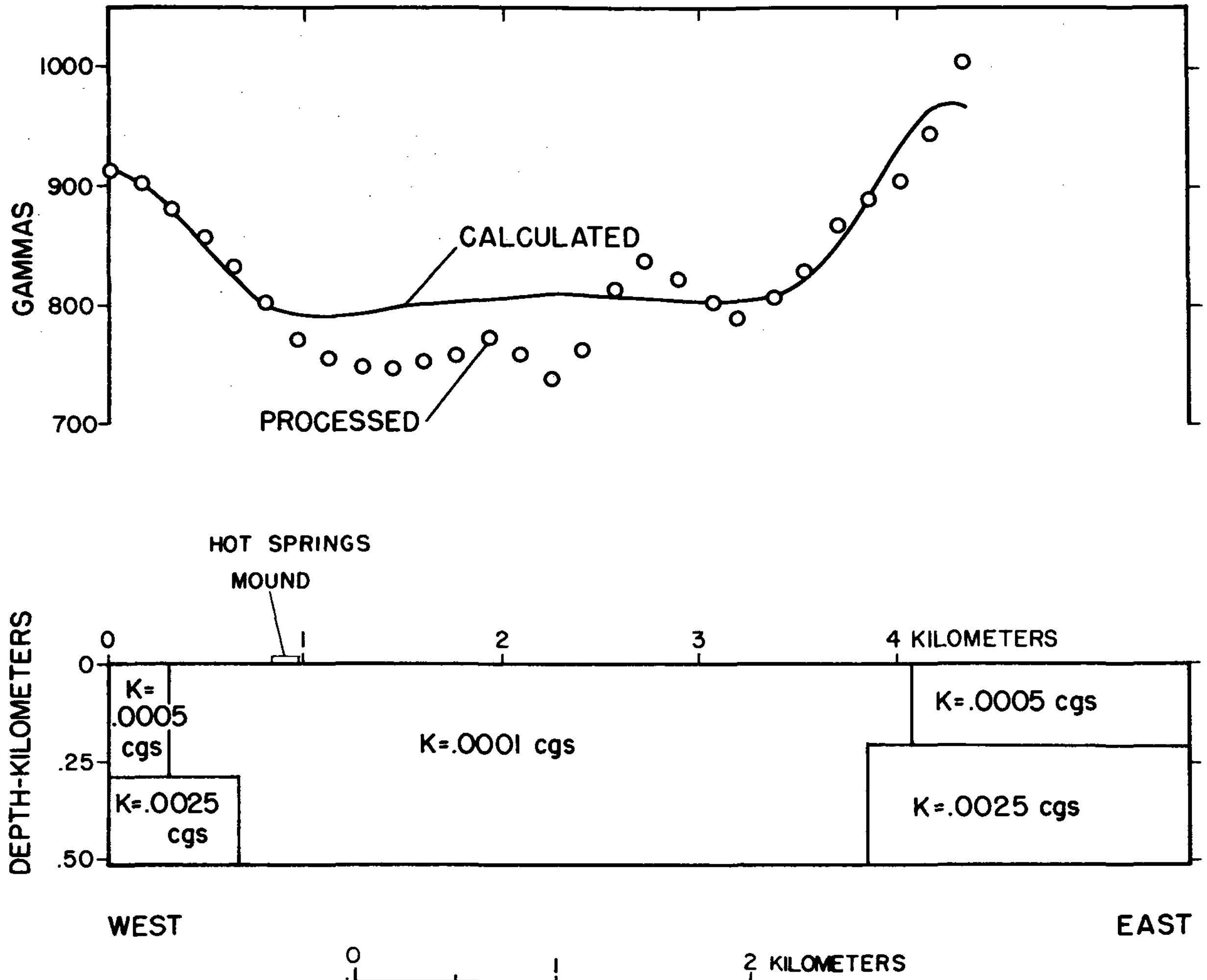

Figure 34. Interpretive two and one-half dimensional model for magnetic profile 1.

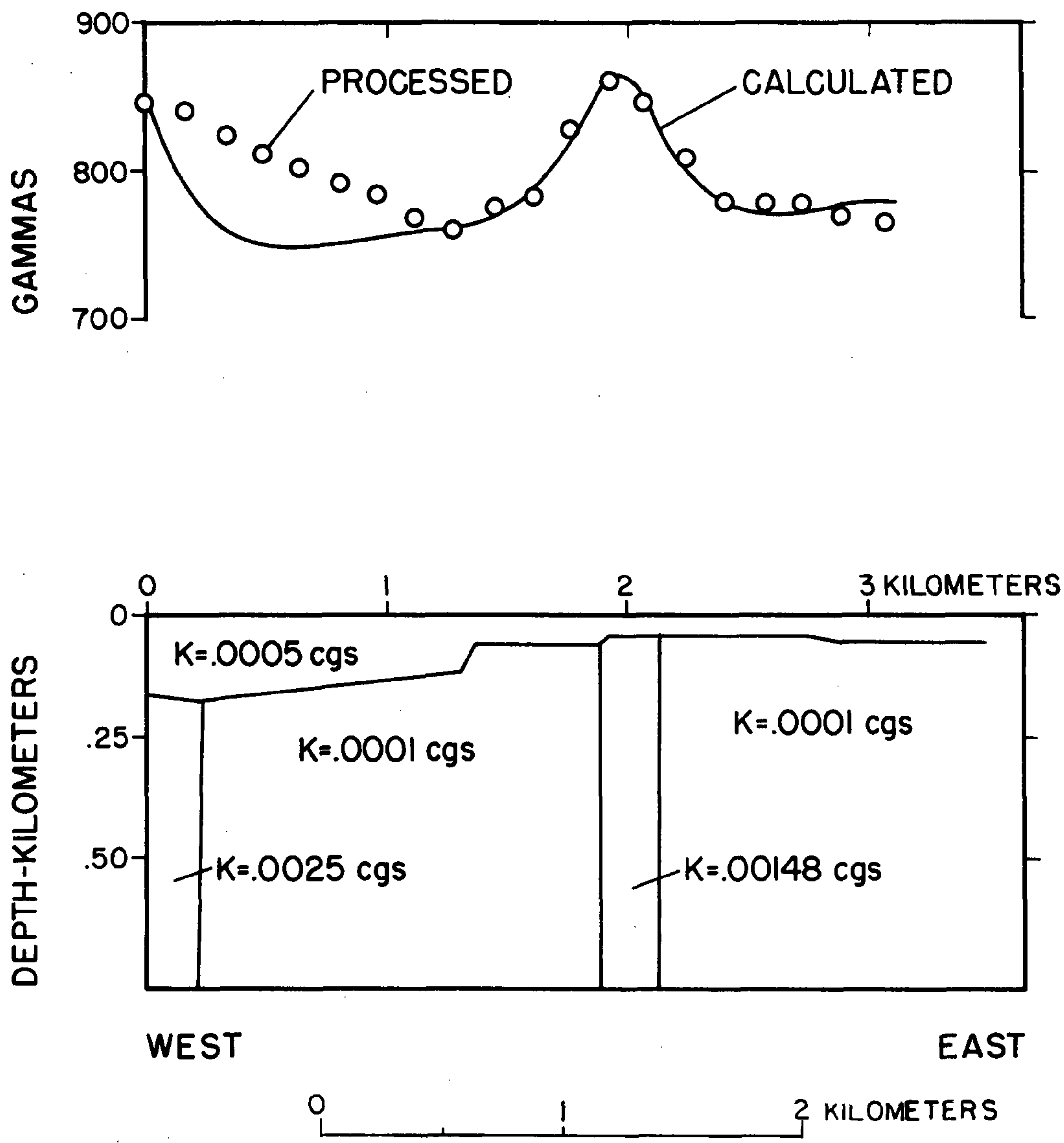

Figure 35. Interpretive two and one-half dimensional model for magnetic profile 2.

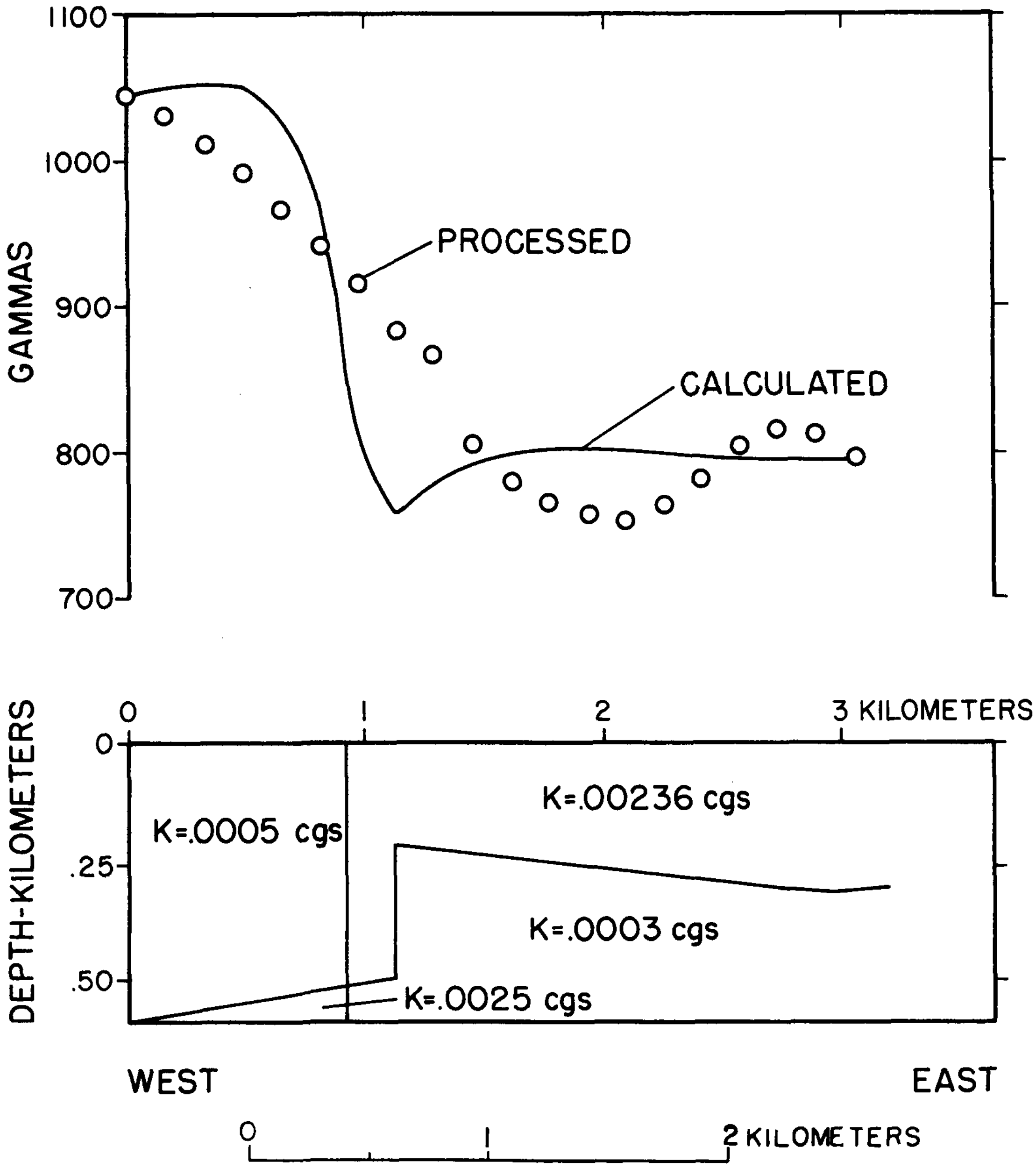

Figure 36. Interpretive two and one-half dimensional model for magnetic profile 3.

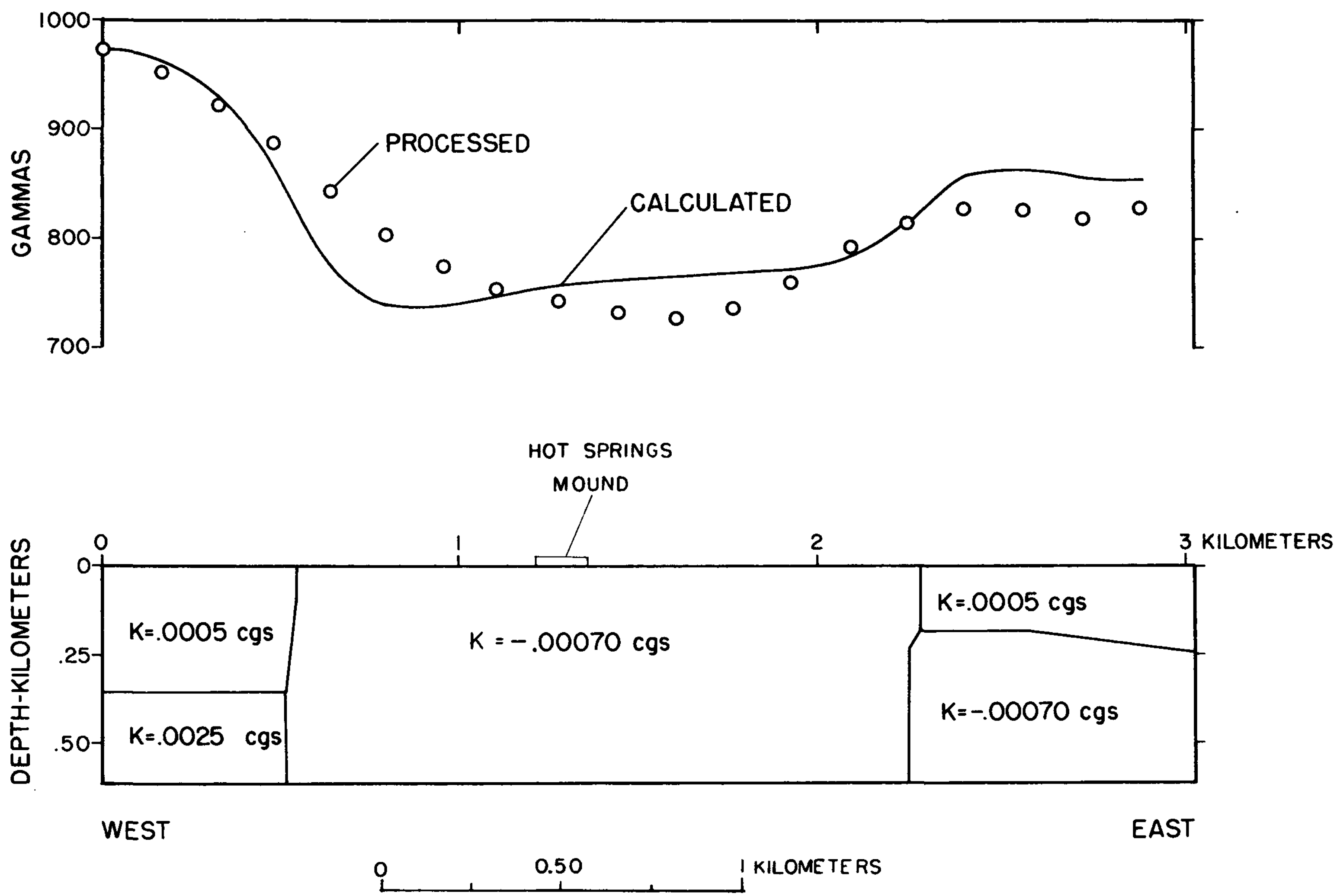

Figure 37. Interpretive two and one-half dimensional model for magnetic profile 4.

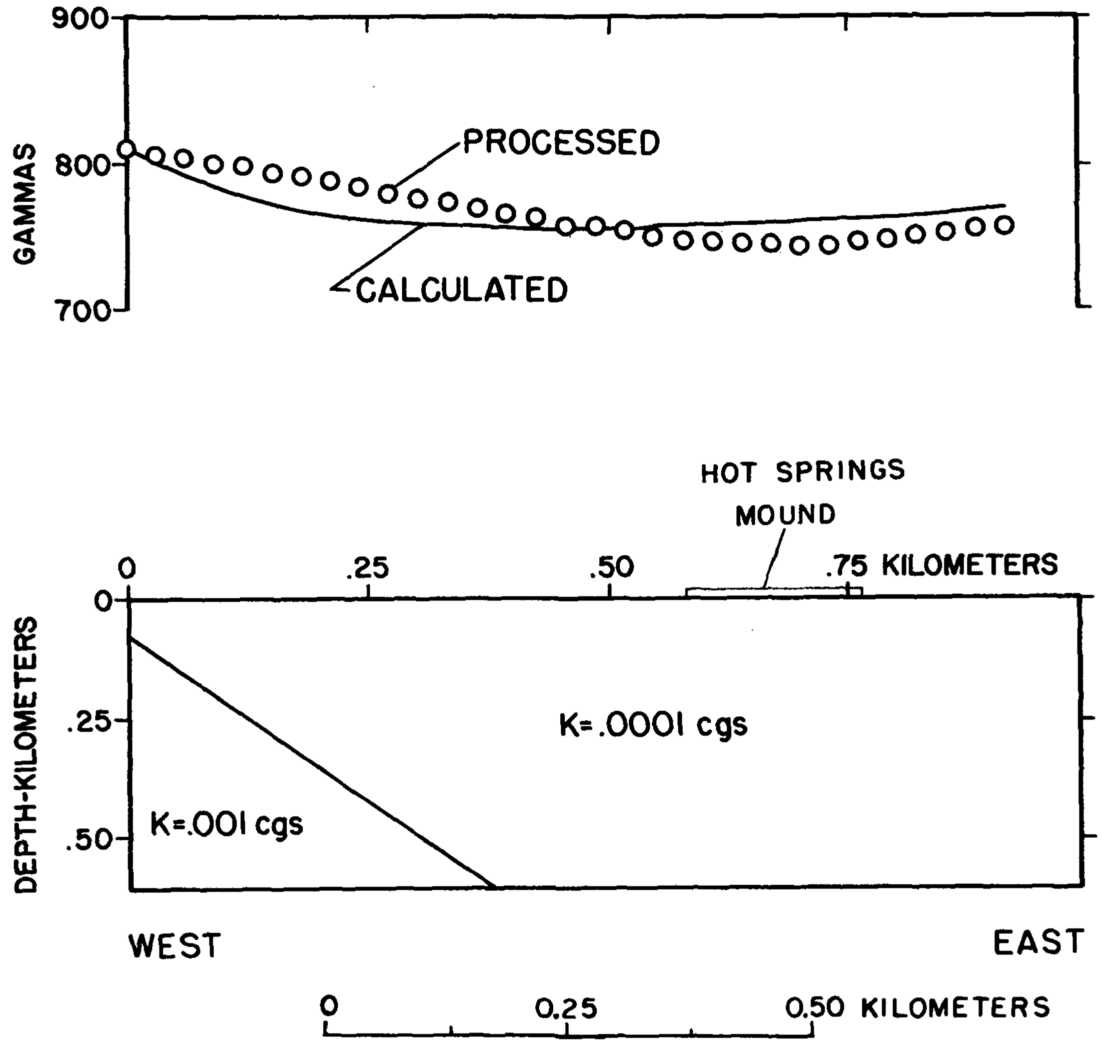

Figure 38. Interpretive two and one-half dimensional model for magnetic profile 5.

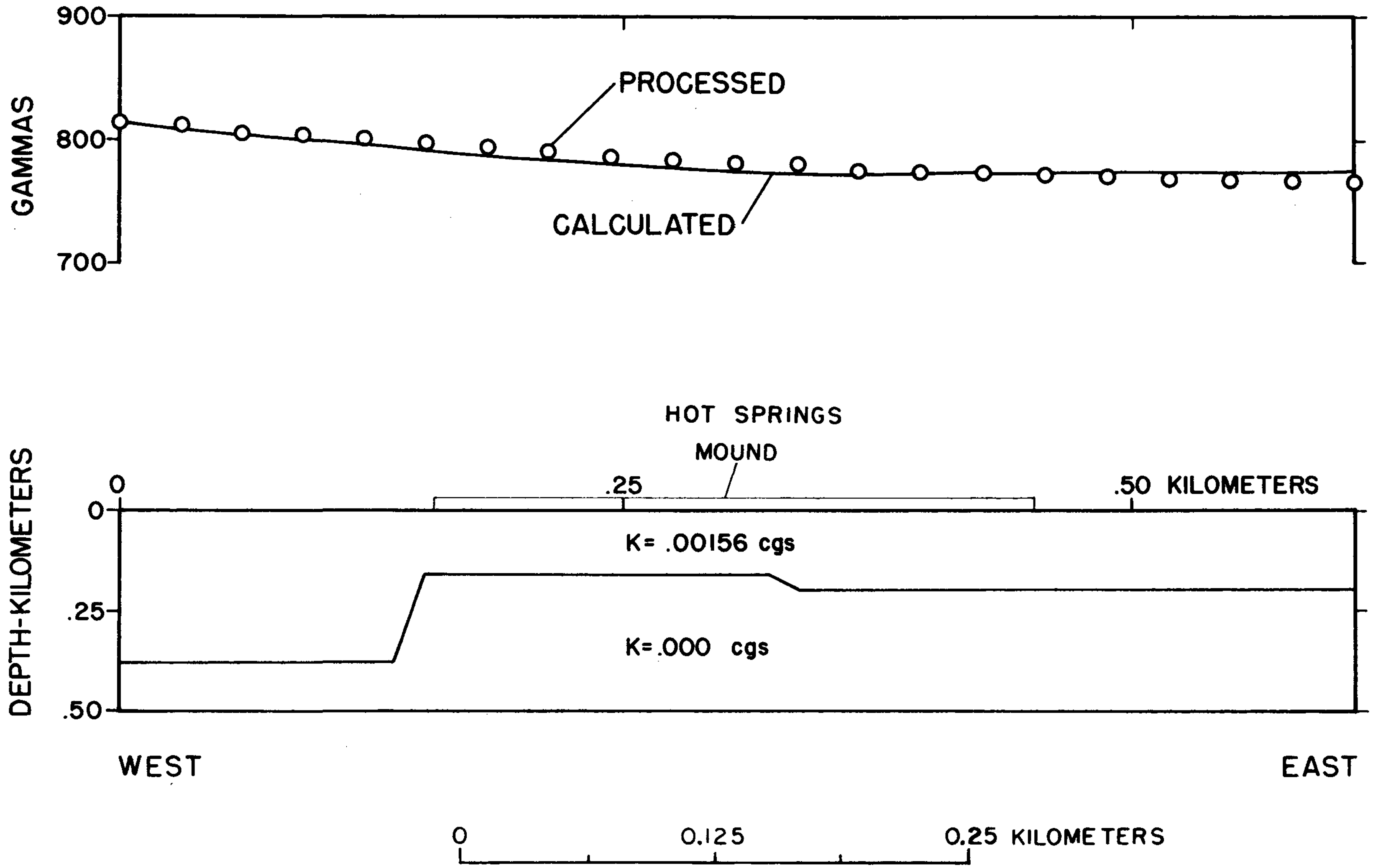

Figure 39. Interpretive two and one-half dimensional model for magnetic profile 6.

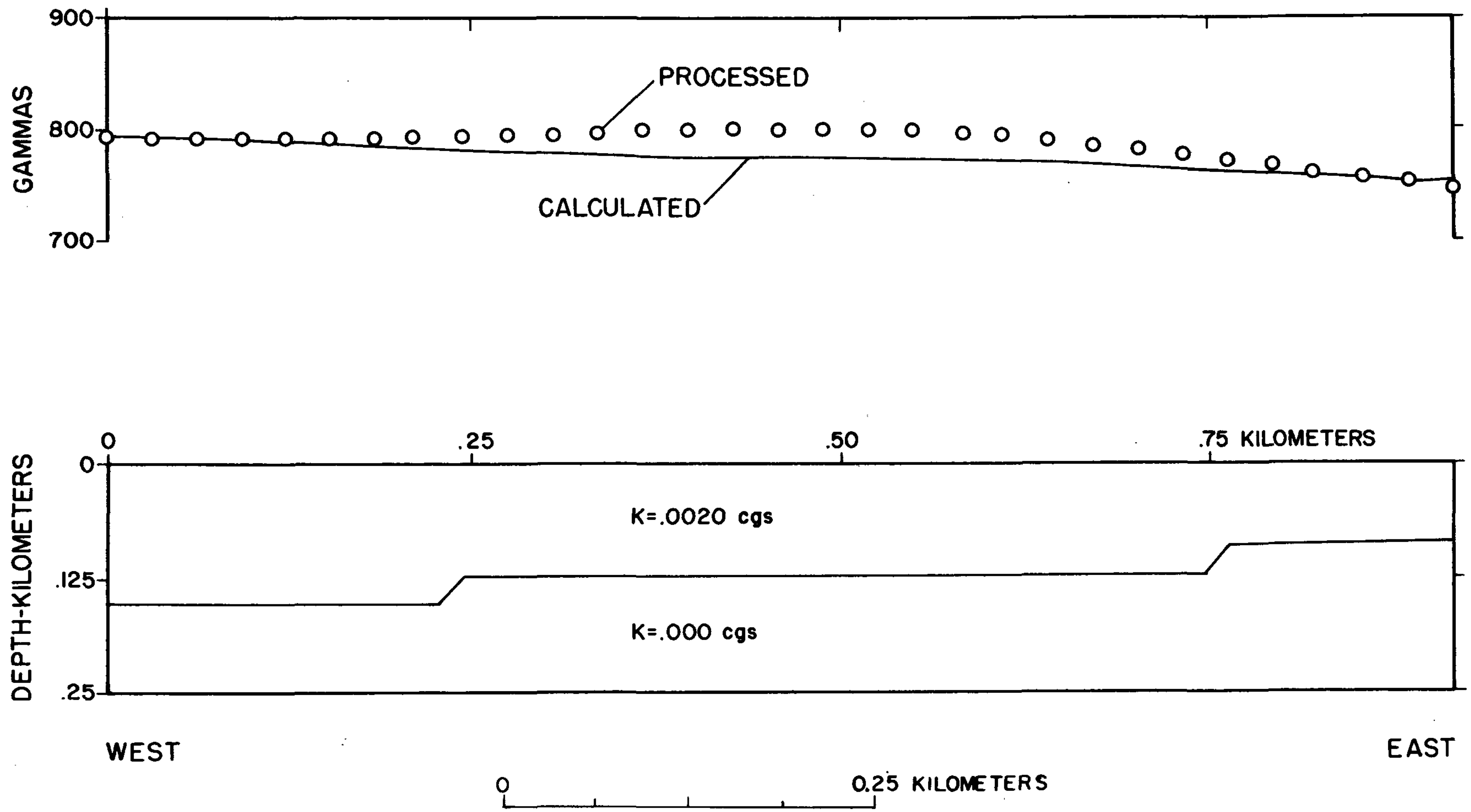

Figure 40. Interpretive two and one-half dimensional model for magnetic profile 7.

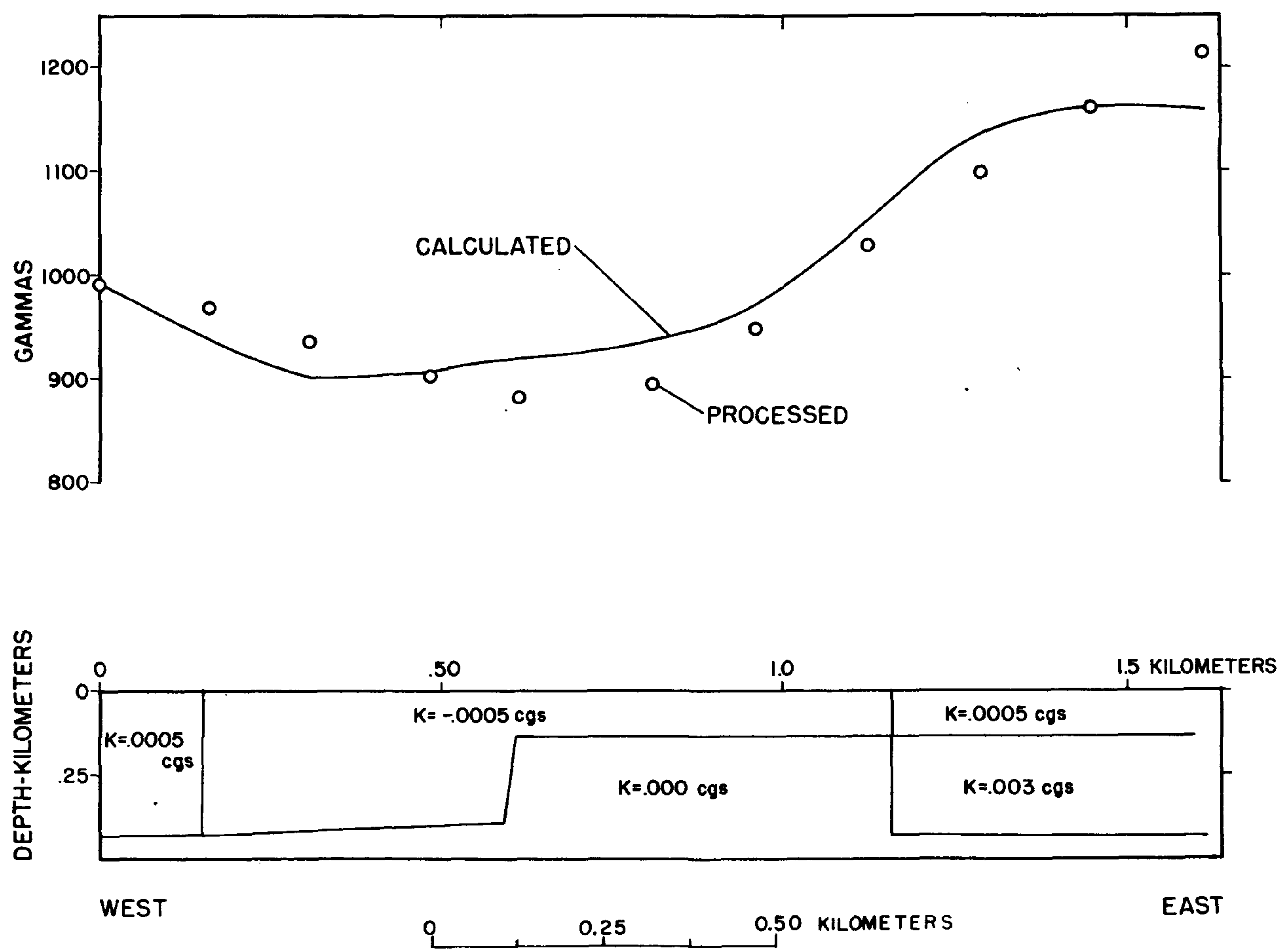

Figure 41. Interpretive two and one-half dimensional model for magnetic profile 8.

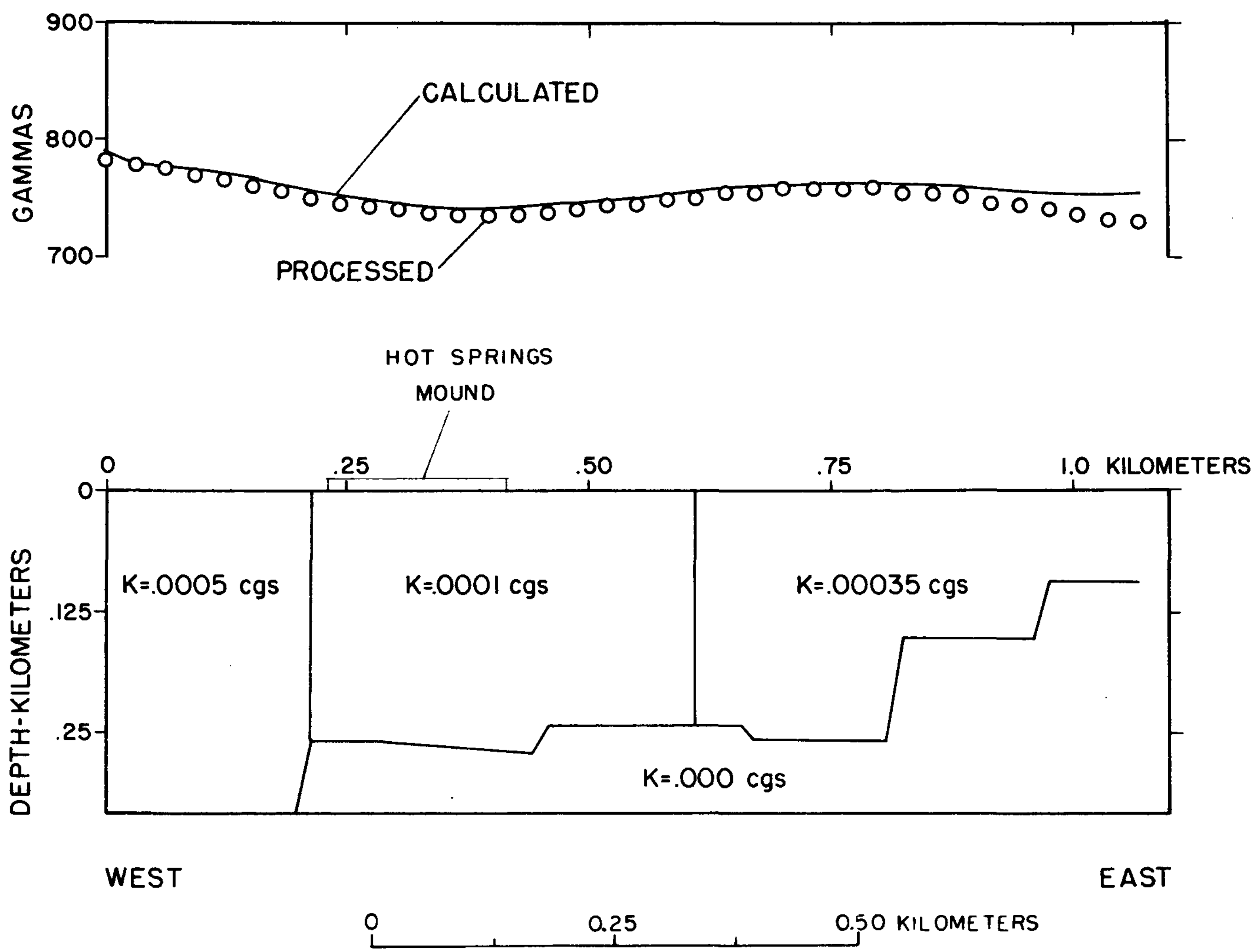

Figure 42. Interpretive two and one-half dimensional model for magnetic profile 9.

springs have sufficient permeability to allow the development of alteration zones as indicated in the models.

The most common type of model resulting from this approach shows an alteration zone which is located in the area of the north-south fault and east of this feature for distances of typically 1.6 km. The models also indicate that such a zone continues to depth.

Two magnetic profiles, 6 and 7, indicate a variation from this general model in that near-surface susceptibilities exceed those at depth. It is possible that the profiles are located west and south of the major surface alteration and perhaps the alteration is more extensive at depth.

SUMMARY AND CONCLUSIONS

The gravity data were reduced and are presented as terrain-corrected Bouguer gravity anomaly maps. Terrain corrections were made to a distance of 18.8 km. The regional gravity map delineates a number of interesting features. A large, elongate north-south trending graben is outlined in the central portion of the survey area. The estimated throw for the normal faulting associated with this graben varies from 200 to 300 m. A conspicuous east-west trend south of the Star Range is interpreted as faulting with downthrow of approximately 200 m to the south. East of Blue Mountain another graben, which appears to be the southern extension of the Wah Wah Valley graben, is interpreted from the regional gravity map. An estimated throw of about 600 m has been interpreted for the normal fault bounding the west side of this graben.

The detailed gravity map indicates two east-west trends insecting a large north-south trend in the immediate vicinity of the Thermo hot springs. These trends have been interpreted as faults which appear to control the location of the hot springs.

To facilitate interpretation of the gravity data, the following processing and modeling techniques were used: 1) high-pass frequency filtering; 2) polynomial fitting; 3) second derivative; 4) strike-filtering; 5) two-dimensional modeling; and 6) three-dimensional modeling. The techniques proved helpful as they more clearly delineated features of interest. The residual maps outlined the north-south graben that extends through the central portion of the survey area and more clearly defined the graben east of Blue Mountain. The strike-filtered maps emphasize the major north-south and east-west faults of the region. The faults controlling the hot springs location are accentuated with these strike filters and, as such, should provide guidelines for future exploration. The two-dimensional and three-dimensional modeling provided reasonable depth estimates for bedrock in the vicinity of the hot springs and supported structural interpretation for the hot springs area. The two-dimensional modeling established the position of the large north-south fault as just west of the hot springs and indicated downthrow to the west of typically 300 m. The three-dimensional model showed fault locations and bedrock depths varying from about 0.15 to 0.45 km. This model should aid further delineation of this known geothermal resource area.

The magnetic data are presented as total magnetic intensity maps for both the regional and detailed surveys. The regional magnetic map delineates a distinct magnetic high of about 600-gammas closure that corresponds with a Tertiary quartz monzonite intrusive in the northeast part of the survey area. A linear trend of approximately 300-gammas relief is delineated south of the Shauntie Hills and Star Range. This trend is interpreted as probably corresponding with an east-west fault which correlates well with the gravity interpretation.

The detailed magnetic map outlines an anomalous low of approximately 100-gammas closure associated with the Thermo Hot Springs. This magnetic low may reflect an alteration zone which is structurally controlled. A north-south trend is apparent on the detailed magnetic map. This trend reflects the normal fault outlined by the gravity.

The following processing and modeling techniques were applied to aid interpretation of the magnetic data: 1) low-pass frequency filtering; 2) strike-filtering; 3) pseudogravity; 4) two and one-half dimensional modeling; and 5) three-dimensional modeling. The low-pass filtering clearly delineates the intrusive and the east-west trend south of the Star Range. Strike-filtering outlines north-south and east-west trends which correlate with faults implied by gravity data. The pseudogravity map indicates that the magnetic and gravity anomalies are not caused by the same bodies. The two and one-half dimensional modeling in the hot springs area provide a possible model for an alteration zone which appears to be structurally controlled. The three-dimensional modeling of the Tertiary quartz monzonite intrusive suggests a reasonable model for that feature. The model shows an elongate east-west intrusive with dimensions approximately 9 km by 5 km. The top of the intrusive is modeled at a depth of 0.14 km and its size increases with depth. The base of the intrusive is modeled at greater than 1 km depth.

APPENDIX 1

DENSITY AND MAGNETIC SUSCEPTIBILITY OF ROCK SAMPLES

SAMPLE NO. AND ROCK TYPE	LATITUDE N. DEG.	LATITUDE N. MIN.	LONGITUDE W. DEG.	LONGITUDE W. MIN.	SAMPLE AREA #	WET BULK DENSITY (gm/cc)	MAGNETIC SUSCEPTIBILITY (in units of 10^{-6} cgs)
Tertiary Intrusives							
S-9 Granitoid	38	22.50	113	04.38	a	2.71	4150
S-14 Granitoid	38	19.90	113	10.10	a	2.54	18.9
S-18 Granitoid	38	21.40	113	04.81	a	2.65	2450
Sedimentary							
S-10 Limestone	38	18.00	113	08.23	a	2.77	4.92
S-11 Sandstone	38	18.00	113	08.03	a	2.36	19.6
S-13 Siltstone	38	18.48	113	08.70	a	2.66	63.4
S-16 Limestone	38	21.53	113	09.84	a	2.68	18.9
S-19 Limestone	38	20.43	113	07.40	c	2.67	21.7
S-25 Limestone	38	13.66	113	23.41	c	2.80	15.8
S-35 Hot springs deposit	38	10.49	113	12.23	e	2.22	9.53

SAMPLE NO. AND ROCK TYPE	LATITUDE N. DEG.	LATITUDE N. MIN.	LONGITUDE W. DEG.	LONGITUDE W. MIN.	SAMPLE AREA #	WET BULK DENSITY (gm/cc)	MAGNETIC SUSCEPTIBILITY (in units of 10^{-6} cgs)
Metamorphic							
S-15 Quartzite	38	21.36	113	9.66	a	2.58	18.5
S-26 Quartzite	38	13.23	113	23.89	c	2.75	11.7
Volcanic							
S-2 Intermediate	38	10.21	113	10.55	d	2.35	28.1
S-3 Intermediate	38	9.48	113	8.38	d	2.23	133
S-4 Intermediate	38	7.59	113	8.21	d	2.35	455
S-5 Basic	38	8.43	113	10.53	d	2.48	2600
S-6 Basic	38	9.20	113	4.85	d	2.69	2880
S-7 Intermediate	38	10.58	113	3.91	e	2.58	269
S-20 Intermediate	38	16.83	113	9.40	e	2.63	1060
S-21 Intermediate	38	15.95	113	10.43	e	2.43	348
S-22 Intermediate	38	15.56	113	13.18	e	2.49	231
S-23 Intermediate	38	14.03	113	20.14	e	2.56	1200
S-24 Intermediate	38	13.06	113	18.10	e	2.61	1830

SAMPLE AND ROCK TYPE	LATITUDE N. DEG.	LATITUDE N. MIN.	LONGITUDE W. DEG.	LONGITUDE W. MIN.	SAMPLE AREA #	WET BULK DENSITY (gm/cc)	MAGNETIC SUSCEPTIBILITY (in units of 10^{-6} cgs)
S-27 Intermediate	38	11.91	113	24.98	c	2.69	4050
S-29 Tuff	38	7.71	113	25.49	c	1.71	160
S-30 Intermediate	38	14.36	113	17.85	e	2.64	867
S-31 Intermediate	38	15.65	113	17.66	b	2.22	488
S-32 Intermediate	38	16.81	113	17.30	b	2.35	676
S-33 Intermediate	38	17.36	113	12.00	b	2.99	1130
S-34 Intermediate	38	17.33	113	11.98	b	2.50	298

Letter subscript denotes general area of sample as follows:

a - Star Range area

b - Shauntie Hills area

c - Blue Mountain area

d - Black Mountains area

e - Escalante Desert area

APPENDIX 2

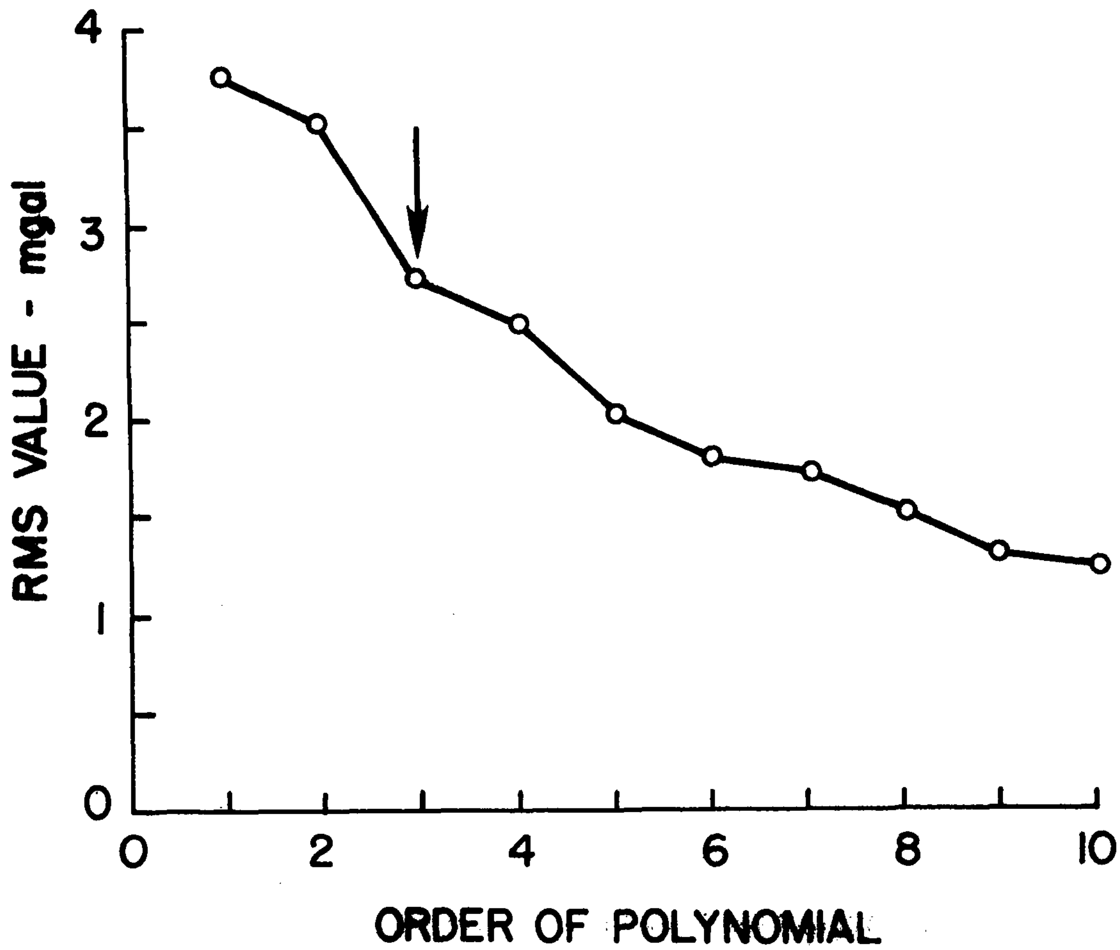

Figure 43. Graph of the RMS value of the difference between observed and calculated gravity values versus polynomial order for the gridded data.

APPENDIX 3

Table of the Gravity and Magnetic Data

NOTES: 1) Units are as follows:

	UNITS
Latitude	degrees, minutes
Longitude	degrees, minutes
Elevation	feet
Free-air anomaly value	mgal
Simple Bouguer anomaly value[1]	mgal
Terrain-correction value[1]	mgal
Terrain-corrected Bouguer anomaly value[1]	mgal
Reduced Magnetic values[2]	gammas

2) Coding is as follows:

RS 105 -number designation of gravity station taken by author

1) A density contrast of 2.67 gm/cc was assumed for both the Bouguer and terrain corrections. Terrain corrections were made from zones B through K using U.S.C. & G.S. zone charts (18.8 km total).

2) Magnetic data were reduced to a datum of 697 gammas at field base, RS-1. A constant value of 179 gammas was added to 1975 University of Utah class data based upon an averaging of common stations.

STATION NUMBER	LATITUDE DEG	MIN	LONGITUDE DEG	MIN	ELEVATION IN FEET	FREE-AIR ANOMALY	SIMPLE BOUGUER	TERRAIN CORRECTION	TERR-CORR BOUGUER
RS-1	38.	10.00	113.	10.38	5075.	-23.64	-196.49	.26	-196.23
RS-2	38.	9.79	113.	9.50	5268.	-16.45	-195.88	.49	-195.39
RS-3	38.	8.91	113.	8.40	5285.	-13.32	-193.33	.55	-192.78
RS-4	38.	7.73	113.	8.45	5487.	-4.39	-191.28	.59	-190.69
RS-5	38.	7.73	113.	10.65	5269.	-18.93	-198.39	.43	-197.96
RS-6	38.	8.91	113.	10.59	5166.	-17.52	-193.48	.30	-193.18
RS-7	38.	9.79	113.	8.43	5168.	-19.24	-195.26	.46	-194.80
RS-8	38.	8.93	113.	11.70	5098.	-21.40	-195.04	.30	-194.74
RS-9	38.	8.93	113.	12.83	5055.	-25.78	-197.95	.20	-197.75
RS10	38.	8.03	113.	14.50	5065.	-28.13	-200.64	.20	-200.44
RS11	38.	8.41	113.	14.87	5063.	-27.41	-199.85	.15	-199.70
RS12	38.	8.93	113.	15.01	5051.	-27.93	-199.97	.15	-199.82
RS13	38.	9.80	113.	15.03	5044.	-28.36	-200.16	.16	-200.00
RS14	38.	10.65	113.	8.43	5071.	-20.91	-193.63	.30	-193.33
RS15	38.	10.65	113.	15.03	5062.	-27.93	-200.34	.15	-200.19
RS16	38.	11.55	113.	15.03	5128.	-24.09	-198.75	.15	-198.60
RS17	38.	12.40	113.	15.01	5200.	-20.34	-197.45	.12	-197.33
RS18	38.	12.40	113.	13.92	5165.	-22.73	-198.65	.13	-198.52
RS19	38.	11.55	113.	13.92	5102.	-25.11	-198.88	.13	-198.75
RS20	38.	13.93	113.	12.60	5208.	-21.75	-199.14	.16	-198.98
RS21	38.	14.19	113.	12.20	5212.	-21.98	-199.50	.21	-199.29
RS22	38.	14.19	113.	11.65	5177.	-21.47	-197.79	.21	-197.58
RS23	38.	14.19	113.	10.60	5131.	-18.58	-193.34	.20	-193.14
RS24	38.	14.19	113.	9.45	5093.	-20.39	-193.86	.18	-193.68
RS25	38.	14.80	113.	14.15	5548.	-6.30	-195.27	.24	-195.03
RS26	38.	12.39	113.	11.70	5046.	-26.78	-198.65	.16	-198.49
RS27	38.	12.44	113.	12.80	5001.	-37.84	-208.17	.16	-208.01
RS28	38.	12.40	113.	10.60	5029.	-22.89	-194.18	.15	-194.03
RS29	38.	12.40	113.	8.43	5022.	-22.90	-193.95	.16	-193.79
RS30	38.	10.68	113.	13.68	5045.	-28.63	-200.46	.15	-200.31

STATION NUMBER	LATITUDE DEG	LATITUDE MIN	LONGITUDE DEG	LONGITUDE MIN	ELEVATION IN FEET	FREE-AIR ANOMALY	SIMPLE BOUGUER	TERRAIN CORRECTION	TERR-CORR BOUGUER
RS31	38.	8.15	113.	20.95	5104.	-32.96	-206.81	.50	-206.31
RS32	38.	8.93	113.	21.70	5114.	-24.66	-198.84	1.17	-197.67
RS33	38.	7.84	113.	21.70	5171.	-25.94	-202.07	.57	-201.50
RS34	38.	8.84	113.	19.58	5071.	-34.33	-207.04	.27	-206.77
RS35	38.	10.65	113.	16.70	5094.	-25.73	-199.23	.19	-199.04
RS36	38.	10.70	113.	17.22	5099.	-26.76	-200.43	.20	-200.23
RS37	38.	10.65	113.	15.51	5073.	-27.57	-200.35	.15	-200.20
RS38	38.	13.15	113.	21.83	5449.	-22.26	-207.85	.90	-206.95
RS39	38.	12.83	113.	21.78	5423.	-22.23	-206.94	.90	-206.04
RS40	38.	12.40	113.	21.63	5367.	-23.16	-205.96	.87	-205.09
RS41	38.	12.40	113.	21.08	5333.	-25.09	-206.73	.65	-206.08
RS42	38.	12.40	113.	20.53	5279.	-25.25	-205.06	.60	-204.46
RS43	38.	14.19	113.	19.43	5388.	-13.91	-197.42	.30	-197.12
RS44	38.	14.75	113.	17.86	5485.	-10.51	-197.33	.23	-197.10
RS45	38.	14.40	113.	17.85	5484.	-9.51	-196.30	.20	-196.10
RS46	38.	13.26	113.	19.99	5302.	-21.50	-202.08	.40	-201.68
RS47	38.	10.65	113.	20.53	5151.	-28.90	-204.34	.72	-203.62
RS48	38.	10.75	113.	19.58	5147.	-27.81	-203.12	.35	-202.77
RS49	38.	10.65	113.	19.43	5140.	-27.99	-203.06	.30	-202.76
RS50	38.	10.21	113.	21.20	5128.	-28.39	-203.05	1.20	-201.85
RS51	38.	9.90	113.	7.43	5098.	-20.29	-193.92	.46	-193.46
RS52	38.	9.79	113.	6.19	5158.	-17.39	-193.07	.43	-192.64
RS53	38.	10.38	113.	4.40	5154.	-15.64	-191.18	.38	-190.80
RS54	38.	9.43	113.	4.85	5268.	-12.36	-191.79	.75	-191.04
RS55	38.	8.91	113.	5.08	5370.	-7.30	-190.21	.85	-189.36
RS56	38.	8.53	113.	4.99	5453.	-3.68	-189.41	.85	-188.56
RS57	38.	10.69	113.	4.18	5125.	-15.15	-189.71	.35	-189.36
RS58	38.	10.68	113.	3.29	5138.	-15.45	-190.45	.42	-190.03
RS59	38.	9.43	113.	3.50	5332.	-8.48	-190.09	.62	-189.47
RS60	38.	11.54	113.	3.94	5076.	-15.76	-188.65	.27	-188.38

STATION NUMBER	LATITUDE DEG MIN		LONGITUDE DEG MIN		ELEVATION IN FEET	FREE-AIR ANOMALY	SIMPLE BOUGUER	TERRAIN CORRECTION	TERR-CORR BOUGUER
RS61	38.	11.54	113.	5.05	5057.	-19.20	-191.44	.27	-191.17
RS62	38.	12.40	113.	5.03	5051.	-20.78	-192.82	.20	-192.62
RS63	38.	12.40	113.	3.94	5064.	-16.85	-189.33	.20	-189.13
RS64	38.	13.70	113.	23.13	5621.	-11.73	-203.19	.58	-202.61
RS65	38.	13.65	113.	23.38	5636.	-8.10	-200.06	.65	-199.41
RS66	38.	13.25	113.	24.00	5751.	-7.04	-202.92	.94	-201.98
RS67	38.	12.78	113.	24.33	5846.	-3.46	-202.58	1.05	-201.53
RS68	38.	12.08	113.	24.99	5999.	4.83	-199.50	1.27	-198.23
RS69	38.	11.73	113.	25.85	6159.	10.18	-199.59	1.30	-198.29
RS70	38.	11.53	113.	26.84	5986.	5.22	-198.66	2.37	-196.29
RS71	38.	11.23	113.	27.61	5940.	2.49	-199.83	1.25	-198.58
RS72	38.	14.30	113.	23.29	5650.	-8.68	-201.12	.56	-200.56
RS73	38.	23.25	113.	2.64	5042.	-19.96	-191.69	.25	-191.44
RS74	38.	23.30	113.	3.96	5083.	-12.14	-185.26	.65	-184.61
RS75	38.	23.44	113.	5.10	5171.	-5.41	-181.54	.85	-180.69
RS76	38.	23.53	113.	5.71	5352.	1.28	-181.01	1.02	-179.99
RS77	38.	21.29	113.	4.83	5109.	-9.58	-183.59	.70	-182.89
RS78	38.	20.51	113.	5.38	5074.	-9.66	-182.48	.72	-181.76
RS79	38.	19.66	113.	6.26	5130.	-7.83	-182.56	.76	-181.80
RS80	38.	20.03	113.	7.48	5426.	1.63	-183.18	1.10	-182.08
RS81	38.	18.43	113.	7.50	5156.	-9.30	-184.91	.55	-184.36
RS82	38.	19.45	113.	6.14	5086.	-9.25	-182.48	.60	-181.88
RS83	38.	19.60	113.	5.73	5042.	-11.00	-182.73	.55	-182.18
RS84	38.	19.93	113.	5.48	5030.	-12.10	-183.43	.55	-182.88
RS85	38.	20.78	113.	4.76	5013.	-12.95	-183.69	.55	-183.14
RS86	38.	21.68	113.	4.19	5016.	-15.23	-186.08	.55	-185.53
RS87	38.	22.10	113.	3.89	5023.	-14.75	-185.83	.50	-185.33
RS88	38.	22.10	113.	1.65	4968.	-26.26	-195.47	.25	-195.22
RS89	38.	21.65	113.	2.15	4970.	-23.44	-192.72	.26	-192.46
RS90	38.	21.63	113.	2.67	4973.	-21.52	-190.90	.27	-190.63

STATION NUMBER	LATITUDE DEG	MIN	LONGITUDE DEG	MIN	ELEVATION IN FEET	FREE-AIR ANOMALY	SIMPLE BOUGUER	TERRAIN CORRECTION	TERR-CORR BOUGUER
RS91	38.	21.83	113.	3.04	4978.	-20.18	-189.73	.28	-189.45
RS92	38.	20.11	113.	3.41	4985.	-18.56	-188.35	.27	-188.08
RS93	38.	19.20	113.	4.16	4991.	-17.80	-187.80	.27	-187.53
RS94	38.	17.86	113.	5.28	5004.	-17.50	-187.93	.25	-187.68
RS95	38.	18.29	113.	6.63	5059.	-14.24	-186.55	.45	-186.10
RS96	38.	18.38	113.	6.91	5083.	-15.53	-188.65	.50	-188.15
RS97	38.	22.48	113.	5.24	5232.	-4.11	-182.31	.90	-181.41
RS98	38.	21.20	113.	7.23	5829.	14.11	-184.42	1.40	-183.02
RS99	38.	22.08	113.	6.13	5415.	2.13	-182.30	1.05	-181.25
RS100	38.	21.59	113.	5.90	5534.	6.44	-182.05	1.03	-181.02
RS101	38.	22.01	113.	7.16	6088.	22.35	-185.01	3.48	-181.53
RS102	38.	20.34	113.	6.13	5240.	-3.59	-182.07	.85	-181.22
RS103	38.	19.45	113.	7.24	5282.	-3.57	-183.47	.85	-182.62
RS104	38.	17.68	113.	8.33	5160.	-10.35	-186.10	.48	-185.62
RS105	38.	16.93	113.	9.03	5203.	-8.57	-185.79	.40	-185.39
RS106	38.	15.93	113.	10.05	5276.	-9.49	-189.19	.28	-188.91
RS107	38.	15.93	113.	9.43	5202.	-11.45	-188.63	.25	-188.38
RS108	38.	15.93	113.	8.33	5096.	-16.80	-190.37	.20	-190.17
RS109	38.	15.93	113.	7.75	5052.	-17.67	-189.74	.18	-189.56
RS110	38.	20.52	113.	3.28	4976.	-18.93	-188.41	.27	-188.14
RS111	38.	15.93	113.	6.90	5014.	-17.95	-188.72	.15	-188.57
RS112	38.	16.80	113.	7.24	5023.	-14.61	-185.70	.30	-185.40
RS113	38.	15.93	113.	10.96	5338.	-12.61	-194.42	.27	-194.15
RS114	38.	15.93	113.	11.35	5351.	-14.12	-196.38	.30	-196.08
RS115	38.	15.93	113.	11.65	5380.	-13.72	-196.96	.30	-196.66
RS116	38.	15.53	113.	13.53	5568.	-4.01	-193.65	.30	-193.35
RS117	38.	15.45	113.	14.16	5534.	-4.43	-192.91	.26	-192.65
RS118	38.	15.33	113.	14.69	5504.	-6.46	-193.92	.30	-193.62
RS119	38.	16.19	113.	11.64	5400.	-12.35	-196.27	.32	-195.95
RS120	38.	16.85	113.	11.43	5483.	-4.22	-190.97	.36	-190.61

STATION NUMBER	LATITUDE DEG MIN	LONGITUDE DEG MIN	ELEVATION IN FEET	FREE-AIR ANOMALY	SIMPLE BOUGUER	TERRAIN CORRECTION	TERR-CORR BOUGUER
RS121	38. 17.83	113. 11.63	5582.	-.39	-190.52	.45	-190.07
RS122	38. 18.21	113. 11.88	5641.	1.06	-191.07	.47	-190.60
RS123	38. 20.05	113. 11.95	5985.	12.56	-191.29	.40	-190.89
RS124	38. 19.74	113. 12.08	5913.	9.53	-191.87	.45	-191.42
RS125	38. 19.25	113. 8.15	5504.	2.56	-184.91	3.06	-181.85
RS126	38. 20.25	113. 7.93	5774.	10.20	-186.47	4.02	-182.45
RS127	38. 22.03	113. 4.51	5088.	-10.78	-184.08	.70	-183.38
RS128	38. 19.13	113. 6.83	5165.	-7.77	-183.69	.70	-182.99
RS129	38. 16.81	113. 8.33	5123.	-12.86	-187.35	.40	-186.95
RS130	38. 16.80	113. 7.74	5072.	-14.44	-187.20	.35	-186.85
RS131	38. 17.68	113. 6.84	5028.	-14.35	-185.60	.40	-185.20
RS132	38. 18.08	113. 5.95	5000.	-15.32	-185.62	.35	-185.27
RS133	38. 16.88	113. 6.10	5005.	-18.16	-188.63	.25	-188.38
RS134	38. 20.86	113. 2.78	4971.	-20.81	-190.12	.27	-189.85
RS135	38. 18.55	113. 4.71	4995.	-17.55	-187.68	.25	-187.43
RS136	38. 21.21	113. 3.89	4995.	-16.87	-187.00	.40	-186.60
RS137	38. 19.45	113. 5.28	5002.	-14.26	-184.63	.40	-184.23
RS138	38. 15.79	113. 12.35	5445.	-11.01	-196.46	.33	-196.13
RS139	38. 16.33	113. 14.94	5696.	3.20	-190.80	.34	-190.46
RS140	38. 16.80	113. 13.85	5763.	7.00	-189.29	.43	-188.86
RS141	38. 17.33	113. 12.59	5666.	1.15	-191.83	.46	-191.37
RS142	38. 17.34	113. 12.03	5590.	-2.10	-192.50	.45	-192.05
RS143	38. 17.19	113. 11.26	5478.	-4.72	-191.30	.40	-190.90
RS144	38. 17.30	113. 10.33	5400.	-1.18	-185.10	.54	-184.56
RS145	38. 18.26	113. 9.54	5455.	1.15	-184.65	.68	-183.97
RS146	38. 18.55	113. 8.33	5263.	-5.49	-184.75	.80	-183.95
RS147	38. 18.53	113. 12.41	5740.	4.96	-190.55	.47	-190.08
RS148	38. 18.90	113. 12.85	5840.	8.44	-190.47	.43	-190.04
RS149	38. 19.50	113. 12.95	6102.	16.52	-191.32	2.47	-188.85
RS150	38. 20.03	113. 13.25	6058.	18.89	-187.45	.35	-187.10

STATION NUMBER	LATITUDE DEG	LATITUDE MIN	LONGITUDE DEG	LONGITUDE MIN	ELEVATION IN FEET	FREE-AIR ANOMALY	SIMPLE BOUGUER	TERRAIN CORRECTION	TERR-CORR BOUGUER
RS151	38.	21.45	113.	13.48	6210.	24.57	-186.95	1.28	-185.67
RS152	38.	20.91	113.	13.65	6186.	23.82	-186.88	.27	-186.61
RS153	38.	20.60	113.	13.90	6185.	24.92	-185.74	.29	-185.45
RS154	38.	18.64	113.	13.18	5845.	8.30	-190.78	.50	-190.28
RS155	38.	18.59	113.	13.78	5955.	15.56	-187.27	.59	-186.68
RS156	38.	18.93	113.	14.73	6275.	33.15	-180.58	.50	-180.08
RS157	38.	18.03	113.	14.33	6033.	18.21	-187.28	.50	-186.78
RS158	38.	18.85	113.	12.05	5750.	2.77	-193.07	.51	-192.56
RS159	38.	19.59	113.	12.18	5880.	9.43	-190.84	.45	-190.39
RS160	38.	19.08	113.	8.64	5505.	3.60	-183.90	1.50	-182.40
RS161	38.	19.65	113.	8.79	5840.	14.12	-184.79	3.31	-181.48
RS162	38.	7.60	113.	16.26	5076.	-26.88	-199.77	.16	-199.61
RS163	38.	7.76	113.	16.75	5065.	-28.72	-201.23	.20	-201.03
RS164	38.	8.70	113.	15.58	5070.	-27.89	-200.57	.18	-200.39
RS165	38.	9.35	113.	16.53	5056.	-28.24	-200.44	.18	-200.26
RS166	38.	8.20	113.	19.56	5073.	-35.94	-208.72	.25	-208.47
RS167	38.	7.74	113.	19.03	5070.	-36.55	-209.23	.25	-208.98
RS168	38.	10.66	113.	21.25	5162.	-27.19	-203.01	1.33	-201.68
RS170	38.	12.09	113.	17.25	5202.	-23.00	-200.18	.18	-200.00
RS171	38.	12.71	113.	17.34	5257.	-21.29	-200.35	.17	-200.18
RS172	38.	13.88	113.	17.52	5368.	-14.28	-197.12	.20	-196.92
RS173	38.	14.59	113.	18.63	5426.	-11.90	-196.71	.25	-196.46
RS174	38.	14.46	113.	17.00	5430.	-13.01	-197.96	.15	-197.81
RS175	38.	13.80	113.	17.10	5366.	-16.40	-199.17	.15	-199.02
RS176	38.	13.95	113.	20.09	5355.	-16.34	-198.73	.40	-198.33
RS177	38.	12.81	113.	19.98	5277.	-22.95	-202.68	.45	-202.23
RS178	38.	12.13	113.	19.98	5239.	-24.09	-202.54	.50	-202.04
RS179	38.	15.04	113.	10.95	5227.	-17.86	-195.89	.20	-195.69
RS180	38.	15.06	113.	10.54	5214.	-16.47	-194.06	.20	-193.86
RS181	38.	15.06	113.	11.65	5270.	-18.87	-198.37	.25	-198.12

STATION NUMBER	LATITUDE DEG	MIN	LONGITUDE DEG	MIN	ELEVATION IN FEET	FREE-AIR ANOMALY	SIMPLE BOUGUER	TERRAIN CORRECTION	TERR-CORR BOUGUER
RS182	38.	15.06	113.	13.86	5495.	-7.89	-195.05	.24	-194.81
RS183	38.	15.15	113.	12.53	5357.	-14.43	-196.89	.28	-196.61
RS184	38.	15.06	113.	9.44	5151.	-15.75	-191.20	.22	-190.98
RS185	38.	15.06	113.	8.33	5078.	-21.51	-194.47	.18	-194.29
RS186	38.	18.57	113.	9.90	5550.	4.28	-184.76	.79	-183.97
RS187	38.	19.19	113.	10.13	5690.	6.47	-187.33	.84	-186.49
RS188	38.	19.73	113.	10.21	5833.	10.19	-188.48	1.00	-187.48
RS189	38.	20.15	113.	9.86	5595.	-23.69	-214.25	1.97	-212.28
RS190	38.	20.54	113.	9.68	6139.	21.76	-187.33	1.40	-185.93
RS191	38.	20.93	113.	9.85	6210.	22.94	-188.57	1.06	-187.51
RS192	38.	21.34	113.	9.71	6437.	31.76	-187.48	.85	-186.63
RS193	38.	22.05	113.	10.45	6240.	24.08	-188.45	.45	-188.00
RS194	38.	22.05	113.	9.08	6315.	33.29	-181.80	.85	-180.95
RS195	38.	21.79	113.	9.75	6325.	29.79	-185.64	.61	-185.03
RS196	38.	20.89	113.	7.60	5770.	17.65	-178.88	1.56	-177.32
RS197	38.	21.20	113.	8.33	5880.	14.54	-185.73	2.69	-183.04
RS198	38.	20.75	113.	8.63	6260.	26.18	-187.03	2.99	-184.04
RS199	38.	15.90	113.	14.49	5605.	-1.22	-192.12	.30	-191.82
RS200	38.	16.54	113.	14.33	5720.	4.44	-190.39	.38	-190.01
RS201	38.	16.55	113.	12.10	5522.	-7.26	-195.34	.38	-194.96
RS202	38.	17.15	113.	13.07	5730.	3.99	-191.18	.45	-190.73
RS203	38.	22.03	113.	12.26	6043.	12.17	-193.65	.22	-193.43
RS204	38.	21.73	113.	12.26	6069.	12.51	-194.20	.22	-193.98
RS205	38.	21.23	113.	12.24	6118.	14.21	-194.17	.23	-193.94
RS206	38.	20.75	113.	12.10	6120.	20.16	-188.29	.23	-188.06
RS207	38.	17.75	113.	9.96	5425.	-.35	-185.12	.60	-184.52
RS208	38.	17.85	113.	12.51	5750.	4.95	-190.89	.45	-190.44
RS209	38.	18.54	113.	10.76	5800.	10.98	-186.57	.91	-185.66
RS210	38.	18.68	113.	10.28	5685.	-7.27	-200.90	.85	-200.05
RS211	38.	15.48	113.	17.76	5600.	-3.58	-194.31	.25	-194.06

STATION NUMBER	LATITUDE DEG	MIN	LONGITUDE DEG	MIN	ELEVATION IN FEET	FREE-AIR ANOMALY	SIMPLE BOUGUER	TERRAIN CORRECTION	TERR-CORR BOUGUER
RS212	38.	16.01	113.	17.70	5680.	.51	-192.95	.30	-192.65
RS213	38.	16.53	113.	18.09	5765.	4.83	-191.53	.34	-191.19
RS214	38.	17.53	113.	18.24	6070.	22.87	-183.87	.65	-183.22
RS215	38.	15.06	113.	17.23	5532.	-7.81	-196.23	.21	-196.02
RS216	38.	15.68	113.	16.46	5592.	-4.33	-194.79	.25	-194.54
RS217	38.	16.25	113.	16.49	5675.	.58	-192.71	.24	-192.47
RS218	38.	16.83	113.	16.66	5765.	8.19	-188.16	.35	-187.81
RS219	38.	16.80	113.	17.23	5808.	9.43	-188.40	.35	-188.05
RS220	38.	17.33	113.	16.44	5795.	10.71	-186.67	.45	-186.22
RS221	38.	17.68	113.	16.28	5825.	12.33	-186.07	.58	-185.49
RS222	38.	15.06	113.	16.13	5486.	-10.38	-197.23	.35	-196.88
RS223	38.	15.06	113.	15.02	5458.	-9.00	-194.90	.35	-194.55
RS224	38.	15.58	113.	15.50	5550.	-6.83	-195.87	.50	-195.37
RS225	38.	16.13	113.	15.18	5668.	2.44	-190.61	.40	-190.21
RS226	38.	15.06	113.	19.44	5505.	-8.72	-196.22	.34	-195.88
RS227	38.	15.06	113.	20.53	5499.	-9.80	-197.10	.35	-196.75
RS228	38.	19.45	113.	17.23	6127.	20.92	-187.76	.26	-187.50
RS229	38.	19.02	113.	16.89	6050.	19.10	-186.96	.30	-186.66
RS230	38.	18.58	113.	16.64	5980.	17.48	-186.20	.35	-185.85
RS231	38.	18.25	113.	17.01	6105.	22.56	-185.38	.42	-184.96
RS232	38.	18.19	113.	16.25	5910.	17.80	-183.49	.45	-183.04
RS233	38.	16.80	113.	15.02	5812.	9.66	-188.30	.38	-187.92
RS234	38.	17.63	113.	15.18	5912.	17.11	-184.25	.45	-183.80
RS235	38.	17.08	113.	16.23	5800.	12.58	-184.97	.50	-184.47
RS236	38.	16.68	113.	16.00	5718.	5.34	-189.42	.45	-188.97
RS237	38.	15.06	113.	18.33	5525.	-7.12	-195.30	.30	-195.00
RS238	38.	15.75	113.	18.64	5912.	4.55	-196.81	.35	-196.46
RS239	38.	14.81	113.	23.40	5672.	-7.80	-200.99	.54	-200.45
RS240	38.	14.75	113.	24.20	5790.	-3.71	-200.91	.75	-200.16
RS241	38.	14.70	113.	24.80	5888.	-2.00	-202.54	.75	-201.79

STATION NUMBER	LATITUDE DEG	MIN	LONGITUDE DEG	MIN	ELEVATION IN FEET	FREE-AIR ANOMALY	SIMPLE BOUGUER	TERRAIN CORRECTION	TERR-CORR BOUGUER
RS242	38.	14.34	113.	24.31	5814.	-5.50	-203.53	.70	-202.83
RS243	38.	13.93	113.	24.57	5874.	-3.03	-203.10	.85	-202.25
RS244	38.	11.63	113.	24.73	6120.	9.66	-198.79	1.50	-197.29
RS245	38.	11.25	113.	24.73	6260.	16.29	-196.92	1.50	-195.42
RS246	38.	10.66	113.	26.88	5850.	-1.05	-200.30	1.50	-198.80
RS247	38.	9.94	113.	26.46	5758.	-7.00	-203.12	1.21	-201.91
RS248	38.	9.43	113.	26.13	5713.	-10.87	-205.45	1.20	-204.25
RS249	38.	8.90	113.	25.85	5635.	-13.87	-205.80	1.20	-204.60
RS250	38.	8.31	113.	25.68	5590.	-12.02	-202.41	1.00	-201.41
RS251	38.	7.55	113.	25.70	5515.	-10.02	-197.87	.75	-197.12
RS252	38.	8.03	113.	25.23	5618.	-9.63	-200.97	.70	-200.27
RS253	38.	8.48	113.	25.08	5690.	-10.20	-204.01	.51	-203.50
RS254	38.	8.93	113.	24.97	5775.	-7.41	-204.10	.75	-203.35
RS255	38.	6.98	113.	25.36	5458.	-9.42	-195.32	.65	-194.67
RS256	38.	7.35	113.	25.71	5499.	-8.51	-195.81	.75	-195.06
RS257	38.	21.23	113.	1.65	4976.	-24.02	-193.50	.26	-193.24
RS258	38.	20.33	113.	1.65	4989.	-23.59	-193.51	.20	-193.31
RS259	38.	20.33	113.	2.78	4982.	-20.36	-190.05	.26	-189.79
RS260	38.	19.23	113.	2.78	4998.	-21.27	-191.50	.20	-191.30
RS261	38.	17.69	113.	2.78	5019.	-23.66	-194.61	.14	-194.47
RS262	38.	17.46	113.	3.90	4998.	-21.93	-192.16	.18	-191.98
RS263	38.	15.93	113.	3.90	5037.	-25.93	-197.49	.14	-197.35
RS264	38.	15.05	113.	3.90	5045.	-25.58	-197.42	.13	-197.29
RS265	38.	15.93	113.	6.13	5015.	-19.84	-190.65	.10	-190.55
RS266	38.	8.36	113.	5.89	5510.	-3.65	-191.32	1.15	-190.17
RS267	38.	7.90	113.	6.05	5610.	-1.73	-192.81	.70	-192.11
RS268	38.	7.79	113.	6.75	5690.	.28	-193.52	.67	-192.85
RS269	38.	8.23	113.	7.49	5538.	-5.10	-193.72	.65	-193.07
RS270	38.	13.30	113.	6.18	5036.	-22.04	-193.57	.08	-193.49
RS271	38.	14.18	113.	5.01	5039.	-24.00	-195.63	.13	-195.50

STATION NUMBER	LATITUDE DEG	MIN	LONGITUDE DEG	MIN	ELEVATION IN FEET	FREE-AIR ANOMALY	SIMPLE BOUGUER	TERRAIN CORRECTION	TERR-CORR BOUGUER
RS272	38.	14.18	113.	2.80	5073.	-19.79	-192.58	.14	-192.44
RS273	38.	12.55	113.	7.25	5029.	-20.21	-191.49	.12	-191.37
75102	38.	10.31	113.	10.15	5056.	-26.65	-198.86	.20	-198.66
75103	38.	10.38	113.	10.37	5046.	-26.88	-198.75	.20	-198.55
75104	38.	10.41	113.	10.59	5046.	-26.18	-198.04	.20	-197.84
75105	38.	10.42	113.	10.80	5043.	-26.05	-197.82	.19	-197.63
75106	38.	10.38	113.	11.03	5044.	-25.48	-197.27	.19	-197.08
75107	38.	10.33	113.	11.25	5036.	-24.88	-196.41	.19	-196.22
75108	38.	10.25	113.	11.44	5033.	-23.97	-195.40	.18	-195.22
75109	38.	10.22	113.	11.55	5030.	-23.86	-195.18	.18	-195.00
75110	38.	10.25	113.	11.65	5030.	-23.98	-195.30	.18	-195.12
75111	38.	10.28	113.	11.74	5030.	-24.42	-195.74	.18	-195.56
75112	38.	10.31	113.	11.83	5031.	-25.05	-196.41	.18	-196.23
75113	38.	10.33	113.	11.93	5031.	-26.04	-197.40	.17	-197.23
75114	38.	10.34	113.	12.03	5032.	-26.44	-197.83	.17	-197.66
75115	38.	10.35	113.	12.11	5035.	-26.87	-198.36	.17	-198.19
75116	38.	10.38	113.	12.16	5037.	-27.35	-198.91	.17	-198.74
75117	38.	10.44	113.	12.22	5045.	-27.68	-199.51	.17	-199.34
75118	38.	10.46	113.	12.31	5039.	-27.31	-198.93	.17	-198.76
75119	38.	10.47	113.	12.41	5038.	-28.44	-200.03	.17	-199.86
75120	38.	10.51	113.	12.50	5037.	-27.74	-199.30	.16	-199.14
75121	38.	10.56	113.	12.58	5035.	-28.20	-199.69	.16	-199.53
75122	38.	10.60	113.	12.67	5034.	-28.63	-200.09	.15	-199.94
75123	38.	10.65	113.	12.76	5033.	-29.33	-200.75	.15	-200.60
75124	38.	10.69	113.	12.85	5033.	-29.78	-201.21	.14	-201.07
75125	38.	10.77	113.	12.93	5040.	-29.89	-201.55	.14	-201.41
75126	38.	10.97	113.	13.05	5052.	-29.82	-201.89	.14	-201.75
75127	38.	11.12	113.	13.13	5052.	-29.72	-201.79	.14	-201.65
75128	38.	11.29	113.	13.21	5063.	-29.29	-201.74	.14	-201.60
75129	38.	11.45	113.	13.29	5073.	-28.72	-201.51	.14	-201.37

STATION NUMBER	LATITUDE DEG	MIN	LONGITUDE DEG	MIN	ELEVATION IN FEET	FREE-AIR ANOMALY	SIMPLE BOUGUER	TERRAIN CORRECTION	TERR-CORR BOUGUER
75130	38.	11.58	113.	13.36	5084.	-28.06	-201.22	.14	-201.08
75131	38.	11.72	113.	13.44	5100.	-26.68	-200.38	.13	-200.25
75132	38.	11.80	113.	13.49	5115.	-25.40	-199.62	.13	-199.49
75133	38.	11.98	113.	13.61	5118.	-25.53	-199.85	.13	-199.72
75134	38.	11.98	113.	13.78	5129.	-24.92	-199.61	.13	-199.48
75135	38.	12.05	113.	13.94	5143.	-23.67	-198.84	.13	-198.71
75136	38.	12.15	113.	14.10	5160.	-22.23	-197.98	.13	-197.85
75137	38.	12.22	113.	14.28	5170.	-21.40	-197.49	.13	-197.36
75138	38.	12.32	113.	14.45	5180.	-20.91	-197.34	.12	-197.22
75139	38.	12.40	113.	14.60	5190.	-20.52	-197.29	.12	-197.17
75140	38.	12.48	113.	14.42	5192.	-20.72	-197.56	.12	-197.44
75141	38.	12.58	113.	14.28	5196.	-20.37	-197.34	.13	-197.21
75142	38.	12.70	113.	14.10	5198.	-19.79	-196.83	.13	-196.70
75143	38.	12.85	113.	13.92	5192.	-19.40	-196.24	.14	-196.10
75144	38.	12.95	113.	13.80	5188.	-19.31	-196.01	.14	-195.87
75145	38.	13.08	113.	13.65	5196.	-19.06	-196.04	.15	-195.89
75146	38.	13.18	113.	13.50	5210.	-18.61	-196.06	.15	-195.91
75147	38.	13.28	113.	13.40	5212.	-19.10	-196.62	.16	-196.46
75148	38.	9.05	113.	12.28	5039.	-24.63	-196.25	.15	-196.10
75149	38.	9.72	113.	12.72	5041.	-27.59	-199.29	.14	-199.15
75150	38.	10.12	113.	12.80	5030.	-29.05	-200.37	.14	-200.23
75151	38.	9.80	113.	14.15	5035.	-28.33	-199.82	.16	-199.66
75152	38.	9.40	113.	14.70	5045.	-28.73	-200.56	.18	-200.38
75153	38.	9.12	113.	14.42	5052.	-28.16	-200.23	.18	-200.05
75154	38.	8.85	113.	14.02	5050.	-25.88	-197.88	.18	-197.70
75155	38.	12.50	113.	9.88	5046.	-29.58	-201.44	.20	-201.24
75156	38.	10.95	113.	9.50	5058.	-23.90	-196.18	.20	-195.98
75157	38.	11.40	113.	8.85	5037.	-23.88	-195.44	.20	-195.24
75158	38.	11.68	113.	8.43	5030.	-24.21	-195.54	.20	-195.34
75160	38.	10.65	113.	9.48	5070.	-24.51	-197.19	.25	-196.94

STATION NUMBER	LATITUDE DEG	LATITUDE MIN	LONGITUDE DEG	LONGITUDE MIN	ELEVATION IN FEET	FREE-AIR ANOMALY	SIMPLE BOUGUER	TERRAIN CORRECTION	TERR-CORR BOUGUER
75161	38.	10.25	113.	9.93	5072.	-25.96	-198.71	.20	-198.51
75162	38.	10.20	113.	9.70	5108.	-23.50	-197.48	.25	-197.23
75163	38.	10.20	113.	9.48	5110.	-22.82	-196.87	.30	-196.57
75164	38.	10.15	113.	9.28	5120.	-21.65	-196.03	.30	-195.73
75165	38.	10.13	113.	9.05	5130.	-20.96	-195.68	.25	-195.43
75166	38.	10.10	113.	8.88	5137.	-20.78	-195.75	.20	-195.55
75167	38.	10.08	113.	8.65	5135.	-20.80	-195.70	.25	-195.45
75168	38.	10.05	113.	8.43	5135.	-20.45	-195.35	.25	-195.10
75169	38.	10.00	113.	8.20	5127.	-20.73	-195.36	.25	-195.11
75170	38.	9.98	113.	7.93	5117.	-21.01	-195.29	.30	-194.99
75171	38.	9.93	113.	7.68	5114.	-20.80	-194.98	.30	-194.68
75173	38.	13.34	113.	5.18	5040.	-23.55	-195.21	.13	-195.08
75174	38.	13.28	113.	7.33	5024.	-21.61	-192.73	.12	-192.61
75178	38.	13.26	113.	9.50	5029.	-23.20	-194.49	.17	-194.32
75179	38.	13.26	113.	9.85	5047.	-21.94	-193.84	.17	-193.67
75180	38.	13.27	113.	8.43	5019.	-24.23	-195.18	.17	-195.01
75181	38.	13.53	113.	9.49	5047.	-22.47	-194.38	.17	-194.21
75182	38.	14.19	113.	8.66	5040.	-24.03	-195.69	.17	-195.52
75183	38.	11.48	113.	9.50	5021.	-22.18	-193.19	.20	-192.99
75184	38.	11.53	113.	9.50	5028.	-24.96	-196.21	.20	-196.01
75186	38.	12.85	113.	6.15	5040.	-21.80	-193.46	.10	-193.36
75187	38.	12.41	113.	6.13	5041.	-21.67	-193.37	.16	-193.21
75188	38.	11.54	113.	6.15	5045.	-19.76	-191.59	.25	-191.34
75189	38.	11.13	113.	6.18	5049.	-20.82	-192.79	.30	-192.49
75190	38.	10.88	113.	6.08	5058.	-20.82	-193.10	.35	-192.75
75191	38.	10.66	113.	6.18	5064.	-20.61	-193.09	.35	-192.74
75192	38.	9.79	113.	6.70	5120.	-19.33	-193.71	.40	-193.31
75193	38.	10.28	113.	4.78	5144.	-16.71	-191.91	.42	-191.49
75194	38.	9.53	113.	14.56	5048.	-28.18	-200.11	.17	-199.94
75195	38.	9.65	113.	14.41	5049.	-27.95	-199.92	.17	-199.75

STATION NUMBER	LATITUDE DEG	LATITUDE MIN	LONGITUDE DEG	LONGITUDE MIN	ELEVATION IN FEET	FREE-AIR ANOMALY	SIMPLE BOUGUER	TERRAIN CORRECTION	TERR-CORR BOUGUER
75196	38.	9.77	113.	14.27	5040.	-28.61	-200.27	.16	-200.11
75197	38.	9.88	113.	14.12	5040.	-28.19	-199.85	.16	-199.69
75198	38.	10.00	113.	13.98	5040.	-28.14	-199.80	.16	-199.64
75199	38.	10.13	113.	13.83	5040.	-28.45	-200.12	.15	-199.97
51100	38.	10.24	113.	13.67	5040.	-29.00	-200.66	.15	-200.51
51101	38.	10.36	113.	13.52	5040.	-29.57	-201.23	.14	-201.09
51102	38.	10.48	113.	13.37	5040.	-29.91	-201.57	.14	-201.43
51103	38.	10.60	113.	13.22	5040.	-30.13	-201.79	.14	-201.65
51104	38.	10.73	113.	13.08	5040.	-30.38	-202.05	.14	-201.91
51106	38.	10.96	113.	12.77	5040.	-30.55	-202.21	.14	-202.07
51107	38.	11.08	113.	12.62	5040.	-30.34	-202.00	.14	-201.86
51108	38.	11.20	113.	12.48	5040.	-30.09	-201.75	.14	-201.61
51109	38.	11.32	113.	12.33	5040.	-29.14	-200.80	.14	-200.66
51111	38.	11.55	113.	12.02	5040.	-28.45	-200.12	.14	-199.98
51112	38.	11.67	113.	11.87	5040.	-27.67	-199.33	.14	-199.19
51113	38.	11.82	113.	11.73	5040.	-26.14	-197.80	.14	-197.66
51114	38.	11.92	113.	11.58	5040.	-24.83	-196.49	.14	-196.35
51115	38.	12.04	113.	11.43	5036.	-24.49	-196.02	.15	-195.87
51116	38.	12.16	113.	11.28	5036.	-24.14	-195.67	.15	-195.52
51117	38.	12.27	113.	11.13	5036.	-23.70	-195.22	.15	-195.07
51118	38.	12.40	113.	10.99	5032.	-23.67	-195.06	.15	-194.91
75203	38.	9.79	113.	15.59	5048.	-28.79	-200.72	.18	-200.54
75204	38.	9.79	113.	16.13	5049.	-29.09	-201.06	.18	-200.88
75205	38.	9.79	113.	16.59	5051.	-29.22	-201.26	.19	-201.07
75206	38.	9.79	113.	17.32	5060.	-31.74	-204.08	.20	-203.88
75207	38.	9.79	113.	17.86	5076.	-30.76	-203.65	.22	-203.43
75208	38.	9.79	113.	18.32	5089.	-29.45	-202.78	.25	-202.53
75209	38.	9.78	113.	18.76	5092.	-30.39	-203.82	.25	-203.57
75210	38.	9.79	113.	19.19	5090.	-31.36	-204.73	.28	-204.45
75211	38.	9.79	113.	19.57	5096.	-31.06	-204.63	.30	-204.33

STATION	LATITUDE		LONGITUDE		ELEVATION	FREE-AIR	SIMPLE	TERRAIN	TERR-CORR
NUMBER	DEG	MIN	DEG	MIN	IN FEET	ANOMALY	BOUGUER	CORRECTION	BOUGUER
75212	38.	9.79	113.	20.13	5100.	-30.65	-204.36	.50	-203.86
75213	38.	9.79	113.	20.52	5104.	-30.14	-203.99	.70	-203.29
75214	38.	9.79	113.	20.91	5101.	-29.29	-203.03	.85	-202.18
75215	38.	9.80	113.	21.20	5103.	-27.88	-201.69	1.05	-200.64
75216	38.	10.24	113.	18.32	5103.	-28.43	-202.23	.25	-201.98
75217	38.	10.70	113.	18.32	5123.	-26.89	-201.38	.25	-201.13
75218	38.	11.52	113.	18.31	5165.	-23.41	-199.33	.25	-199.08
75219	38.	11.52	113.	18.87	5176.	-23.89	-200.18	.30	-199.88
75220	38.	11.52	113.	19.70	5192.	-25.34	-202.18	.50	-201.68
75221	38.	11.57	113.	20.58	5222.	-27.45	-205.31	.70	-204.61
75222	38.	11.52	113.	20.95	5230.	-26.89	-205.03	.90	-204.13
75223	38.	11.52	113.	21.32	5252.	-25.94	-204.83	1.10	-203.73
75224	38.	11.52	113.	21.38	5355.	-21.66	-204.05	1.35	-202.70
75226	38.	11.53	113.	17.66	5152.	-24.14	-199.61	.20	-199.41
75227	38.	11.60	113.	17.24	5163.	-24.33	-200.18	.19	-199.99
75228	38.	11.73	113.	16.79	5168.	-27.79	-203.81	.18	-203.63
75229	38.	11.84	113.	16.46	5168.	-27.95	-203.97	.17	-203.80
75230	38.	12.00	113.	15.91	5174.	-24.19	-200.41	.16	-200.25
75231	38.	12.15	113.	15.45	5174.	-24.10	-200.33	.15	-200.18
75232	38.	12.31	113.	14.91	5193.	-20.69	-197.56	.12	-197.44
75240	38.	13.76	113.	22.80	5584.	-15.38	-205.57	.56	-205.01
75241	38.	13.88	113.	22.24	5507.	-20.02	-207.59	.50	-207.09
75242	38.	13.93	113.	21.90	5469.	-20.79	-207.06	.45	-206.61
75243	38.	14.11	113.	21.15	5400.	-25.89	-209.81	.40	-209.41
75244	38.	14.19	113.	20.07	5383.	-15.16	-198.50	.32	-198.18
75246	38.	13.57	113.	18.22	5330.	-16.32	-197.86	.20	-197.66
75247	38.	13.27	113.	17.22	5308.	-19.06	-199.85	.15	-199.70
75248	38.	12.79	113.	15.85	5251.	-20.28	-199.13	.13	-199.00
75249	38.	8.92	113.	20.53	5079.	-32.93	-205.92	.50	-205.42
75250	38.	8.19	113.	20.68	5092.	-33.86	-207.29	.40	-206.89

STATION NUMBER	LATITUDE DEG	LATITUDE MIN	LONGITUDE DEG	LONGITUDE MIN	ELEVATION IN FEET	FREE-AIR ANOMALY	SIMPLE BOUGUER	TERRAIN CORRECTION	TERR-CORR BOUGUER
75251	38.	7.74	113.	20.68	5101.	-33.68	-207.42	.40	-207.02
75252	38.	7.01	113.	20.64	5106.	-34.04	-207.95	.35	-207.60
75253	38.	6.85	113.	21.70	5168.	-28.35	-204.37	.40	-203.97
75254	38.	6.84	113.	22.80	5287.	-19.67	-199.75	.50	-199.25
75255	38.	6.51	113.	23.58	5330.	-12.35	-193.89	.50	-193.39
75256	38.	6.16	113.	24.30	5358.	-10.91	-193.40	.50	-192.90
75258	38.	9.41	113.	12.35	5048.	-25.14	-197.07	.16	-196.91
75259	38.	8.93	113.	12.39	5060.	-23.92	-196.26	.20	-196.06
75260	38.	7.72	113.	12.84	5082.	-24.99	-198.09	.21	-197.88
75261	38.	8.72	113.	11.85	5148.	-24.46	-199.80	.30	-199.50
75262	38.	8.44	113.	10.38	5220.	-15.82	-193.61	.30	-193.31
75263	38.	8.42	113.	9.55	5247.	-13.88	-192.59	.30	-192.29
75264	38.	9.28	113.	8.54	5240.	-15.06	-193.54	.40	-193.14
75267	38.	8.18	113.	16.23	5064.	-23.26	-195.74	.18	-195.56
75268	38.	8.19	113.	15.69	5072.	-26.33	-199.09	.18	-198.91
75269	38.	8.20	113.	15.22	5061.	-25.99	-198.37	.18	-198.19
2-1E	38.	9.79	113.	10.59	5124.	-20.02	-194.54	.20	-194.34
2-.9E	38.	9.79	113.	10.70	5106.	-20.59	-194.49	.20	-194.29
2-.8E	38.	9.79	113.	10.81	5099.	-21.03	-194.69	.20	-194.49
2-.7E	38.	9.79	113.	10.92	5091.	-21.02	-194.42	.19	-194.23
2-.6E	38.	9.79	113.	11.03	5085.	-21.27	-194.48	.19	-194.29
2-.5E	38.	9.79	113.	11.14	5078.	-21.52	-194.48	.19	-194.29
2-.4E	38.	9.79	113.	11.26	5075.	-21.69	-194.54	.18	-194.36
2-.3E	38.	9.79	113.	11.37	5072.	-21.92	-194.68	.18	-194.50
2-.2E	38.	9.79	113.	11.48	5069.	-22.13	-194.79	.18	-194.61
2-.1E	38.	9.79	113.	11.59	5062.	-22.58	-194.99	.17	-194.82
2-0E	38.	9.79	113.	11.70	5060.	-22.86	-195.21	.17	-195.04
2-.1W	38.	9.79	113.	11.81	5058.	-23.22	-195.51	.17	-195.34
2-.2W	38.	9.79	113.	11.92	5052.	-24.23	-196.30	.16	-196.14
2-.3W	38.	9.79	113.	12.03	5051.	-24.85	-196.89	.16	-196.73

STATION NUMBER	LATITUDE DEG	LATITUDE MIN	LONGITUDE DEG	LONGITUDE MIN	ELEVATION IN FEET	FREE-AIR ANOMALY	SIMPLE BOUGUER	TERRAIN CORRECTION	TERR-CORR BOUGUER
2-.4W	38.	9.79	113.	12.15	5047.	-25.32	-197.21	.16	-197.05
2-.5W	38.	9.79	113.	12.26	5042.	-25.67	-197.40	.15	-197.25
2-.6W	38.	9.79	113.	12.37	5040.	-25.94	-197.59	.15	-197.44
2-.7W	38.	9.79	113.	12.48	5042.	-26.10	-197.83	.15	-197.68
2-.8W	38.	9.79	113.	12.59	5044.	-26.50	-198.28	.14	-198.14
2-.9W	38.	9.79	113.	12.70	5045.	-26.97	-198.81	.14	-198.67
2-1W	38.	9.79	113.	12.81	5040.	-27.53	-199.18	.14	-199.04
6-0	38.	11.32	113.	11.60	5040.	-24.62	-196.29	.14	-196.15
6-1CW	38.	11.32	113.	11.62	5042.	-24.53	-196.26	.14	-196.12
6-2CW	38.	11.32	113.	11.64	5044.	-24.43	-196.22	.14	-196.08
6-3CW	38.	11.32	113.	11.66	5047.	-24.35	-196.26	.14	-196.12
6-4CW	38.	11.32	113.	11.68	5050.	-24.28	-196.29	.14	-196.15
6-5CW	38.	11.32	113.	11.70	5053.	-24.15	-196.26	.14	-196.12
6-6CW	38.	11.32	113.	11.72	5065.	-23.93	-196.45	.14	-196.31
6-7CW	38.	11.32	113.	11.74	5070.	-23.82	-196.51	.14	-196.37
6-8CW	38.	11.32	113.	11.76	5070.	-23.89	-196.56	.14	-196.42
6-9CW	38.	11.32	113.	11.78	5072.	-23.93	-196.67	.14	-196.53
610CW	38.	11.32	113.	11.80	5070.	-24.11	-196.79	.14	-196.65
611CW	38.	11.32	113.	11.82	5066.	-24.34	-196.88	.14	-196.74
612CW	38.	11.32	113.	11.84	5057.	-24.69	-196.94	.14	-196.80
613CW	38.	11.32	113.	11.86	5053.	-25.03	-197.12	.14	-196.98
614CW	38.	11.32	113.	11.88	5050.	-25.25	-197.25	.14	-197.11
615CW	38.	11.32	113.	11.90	5049.	-25.45	-197.42	.14	-197.28
616CW	38.	11.32	113.	11.92	5046.	-25.69	-197.57	.14	-197.43
617CW	38.	11.32	113.	11.94	5044.	-25.94	-197.75	.14	-197.61
618CW	38.	11.32	113.	11.96	5041.	-26.19	-197.89	.14	-197.75
619CW	38.	11.32	113.	11.98	5041.	-26.36	-198.07	.14	-197.93
6-2KW	38.	11.32	113.	12.00	5041.	-26.56	-198.27	.14	-198.13
4-0	38.	11.09	113.	12.60	5040.	-29.12	-200.79	.14	-200.65
4-.1E	38.	11.09	113.	12.49	5039.	-28.85	-200.47	.14	-200.33

STATION NUMBER	LATITUDE DEG MIN	LONGITUDE DEG MIN	ELEVATION IN FEET	FREE-AIR ANOMALY	SIMPLE BOUGUER	TERRAIN CORRECTION	TERR-CORR BOUGUER
4-.2E	38. 11.09	113. 12.38	5038.	-28.38	-199.98	.14	-199.84
4-.3E	38. 11.09	113. 12.27	5038.	-27.80	-199.39	.14	-199.25
4-.4E	38. 11.09	113. 12.16	5038.	-27.16	-198.75	.14	-198.61
4-.5E	38. 11.09	113. 12.04	5045.	-26.12	-197.96	.14	-197.82
4-.6E	38. 11.09	113. 11.93	5059.	-24.83	-197.13	.14	-196.99
4-.7E	38. 11.09	113. 11.82	5053.	-24.81	-196.92	.14	-196.78
4-.8E	38. 11.09	113. 11.71	5035.	-25.62	-197.12	.14	-196.98
4-.9E	38. 11.09	113. 11.60	5029.	-26.34	-197.64	.14	-197.50
4-1E	38. 11.09	113. 11.49	5027.	-26.53	-197.76	.14	-197.62
41.1E	38. 11.09	113. 11.38	5027.	-26.76	-197.99	.14	-197.85
41.2E	38. 11.09	113. 11.27	5027.	-26.87	-198.09	.14	-197.95
41.3E	38. 11.09	113. 11.15	5026.	-26.80	-197.99	.14	-197.85
41.4E	38. 11.09	113. 11.04	5026.	-26.66	-197.83	.14	-197.69
41.5E	38. 11.09	113. 10.93	5027.	-26.54	-197.75	.14	-197.61
41.6E	38. 11.09	113. 10.82	5026.	-26.58	-197.78	.14	-197.64
41.7E	38. 11.09	113. 10.71	5026.	-26.74	-197.94	.14	-197.80
41.8E	38. 11.09	113. 10.60	5027.	-26.90	-198.12	.14	-197.98
3-.3W	38. 11.53	113. 11.93	5042.	-26.81	-198.53	.14	-198.39
3-.2W	38. 11.53	113. 11.82	5040.	-26.34	-197.99	.14	-197.85
3-.1W	38. 11.53	113. 11.71	5037.	-25.80	-197.37	.14	-197.23
3-0	38. 11.53	113. 11.60	5036.	-25.27	-196.78	.14	-196.64
3-.1E	38. 11.53	113. 11.49	5034.	-25.01	-196.48	.13	-196.35
3-.2E	38. 11.53	113. 11.38	5033.	-25.07	-196.48	.13	-196.35
3-.3E	38. 11.53	113. 11.27	5032.	-25.18	-196.58	.13	-196.45
3-.4E	38. 11.53	113. 11.16	5027.	-25.34	-196.56	.13	-196.43
3-.5E	38. 11.53	113. 11.04	5027.	-25.36	-196.58	.13	-196.45
3-.6E	38. 11.53	113. 10.93	5027.	-25.49	-196.73	.13	-196.60
3-.7E	38. 11.53	113. 10.82	5026.	-25.56	-196.74	.13	-196.61
3-.8E	38. 11.53	113. 10.71	5025.	-25.54	-196.70	.13	-196.57
3-.9E	38. 11.53	113. 10.60	5025.	-25.43	-196.58	.13	-196.45

STATION NUMBER	LATITUDE DEG MIN	LONGITUDE DEG MIN	ELEVATION IN FEET	FREE-AIR ANOMALY	SIMPLE BOUGUER	TERRAIN CORRECTION	TERR-CORR BOUGUER
3-1E	38. 11.53	113. 10.49	5024.	-24.99	-196.11	.13	-195.98
3-.4W	38. 11.53	113. 12.04	5044.	-27.48	-199.26	.14	-199.12
3-.5W	38. 11.53	113. 12.16	5047.	-27.99	-199.88	.14	-199.74
3-.6W	38. 11.53	113. 12.27	5049.	-28.55	-200.52	.14	-200.38
3-.7W	38. 11.53	113. 12.38	5051.	-28.93	-200.98	.14	-200.84
3-.8W	38. 11.53	113. 12.49	5057.	-29.20	-201.43	.14	-201.29
3-.9W	38. 11.53	113. 12.60	5074.	-29.03	-201.87	.14	-201.73
3-1W	38. 11.53	113. 12.71	5079.	-29.13	-202.13	.14	-201.99
3-.3W	38. 11.53	113. 11.93	5042.	-26.81	-198.53	.15	-198.38
5-6CW	38. 10.89	113. 11.82	5063.	-25.26	-197.71	.15	-197.56
5-5CW	38. 10.89	113. 11.80	5054.	-25.47	-197.61	.15	-197.46
5-4CW	38. 10.89	113. 11.78	5048.	-25.67	-197.61	.15	-197.46
5-3CW	38. 10.89	113. 11.76	5043.	-25.81	-197.58	.15	-197.43
5-2CW	38. 10.89	113. 11.74	5039.	-25.87	-197.50	.15	-197.35
5-1CW	38. 10.89	113. 11.72	5038.	-25.98	-197.59	.15	-197.44
5-0	38. 10.89	113. 11.70	5036.	-26.05	-197.56	.15	-197.41
5-8CW	38. 10.89	113. 11.86	5059.	-25.36	-197.66	.15	-197.51
5-9CW	38. 10.89	113. 11.88	5053.	-25.63	-197.72	.15	-197.57
5-1KW	38. 10.89	113. 11.90	5048.	-25.84	-197.77	.15	-197.62
511CW	38. 10.89	113. 11.92	5046.	-25.90	-197.77	.15	-197.62
512CW	38. 10.89	113. 11.94	5044.	-26.05	-197.85	.15	-197.70
513CW	38. 10.89	113. 11.96	5045.	-26.09	-197.91	.15	-197.76
514CW	38. 10.89	113. 11.98	5044.	-26.24	-198.05	.15	-197.90
515CW	38. 10.89	113. 12.00	5042.	-26.27	-198.01	.15	-197.86
516CW	38. 10.89	113. 12.02	5042.	-26.38	-198.11	.15	-197.96
517CW	38. 10.89	113. 12.04	5042.	-26.45	-198.19	.15	-198.04
518CW	38. 10.89	113. 12.06	5042.	-26.54	-198.26	.15	-198.11
519CW	38. 10.89	113. 12.08	5043.	-26.54	-198.31	.15	-198.16
5-2KW	38. 10.89	113. 12.10	5041.	-26.64	-198.35	.15	-198.20
6-7CW	38. 11.32	113. 11.74	5070.	-23.88	-196.57	.14	-196.43

STATION NUMBER	LATITUDE DEG MIN	LONGITUDE DEG MIN	ELEVATION IN FEET	FREE-AIR ANOMALY	SIMPLE BOUGUER	TERRAIN CORRECTION	TERR-CORR BOUGUER
6-6CW	38. 11.32	113. 11.72	5065.	-23.96	-196.48	.14	-196.34
6-5CW	38. 11.32	113. 11.70	5053.	-24.18	-196.29	.14	-196.15
6-4CW	38. 11.32	113. 11.68	5050.	-24.28	-196.30	.14	-196.16
6-3CW	38. 11.32	113. 11.66	5047.	-24.38	-196.29	.14	-196.15
6-2CW	38. 11.32	113. 11.64	5044.	-24.46	-196.26	.14	-196.12
6-1CW	38. 11.32	113. 11.62	5042.	-24.57	-196.31	.14	-196.17
6-0	38. 11.32	113. 11.60	5040.	-24.69	-196.36	.14	-196.22
6-8CW	38. 11.32	113. 11.76	5070.	-23.96	-196.63	.14	-196.49
6-9CW	38. 11.32	113. 11.78	5072.	-24.05	-196.79	.14	-196.65
6-1KW	38. 11.32	113. 11.80	5070.	-24.15	-196.83	.14	-196.69
611CW	38. 11.32	113. 11.82	5066.	-24.45	-197.00	.14	-196.86
612CW	38. 11.32	113. 11.84	5057.	-24.82	-197.08	.14	-196.94
613CW	38. 11.32	113. 11.86	5053.	-25.07	-197.16	.14	-197.02
614CW	38. 11.32	113. 11.88	5050.	-25.32	-197.33	.14	-197.19
615CW	38. 11.32	113. 11.90	5049.	-25.54	-197.51	.14	-197.37
616CW	38. 11.32	113. 11.92	5046.	-25.82	-197.70	.14	-197.56
617CW	38. 11.32	113. 11.94	5044.	-26.03	-197.84	.14	-197.70
618CW	38. 11.32	113. 11.96	5041.	-26.32	-198.03	.14	-197.89
619CW	38. 11.32	113. 11.98	5041.	-26.54	-198.25	.14	-198.11
6-2KW	38. 11.32	113. 12.00	5041.	-26.65	-198.36	.14	-198.22
4-.3E	38. 11.09	113. 12.27	5038.	-27.39	-198.99	.14	-198.85
4-.4E	38. 11.09	113. 12.16	5038.	-26.88	-198.47	.14	-198.33
4-.5E	38. 11.09	113. 12.04	5045.	-25.87	-197.71	.14	-197.57
4-.6E	38. 11.09	113. 11.93	5059.	-24.65	-196.95	.14	-196.81
4-.7E	38. 11.09	113. 11.82	5053.	-24.67	-196.79	.14	-196.65
4-.8E	38. 11.09	113. 11.71	5035.	-25.52	-197.01	.14	-196.87
4-.9E	38. 11.09	113. 11.60	5029.	-26.32	-197.61	.14	-197.47
4-1E	38. 11.09	113. 11.49	5027.	-26.54	-197.77	.14	-197.63
7-0	38. 10.11	113. 12.25	5035.	-26.07	-197.56	.16	-197.40
7-1CE	38. 10.11	113. 12.23	5035.	-26.02	-197.50	.16	-197.34

STATION NUMBER	LATITUDE DEG MIN		LONGITUDE DEG MIN		ELEVATION IN FEET	FREE-AIR ANOMALY	SIMPLE BOUGUER	TERRAIN CORRECTION	TERR-CORR BOUGUER
7-2CE	38.	10.11	113.	12.21	5035.	-26.02	-197.49	.16	-197.33
7-3CE	38.	10.11	113.	12.19	5034.	-26.01	-197.48	.16	-197.32
7-4CE	38.	10.11	113.	12.17	5034.	-25.99	-197.45	.16	-197.29
7-5CE	38.	10.11	113.	12.15	5034.	-26.01	-197.48	.16	-197.32
7-6CE	38.	10.11	113.	12.13	5034.	-26.06	-197.53	.16	-197.37
7-7CE	38.	10.11	113.	12.11	5034.	-26.05	-197.52	.16	-197.36
7-8CE	38.	10.11	113.	12.09	5034.	-26.06	-197.53	.16	-197.37
7-9CE	38.	10.11	113.	12.07	5034.	-25.99	-197.46	.16	-197.30
7-1KE	38.	10.11	113.	12.05	5036.	-25.91	-197.42	.16	-197.26
711CE	38.	10.11	113.	12.03	5036.	-25.84	-197.38	.16	-197.22
712CE	38.	10.11	113.	12.01	5035.	-25.77	-197.27	.16	-197.11
713CE	38.	10.11	113.	11.99	5035.	-25.70	-197.21	.16	-197.05
714CE	38.	10.11	113.	11.97	5035.	-25.63	-197.14	.16	-196.98
715CE	38.	10.11	113.	11.95	5036.	-25.76	-197.27	.16	-197.11
716CE	38.	10.11	113.	11.93	5035.	-25.43	-196.92	.16	-196.76
717CE	38.	10.11	113.	11.91	5035.	-25.32	-196.81	.16	-196.65
718CE	38.	10.11	113.	11.89	5035.	-25.20	-196.69	.16	-196.53
719CE	38.	10.11	113.	11.87	5035.	-25.07	-196.55	.16	-196.39
7-2KE	38.	10.11	113.	11.85	5035.	-24.86	-196.33	.16	-196.17
7-1CW	38.	10.11	113.	12.27	5035.	-26.08	-197.57	.15	-197.42
7-2CW	38.	10.11	113.	12.29	5035.	-26.10	-197.59	.15	-197.44
7-3CW	38.	10.11	113.	12.31	5035.	-26.21	-197.71	.15	-197.56
7-4CW	38.	10.11	113.	12.33	5035.	-26.24	-197.75	.15	-197.60
7-5CW	38.	10.11	113.	12.35	5036.	-26.21	-197.73	.15	-197.58
7-6CW	38.	10.11	113.	12.37	5035.	-26.32	-197.83	.15	-197.68
7-7CW	38.	10.11	113.	12.39	5035.	-26.43	-197.93	.15	-197.78
7-8CW	38.	10.11	113.	12.41	5035.	-26.53	-198.02	.15	-197.87
7-9CW	38.	10.11	113.	12.43	5035.	-26.55	-198.04	.15	-197.89
7-1KW	38.	10.11	113.	12.45	5035.	-26.65	-198.16	.15	-198.01
521CW	38.	10.89	113.	12.12	5040.	-26.72	-198.39	.15	-198.24

STATION NUMBER	LATITUDE DEG MIN	LONGITUDE DEG MIN	ELEVATION IN FEET	FREE-AIR ANOMALY	SIMPLE BOUGUER	TERRAIN CORRECTION	TERR-CORR BOUGUER
522CW	38. 10.89	113. 12.14	5040.	-26.84	-198.52	.15	-198.37
523CW	38. 10.89	113. 12.16	5039.	-27.06	-198.69	.15	-198.54
524CW	38. 10.89	113. 12.18	5038.	-27.19	-198.80	.15	-198.65
525CW	38. 10.89	113. 12.20	5040.	-27.25	-198.90	.15	-198.75
526CW	38. 10.89	113. 12.22	5038.	-27.35	-198.95	.15	-198.80
527CW	38. 10.89	113. 12.24	5038.	-27.43	-199.01	.15	-198.86
528CW	38. 10.89	113. 12.26	5036.	-27.57	-199.10	.15	-198.95
529CW	38. 10.89	113. 12.28	5035.	-27.69	-109.20	.15	-109.05
5-3KW	38. 10.89	113. 12.30	5035.	-27.81	-199.31	.15	-199.16
1-0	38. 10.67	113. 11.69	5028.	-26.15	-197.40	.15	-197.25
1-.1E	38. 10.67	113. 11.58	5028.	-26.11	-197.36	.15	-197.21
1-.2E	38. 10.67	113. 11.47	5027.	-25.97	-197.20	.15	-197.05
1-.3E	38. 10.67	113. 11.36	5027.	-26.09	-197.30	.16	-197.14
1-.4E	38. 10.67	113. 11.25	5027.	-26.19	-197.41	.16	-197.25
1-.5E	38. 10.67	113. 11.13	5027.	-26.40	-197.61	.16	-197.45
1-.6E	38. 10.67	113. 11.02	5028.	-26.41	-197.66	.16	-197.50
1-.7E	38. 10.67	113. 10.91	5028.	-26.34	-197.59	.17	-197.42
1-.8E	38. 10.67	113. 10.80	5029.	-26.52	-197.80	.17	-197.63
1-.9E	38. 10.67	113. 10.69	5033.	-26.69	-198.13	.17	-197.96
1-1E	38. 10.67	113. 10.58	5031.	-27.00	-198.35	.17	-198.18
1-.1W	38. 10.67	113. 11.80	5032.	-26.20	-197.60	.15	-197.45
1-.2W	38. 10.67	113. 11.91	5034.	-26.35	-197.81	.16	-197.65
1-.3W	38. 10.67	113. 12.02	5043.	-26.45	-198.22	.16	-198.06
.3-1C	38. 10.67	113. 12.04	5046.	-26.45	-198.30	.16	-198.14
.3-2C	38. 10.67	113. 12.06	5049.	-26.48	-198.44	.16	-198.28
.3-3C	38. 10.67	113. 12.08	5053.	-26.37	-198.47	.16	-198.31
.3-4C	38. 10.67	113. 12.10	5060.	-26.32	-198.66	.16	-198.50
.3-5C	38. 10.67	113. 12.12	5062.	-26.24	-198.66	.16	-198.50
.3-6C	38. 10.67	113. 12.14	5056.	-26.58	-198.79	.16	-198.63
.3-7C	38. 10.67	113. 12.16	5052.	-26.69	-198.77	.16	-198.61

STATION NUMBER	LATITUDE DEG MIN		LONGITUDE DEG MIN		ELEVATION IN FEET	FREE-AIR ANOMALY	SIMPLE BOUGUER	TERRAIN CORRECTION	TERR-CORR BOUGUER
.3-8C	38.	10.67	113.	12.18	5048.	-26.92	-198.87	.16	-198.71
.3-9C	38.	10.67	113.	12.20	5047.	-27.23	-199.12	.16	-198.96
.3-1K	38.	10.67	113.	12.22	5045.	-27.19	-199.01	.16	-198.85
1-.6W	38.	10.67	113.	12.36	5034.	-27.96	-199.42	.15	-199.27
1-.7W	38.	10.67	113.	12.47	5034.	-28.31	-199.76	.15	-199.61
1-.8W	38.	10.67	113.	12.58	5033.	-28.59	-200.03	.14	-199.89
1-.9W	38.	10.67	113.	12.69	5034.	-28.99	-200.46	.14	-200.32
1-1W	38.	10.67	113.	12.80	5034.	-29.42	-200.90	.14	-200.76
9-0	38.	10.38	113.	12.16	5037.	-27.14	-198.70	.17	-198.53
9-1CE	38.	10.38	113.	12.15	5036.	-27.13	-198.66	.17	-198.49
9-2CE	38.	10.36	113.	12.13	5032.	-27.17	-198.57	.17	-198.40
9-3CE	38.	10.36	113.	12.11	5030.	-27.18	-198.49	.17	-198.32
9-4CE	38.	10.35	113.	12.10	5028.	-27.16	-198.41	.17	-198.24
9-5CE	38.	10.34	113.	12.07	5026.	-27.13	-198.32	.17	-198.15
9-6CE	38.	10.34	113.	12.05	5026.	-27.07	-198.24	.17	-198.07
9-7CE	38.	10.34	113.	12.03	5025.	-27.00	-198.16	.17	-197.99
9-8CE	38.	10.34	113.	12.01	5025.	-26.93	-198.09	.17	-197.92
9-9CE	38.	10.34	113.	11.99	5025.	-26.86	-198.00	.17	-197.83
9-1KE	38.	10.33	113.	11.97	5025.	-26.71	-197.86	.17	-197.69
911CE	38.	10.33	113.	11.95	5025.	-26.59	-197.73	.18	-197.55
912CE	38.	10.33	113.	11.93	5025.	-26.45	-197.59	.18	-197.41
913CE	38.	10.33	113.	11.90	5025.	-26.28	-197.42	.18	-197.24
914CE	38.	10.32	113.	11.88	5025.	-26.08	-197.22	.18	-197.04
915CE	38.	10.32	113.	11.86	5025.	-25.92	-197.06	.18	-196.88
916CE	38.	10.31	113.	11.84	5025.	-25.71	-196.84	.18	-196.66
917CE	38.	10.31	113.	11.82	5024.	-25.54	-196.67	.18	-196.49
918CE	38.	10.30	113.	11.80	5024.	-25.37	-196.50	.18	-196.32
919CE	38.	10.29	113.	11.78	5024.	-25.19	-196.33	.18	-196.15
9-2KE	38.	10.28	113.	11.76	5024.	-25.06	-196.18	.18	-196.00
9-1CW	38.	10.39	113.	12.18	5037.	-27.26	-198.82	.17	-198.65

STATION NUMBER	LATITUDE DEG	MIN	LONGITUDE DEG	MIN	ELEVATION IN FEET	FREE-AIR ANOMALY	SIMPLE BOUGUER	TERRAIN CORRECTION	TERR-CORR BOUGUER
9-2CW	38.	10.40	113.	12.20	5039.	-27.26	-198.88	.17	-198.71
9-3CW	38.	10.42	113.	12.20	5044.	-27.29	-199.09	.17	-198.92
9-4CW	38.	10.44	113.	12.21	5050.	-27.13	-199.12	.17	-198.95
9-5CW	38.	10.45	113.	12.23	5049.	-27.19	-199.16	.17	-198.99
9-6CW	38.	10.46	113.	12.25	5043.	-27.37	-199.13	.17	-198.96
9-7CW	38.	10.46	113.	12.27	5039.	-27.51	-199.15	.17	-198.98
9-8CW	38.	10.46	113.	12.29	5036.	-27.69	-199.21	.17	-199.04
9-9CW	38.	10.46	113.	12.32	5033.	-27.95	-199.38	.17	-199.21
9-1KW	38.	10.46	113.	12.33	5032.	-28.03	-199.41	.17	-199.24
911CW	38.	10.46	113.	12.36	5031.	-28.15	-199.51	.16	-199.35
912CW	38.	10.46	113.	12.38	5027.	-28.29	-199.53	.16	-199.37
913CW	38.	10.48	113.	12.40	5027.	-28.40	-199.63	.16	-199.47
914CW	38.	10.48	113.	12.42	5027.	-28.44	-199.67	.16	-199.51
915CW	38.	10.49	113.	12.44	5027.	-28.51	-199.74	.16	-199.58
.311C	38.	10.67	113.	12.24	5041.	-27.36	-199.06	.16	-198.90
.312C	38.	10.67	113.	12.26	5040.	-27.46	-199.12	.16	-198.96
.313C	38.	10.67	113.	12.28	5038.	-27.57	-199.15	.16	-198.99
.314C	38.	10.67	113.	12.30	5035.	-27.69	-199.18	.16	-199.02
.315C	38.	10.67	113.	12.32	5035.	-27.79	-109.27	.16	-109.11
8-.2E	38.	11.97	113.	11.44	5037.	-23.75	-195.30	.15	-195.15
8-.1E	38.	11.97	113.	11.55	5038.	-24.35	-195.95	.15	-195.80
8-0	38.	11.97	113.	11.66	5040.	-24.84	-196.50	.15	-196.35
8-.1W	38.	11.97	113.	11.77	5042.	-25.57	-197.30	.15	-197.15
8-.2W	38.	11.97	113.	11.88	5044.	-26.40	-198.21	.15	-198.06
8-.3W	38.	11.97	113.	11.99	5048.	-27.14	-199.07	.15	-198.92
8-.4W	38.	11.97	113.	12.10	5052.	-27.74	-199.82	.15	-199.67
8-.5W	38.	11.97	113.	12.21	5055.	-28.27	-200.46	.15	-200.31
8-.3E	38.	11.97	113.	11.33	5035.	-23.51	-195.01	.15	-194.86
8-.4E	38.	11.97	113.	11.22	5034.	-34.04	-205.49	.15	-205.34
8-.5E	38.	11.97	113.	11.11	5033.	-23.39	-194.80	.15	-194.65

STATION NUMBER	LATITUDE	LONGITUDE	REDUCED MAGNETIC VALUE
RS1	38. 10.00	113. 10.38	697.0
RS2	38. 9.79	113. 9.50	485.0
RS3	38. 8.91	113. 8.40	972.0
RS4	38. 7.73	113. 8.45	973.0
RS5	38. 7.73	113. 10.65	1092.0
RS6	38. 8.91	113. 10.59	440.0
RS7	38. 9.79	113. 8.43	442.0
RS8	38. 8.93	113. 11.70	834.0
RS9	38. 8.93	113. 12.83	470.0
RS10	38. 8.03	113. 14.50	716.0
RS11	38. 8.41	113. 14.87	478.0
RS12	38. 8.93	113. 15.01	606.0
RS13	38. 9.80	113. 15.03	814.0
RS14	38. 10.65	113. 8.43	641.0
RS15	38. 10.65	113. 15.03	895.0
RS16	38. 11.55	113. 15.03	1119.0
RS17	38. 12.40	113. 15.01	1199.0
RS18	38. 12.40	113. 13.92	872.0
RS19	38. 11.55	113. 13.92	1198.0
RS20	38. 13.93	113. 12.60	988.0
RS21	38. 14.19	113. 12.20	1023.0
RS22	38. 14.19	113. 11.65	1026.0
RS23	38. 14.19	113. 10.60	1200.0
RS24	38. 14.19	113. 9.45	1151.0
RS25	38. 14.80	113. 14.15	1053.0
RS26	38. 12.39	113. 11.70	934.0
RS27	38. 12.44	113. 12.80	1126.0
RS28	38. 12.40	113. 10.60	1117.0
RS29	38. 12.40	113. 8.43	911.0
RS30	38. 10.68	113. 13.68	884.0

STATION NUMBER	LATITUDE	LONGITUDE	REDUCED MAGNETIC VALUE
RS31	38. 8.15	113. 20.95	669.0
RS32	38. 8.93	113. 21.70	633.0
RS33	38. 7.84	113. 21.70	595.0
RS34	38. 8.84	113. 19.58	664.0
RS35	38. 10.65	113. 16.70	921.0
RS36	38. 10.70	113. 17.22	816.0
RS37	38. 10.65	113. 15.51	889.0
RS38	38. 13.15	113. 21.83	819.0
RS39	38. 12.83	113. 21.78	764.0
RS40	38. 12.40	113. 21.63	774.0
RS41	38. 12.40	113. 21.08	762.0
RS42	38. 12.40	113. 20.53	690.0
RS43	38. 14.19	113. 19.43	548.0
RS44	38. 14.75	113. 17.86	722.0
RS45	38. 14.40	113. 17.85	904.0
RS46	38. 13.26	113. 19.99	870.0
RS47	38. 10.65	113. 20.53	838.0
RS48	38. 10.75	113. 19.58	863.0
RS49	38. 10.65	113. 19.43	868.0
RS50	38. 10.21	113. 21.20	821.0
RS51	38. 9.90	113. 7.43	222.0
RS52	38. 9.79	113. 6.19	706.0
RS53	38. 10.38	113. 4.40	595.0
RS54	38. 9.43	113. 4.85	805.0
RS55	38. 8.91	113. 5.08	287.0
RS56	38. 8.53	113. 4.99	809.0
RS57	38. 10.69	113. 4.18	682.0
RS58	38. 10.68	113. 3.29	745.0
RS59	38. 9.43	113. 3.50	1072.0
RS60	38. 11.54	113. 3.94	681.0

STATION NUMBER	LATITUDE	LONGITUDE	REDUCED MAGNETIC VALUE
RS61	38. 11.54	113. 5.05	852.0
RS62	38. 12.40	113. 5.03	931.0
RS63	38. 12.40	113. 3.94	721.0
RS64	38. 13.70	113. 23.13	743.0
RS65	38. 13.65	113. 23.38	742.0
RS66	38. 13.25	113. 24.00	655.0
RS67	38. 12.78	113. 24.33	834.0
RS68	38. 12.08	113. 24.99	501.0
RS69	38. 11.73	113. 25.85	764.0
RS70	38. 11.53	113. 26.84	682.0
RS71	38. 11.23	113. 27.61	599.0
RS72	38. 14.30	113. 23.29	731.0
RS73	38. 23.25	113. 2.64	768.0
RS74	38. 23.30	113. 3.96	730.0
RS75	38. 23.44	113. 5.10	759.0
RS76	38. 23.53	113. 5.71	742.0
RS77	38. 21.29	113. 4.83	1463.0
RS78	38. 20.51	113. 5.38	1532.0
RS79	38. 19.66	113. 6.26	938.0
RS80	38. 20.03	113. 7.48	997.0
RS81	38. 18.43	113. 7.50	829.0
RS82	38. 19.45	113. 6.14	892.0
RS83	38. 19.60	113. 5.73	912.0
RS84	38. 19.93	113. 5.48	1027.0
RS85	38. 20.78	113. 4.76	1624.0
RS86	38. 21.68	113. 4.19	1140.0
RS87	38. 22.10	113. 3.89	1066.0
RS88	38. 22.10	113. 1.65	737.0
RS89	38. 21.65	113. 2.15	961.0
RS90	38. 21.63	113. 2.67	954.0

STATION NUMBER	LATITUDE	LONGITUDE	REDUCED MAGNETIC VALUE
RS91	38. 21.83	113. 3.04	1027.0
RS92	38. 20.11	113. 3.41	926.0
RS93	38. 19.20	113. 4.16	741.0
RS94	38. 17.86	113. 5.28	810.0
RS95	38. 18.29	113. 6.63	878.0
RS96	38. 18.38	113. 6.91	853.0
RS97	38. 22.48	113. 5.24	825.0
RS98	38. 21.20	113. 7.23	1000.0
RS99	38. 22.08	113. 6.13	824.0
RS100	38. 21.59	113. 5.90	1464.0
RS101	38. 22.01	113. 7.16	844.0
RS102	38. 20.34	113. 6.13	1324.0
RS103	38. 19.45	113. 7.24	927.0
RS104	38. 17.68	113. 8.33	698.0
RS105	38. 16.93	113. 9.03	605.0
RS106	38. 15.93	113. 10.05	550.0
RS107	38. 15.93	113. 9.43	493.0
RS108	38. 15.93	113. 8.33	719.0
RS109	38. 15.93	113. 7.75	613.0
RS110	38. 20.52	113. 3.28	1423.0
RS111	38. 15.93	113. 6.90	511.0
RS112	38. 16.80	113. 7.24	761.0
RS113	38. 15.93	113. 10.96	703.0
RS114	38. 15.93	113. 11.35	771.0
RS115	38. 15.93	113. 11.65	658.0
RS116	38. 15.93	113. 13.53	336.0
RS117	38. 15.45	113. 14.16	337.0
RS118	38. 15.33	113. 14.69	429.0
RS119	38. 16.19	113. 11.64	760.0
RS120	38. 16.85	113. 11.43	647.0

STATION NUMBER	LATITUDE	LONGITUDE	REDUCED MAGNETIC VALUE
RS121	38. 17.83	113. 11.63	770.0
RS122	38. 18.21	113. 11.88	366.0
RS123	38. 20.05	113. 11.95	614.0
RS124	38. 19.74	113. 12.08	842.0
RS125	38. 19.25	113. 8.15	829.0
RS126	38. 20.25	113. 7.93	927.0
RS127	38. 22.03	113. 4.51	1109.0
RS128	38. 19.13	113. 6.83	843.0
RS129	38. 16.81	113. 8.33	912.0
RS130	38. 16.80	113. 7.74	801.0
RS131	38. 17.68	113. 6.84	821.0
RS132	38. 18.08	113. 5.95	779.0
RS133	38. 16.88	113. 6.10	942.0
RS134	38. 20.86	113. 2.78	1365.0
RS135	38. 18.55	113. 4.71	685.0
RS136	38. 21.21	113. 3.89	1383.0
RS137	38. 19.45	113. 5.28	814.0
RS138	38. 15.79	113. 12.35	1013.0
RS139	38. 16.33	113. 14.94	479.0
RS140	38. 16.80	113. 13.85	757.0
RS141	38. 17.33	113. 12.59	251.0
RS142	38. 17.34	113. 12.03	1429.0
RS143	38. 17.19	113. 11.26	711.0
RS144	38. 17.30	113. 10.33	143.0
RS145	38. 18.26	113. 9.54	712.0
RS146	38. 18.55	113. 8.33	795.0
RS147	38. 18.53	113. 12.41	663.0
RS148	38. 18.90	113. 12.85	773.0
RS149	38. 19.50	113. 12.95	1290.0
RS150	38. 20.03	113. 13.25	658.0

STATION NUMBER	LATITUDE	LONGITUDE	REDUCED MAGNETIC VALUE
RS151	38. 21.45	113. 13.48	950.0
RS152	38. 20.91	113. 13.65	768.0
RS153	38. 20.60	113. 13.90	658.0
RS154	38. 18.64	113. 13.18	577.0
RS155	38. 18.59	113. 13.78	478.0
RS156	38. 18.93	113. 14.73	662.0
RS157	38. 18.03	113. 14.33	527.0
RS158	38. 18.85	113. 12.05	774.0
RS159	38. 19.59	113. 12.18	808.0
RS160	38. 19.08	113. 8.64	834.0
RS161	38. 19.65	113. 8.79	827.0
RS162	38. 7.60	113. 16.26	604.0
RS163	38. 7.76	113. 16.75	639.0
RS164	38. 8.70	113. 15.58	504.0
RS165	38. 9.35	113. 16.53	646.0
RS166	38. 8.20	113. 19.56	627.0
RS167	38. 7.74	113. 19.03	625.0
RS168	38. 10.66	113. 21.25	751.0
RS169	38. 11.11	113. 20.15	831.0
RS170	38. 12.09	113. 17.25	1061.0
RS171	38. 12.71	113. 17.34	778.0
RS172	38. 13.88	113. 17.52	694.0
RS173	38. 14.59	113. 18.63	1393.0
RS174	38. 14.46	113. 17.00	576.0
RS175	38. 13.80	113. 17.10	954.0
RS176	38. 13.95	113. 20.09	688.0
RS177	38. 12.81	113. 19.98	757.0
RS178	38. 12.13	113. 19.98	710.0
RS179	38. 15.04	113. 10.95	889.0
RS180	38. 15.06	113. 10.54	811.0

STATION NUMBER	LATITUDE	LONGITUDE	REDUCED MAGNETIC VALUE
RS181	38. 15.06	113. 11.65	982.0
RS182	38. 15.06	113. 13.86	536.0
RS183	38. 15.15	113. 12.53	865.0
RS184	38. 15.06	113. 9.44	907.0
RS185	38. 15.06	113. 8.33	1055.0
RS186	38. 18.57	113. 9.90	805.0
RS187	38. 19.19	113. 10.13	718.0
RS188	38. 19.73	113. 10.21	699.0
RS189	38. 20.15	113. 9.86	751.0
RS190	38. 20.54	113. 9.68	829.0
RS191	38. 20.93	113. 9.85	917.0
RS192	38. 21.34	113. 9.71	862.0
RS193	38. 22.05	113. 10.45	883.0
RS194	38. 22.05	113. 9.08	1201.0
RS195	38. 21.79	113. 9.75	865.0
RS196	38. 20.89	113. 7.60	950.0
RS197	38. 21.20	113. 8.33	805.0
RS198	38. 20.75	113. 8.63	800.0
RS199	38. 15.90	113. 14.49	665.0
RS200	38. 16.54	113. 14.33	266.0
RS201	38. 16.55	113. 12.10	714.0
RS202	38. 17.15	113. 13.07	670.0
RS203	38. 22.03	113. 12.26	929.0
RS204	38. 21.73	113. 12.26	966.0
RS205	38. 21.23	113. 12.24	938.0
RS206	38. 20.75	113. 12.10	833.0
RS207	38. 17.75	113. 9.96	707.0
RS208	38. 17.85	113. 12.51	1315.0
RS209	38. 18.54	113. 10.76	857.0
RS210	38. 18.68	113. 10.28	814.0

STATION NUMBER	LATITUDE	LONGITUDE	REDUCED MAGNETIC VALUE
RS211	38. 15.48	113. 17.76	313.0
RS212	38. 16.01	113. 17.70	397.0
RS213	38. 16.53	113. 18.09	570.0
RS214	38. 17.53	113. 18.24	1190.0
RS215	38. 15.06	113. 17.23	895.0
RS216	38. 15.68	113. 16.46	532.0
RS217	38. 16.25	113. 16.49	401.0
RS218	38. 16.83	113. 16.66	488.0
RS219	38. 16.80	113. 17.23	382.0
RS220	38. 17.33	113. 16.44	458.0
RS221	38. 17.68	113. 16.28	652.0
RS222	38. 15.06	113. 16.13	594.0
RS223	38. 15.06	113. 15.02	604.0
RS224	38. 15.58	113. 15.50	350.0
RS225	38. 16.13	113. 15.18	227.0
RS226	38. 15.06	113. 19.44	395.0
RS227	38. 15.06	113. 20.53	365.0
RS228	38. 19.45	113. 17.23	785.0
RS229	38. 19.02	113. 16.89	733.0
RS230	38. 18.58	113. 16.64	609.0
RS231	38. 18.25	113. 17.01	590.0
RS232	38. 18.19	113. 16.25	583.0
RS233	38. 16.80	113. 15.02	1126.0
RS234	38. 17.63	113. 15.18	416.0
RS235	38. 17.08	113. 16.23	431.0
RS236	38. 16.68	113. 16.00	-75.0
RS237	38. 15.06	113. 18.33	261.0
RS238	38. 15.75	113. 18.64	2468.0
RS239	38. 14.81	113. 23.40	816.0
RS240	38. 14.75	113. 24.20	514.0

STATION NUMBER	LATITUDE	LONGITUDE	REDUCED MAGNETIC VALUE
RS241	38. 14.70	113. 24.80	574.0
RS242	38. 14.34	113. 24.31	783.0
RS243	38. 13.93	113. 24.57	752.0
RS244	38. 11.63	113. 24.73	656.0
RS245	38. 11.25	113. 24.73	476.0
RS246	38. 10.66	113. 26.88	757.0
RS247	38. 9.94	113. 26.46	665.0
RS248	38. 9.43	113. 26.13	609.0
RS249	38. 8.90	113. 25.85	625.0
RS250	38. 8.31	113. 25.68	592.0
RS251	38. 7.55	113. 25.70	351.0
RS252	38. 8.03	113. 25.23	598.0
RS253	38. 8.48	113. 25.08	600.0
RS254	38. 8.93	113. 24.97	722.0
RS255	38. 6.98	113. 25.36	624.0
RS256	38. 7.35	113. 25.71	431.0
RS257	38. 21.23	113. 1.65	1018.0
RS258	38. 20.33	113. 1.65	897.0
RS259	38. 20.33	113. 2.78	1208.0
RS260	38. 19.23	113. 2.78	816.0
RS261	38. 17.69	113. 2.78	770.0
RS262	38. 17.46	113. 3.90	993.0
RS263	38. 15.93	113. 3.90	870.0
RS264	38. 15.05	113. 3.90	999.0
RS265	38. 15.93	113. 6.13	704.0
RS266	38. 8.36	113. 5.89	-97.0
RS267	38. 7.90	113. 6.05	609.0
RS268	38. 7.79	113. 6.75	1413.0
RS269	38. 8.23	113. 7.49	1024.0
RS270	38. 13.30	113. 6.18	1060.0

STATION NUMBER	LATITUDE	LONGITUDE	REDUCED MAGNETIC VALUE
RS271	38. 14.18	113. 5.01	1204.0
RS272	38. 14.18	113. 2.80	1207.0
RS273	38. 12.55	113. 7.25	833.0
75110	38. 10.25	113. 11.65	726.0
75115	38. 10.35	113. 12.11	739.0
75120	38. 10.51	113. 12.50	856.0
75125	38. 10.77	113. 12.93	1014.0
75128	38. 11.29	113. 13.21	1160.0
75131	38. 11.72	113. 13.44	1217.0
75133	38. 11.98	113. 13.61	1121.0
75135	38. 12.05	113. 13.94	1197.0
75137	38. 12.22	113. 14.28	922.0
75143	38. 12.85	113. 13.92	500.0
75148	38. 9.05	113. 12.28	794.0
75152	38. 9.40	113. 14.70	830.0
75153	38. 9.12	113. 14.42	643.0
75154	38. 8.85	113. 14.02	583.0
75155	38. 12.50	113. 9.88	1131.0
75156	38. 10.95	113. 9.50	767.0
75157	38. 11.40	113. 8.85	787.0
75158	38. 11.68	113. 8.43	858.0
75159	38. 10.65	113. 8.43	631.0
75162	38. 10.20	113. 9.70	828.0
75165	38. 10.13	113. 9.05	683.0
75168	38. 10.05	113. 8.43	281.0
75171	38. 9.93	113. 7.68	36.0
75232	38. 12.31	113. 14.91	1079.0
52102	38. 9.80	113. 13.81	903.0
52106	38. 9.80	113. 13.35	897.0
52110	38. 9.80	113. 12.90	854.0

STATION NUMBER	LATITUDE	LONGITUDE	REDUCED MAGNETIC VALUE
52114	38. 9.80	113. 12.40	803.0
52118	38. 9.82	113. 11.98	714.0
52122	38. 9.84	113. 11.58	936.0
52126	38. 9.86	113. 11.18	840.0
52129	38. 9.88	113. 10.88	798.0
52133	38. 9.02	113. 13.65	654.0
52138	38. 9.17	113. 13.18	531.0
52143	38. 9.32	113. 12.69	769.0
52148	38. 9.47	113. 12.20	821.0
52153	38. 9.62	113. 11.70	1082.0
51205	38. 10.67	113. 12.30	806.0
51210	38. 10.67	113. 11.73	746.0
51215	38. 10.66	113. 11.14	855.0
51225	38. 10.66	113. 10.04	908.0
51220	38. 10.66	113. 10.60	800.0
51231	38. 11.09	113. 12.56	993.0
51236	38. 11.09	113. 12.01	797.0
51241	38. 11.09	113. 11.46	707.0
51246	38. 11.09	113. 10.91	848.0
51250	38. 11.53	113. 10.59	780.0
51253	38. 11.53	113. 10.91	838.0
51256	38. 11.53	113. 11.24	754.0
75202	38. 9.79	113. 15.03	810.0
75203	38. 9.79	113. 15.59	879.0
75204	38. 9.79	113. 16.13	802.0
75205	38. 9.79	113. 16.59	839.0
75206	38. 9.79	113. 17.32	805.0
75207	38. 9.79	113. 17.86	758.0
75208	38. 9.79	113. 18.32	733.0
75209	38. 9.78	113. 18.76	701.0

STATION NUMBER	LATITUDE	LONGITUDE	REDUCED MAGNETIC VALUE
75210	38. 9.79	113. 19.19	699.0
75211	38. 9.79	113. 19.57	715.0
75212	38. 9.79	113. 20.13	742.0
75213	38. 9.79	113. 20.52	764.0
75214	38. 9.79	113. 20.91	743.0
75215	38. 9.83	113. 21.20	758.0
75216	38. 10.24	113. 18.32	819.0
75217	38. 10.70	113. 18.32	935.0
75218	38. 11.52	113. 18.31	983.0
75219	38. 11.52	113. 18.87	729.0
75220	38. 11.52	113. 19.70	760.0
75221	38. 11.57	113. 20.58	838.0
75222	38. 11.52	113. 20.95	783.0
75223	38. 11.52	113. 21.32	706.0
75225	38. 12.38	113. 14.61	1024.0
75226	38. 11.53	113. 17.66	1002.0
75227	38. 11.60	113. 17.24	1154.0
75228	38. 11.73	113. 16.79	1102.0
75229	38. 11.84	113. 16.46	1030.0
75230	38. 12.00	113. 15.91	1078.0
75231	38. 12.15	113. 15.45	1259.0
75241	38. 13.88	113. 22.24	828.0
75242	38. 13.93	113. 21.90	839.0
75243	38. 14.11	113. 21.15	697.0
75244	38. 14.19	113. 20.07	468.0
75245	38. 13.88	113. 19.15	1160.0
75246	38. 13.57	113. 18.22	929.0
75247	38. 13.24	113. 17.22	657.0
75248	38. 12.79	113. 15.85	1313.0
74252	38. 13.25	113. 9.85	860.0

STATION NUMBER	LATITUDE	LONGITUDE	REDUCED MAGNETIC VALUE
74255	38. 13.27	113. 10.57	821.0
74258	38. 13.27	113. 11.47	760.0
74260	38. 13.27	113. 12.05	842.0
74263	38. 13.27	113. 12.80	904.0
8-0	38. 11.97	113. 11.66	842.0
8-.1W	38. 11.97	113. 11.77	845.0
8-.2W	38. 11.97	113. 11.88	877.0
8-.3W	38. 11.97	113. 11.99	949.0
8-.4W	38. 11.97	113. 12.10	995.0
8-.5W	38. 11.97	113. 12.21	1021.0
8-.1E	38. 11.97	113. 11.55	910.0
8-.2E	38. 11.97	113. 11.44	1054.0
8-.3E	38. 11.97	113. 11.33	1117.0
8-.4E	38. 11.97	113. 11.22	1182.0
8-.5E	38. 11.97	113. 11.11	1272.0
7-0	38. 10.11	113. 12.25	790.0
7-1CE	38. 10.11	113. 12.23	804.0
7-2CE	38. 10.11	113. 12.21	804.0
7-3CE	38. 10.11	113. 12.19	811.0
7-4CE	38. 10.11	113. 12.17	819.0
7-5CE	38. 10.11	113. 12.15	821.0
7-6CE	38. 10.11	113. 12.13	818.0
7-7CE	38. 10.11	113. 12.11	823.0
7-8CE	38. 10.11	113. 12.09	822.0
7-9CE	38. 10.11	113. 12.07	819.0
7-1KE	38. 10.11	113. 12.05	821.0
711CE	38. 10.11	113. 12.03	814.0
712CE	38. 10.11	113. 12.01	799.0
713CE	38. 10.11	113. 11.99	780.0
714CE	38. 10.11	113. 11.97	783.0

STATION NUMBER	LATITUDE	LONGITUDE	REDUCED MAGNETIC VALUE
715CE	38. 10.11	113. 11.95	783.0
716CE	38. 10.11	113. 11.93	773.0
717CE	38. 10.11	113. 11.91	762.0
718CE	38. 10.11	113. 11.89	761.0
719CE	38. 10.11	113. 11.87	732.0
7-2KE	38. 10.11	113. 11.85	721.0
7-1CW	38. 10.11	113. 12.27	786.0
7-2CW	38. 10.11	113. 12.29	781.0
7-3CW	38. 10.11	113. 12.31	778.0
7-4CW	38. 10.11	113. 12.33	792.0
7-5CW	38. 10.11	113. 12.35	798.0
7-6CW	38. 10.11	113. 12.37	787.0
7-7CW	38. 10.11	113. 12.39	780.0
7-8CW	38. 10.11	113. 12.41	776.0
7-9CW	38. 10.11	113. 12.43	783.0
7-1KW	38. 10.11	113. 12.45	796.0
.34CW	38. 10.67	113. 12.10	742.0
.33CW	38. 10.67	113. 12.08	738.0
.32CW	38. 10.67	113. 12.06	741.0
.31CW	38. 10.67	113. 12.04	738.0
1.3W	38. 10.67	113. 12.02	736.0
.35CW	38. 10.67	113. 12.12	748.0
.36CW	38. 10.67	113. 12.14	748.0
.37CW	38. 10.67	113. 12.16	764.0
.38CW	38. 10.67	113. 12.18	757.0
.39CW	38. 10.67	113. 12.19	778.0
.31KW	38. 10.67	113. 12.20	786.0
5-7CW	38. 10.89	113. 11.84	719.0
5-6CW	38. 10.89	113. 11.82	719.0
5-5CW	38. 10.89	113. 11.80	727.0

STATION NUMBER	LATITUDE	LONGITUDE	REDUCED MAGNETIC VALUE
5-4CW	38. 10.89	113. 11.78	734.0
5-3CW	38. 10.89	113. 11.76	741.0
5-2CW	38. 10.89	113. 11.74	747.0
5-1CW	38. 10.89	113. 11.72	758.0
5-0	38. 10.89	113. 11.70	769.0
5-8CW	38. 10.89	113. 11.86	716.0
5-9CW	38. 10.89	113. 11.88	715.0
5-1KW	38. 10.89	113. 11.90	722.0
511CW	38. 10.89	113. 11.92	728.0
512CW	38. 10.89	113. 11.94	737.0
513CW	38. 10.89	113. 11.96	742.0
514CW	38. 10.89	113. 11.98	743.0
515CW	38. 10.89	113. 12.00	750.0
516CW	38. 10.89	113. 12.02	756.0
517CW	38. 10.89	113. 12.04	767.0
518CW	38. 10.89	113. 12.06	762.0
519CW	38. 10.89	113. 12.08	775.0
5-2KW	38. 10.89	113. 12.10	774.0
521CW	38. 10.89	113. 12.12	782.0
522CW	38. 10.89	113. 12.14	790.0
523CW	38. 10.89	113. 12.16	786.0
524CW	38. 10.89	113. 12.18	793.0
525CW	38. 10.89	113. 12.20	795.0
526CW	38. 10.89	113. 12.22	802.0
527CW	38. 10.89	113. 12.24	816.0
528CW	38. 10.89	113. 12.26	815.0
529CW	38. 10.89	113. 12.28	814.0
5-3KW	38. 10.89	113. 12.30	825.0
6-2KW	38. 11.32	113. 12.00	837.0
619CW	38. 11.32	113. 11.98	814.0

STATION NUMBER	LATITUDE	LONGITUDE	REDUCED MAGNETIC VALUE
618CW	38. 11.32	113. 11.96	812.0
617CW	38. 11.32	113. 11.94	799.0
616CW	38. 11.32	113. 11.92	802.0
615CW	38. 11.32	113. 11.90	786.0
614CW	38. 11.32	113. 11.88	786.0
613CW	38. 11.32	113. 11.86	782.0
612CW	38. 11.32	113. 11.84	782.0
611CW	38. 11.32	113. 11.82	783.0
6-1KW	38. 11.32	113. 11.80	776.0
6-9CW	38. 11.32	113. 11.78	776.0
6-8CW	38. 11.32	113. 11.76	771.0
6-7CW	38. 11.32	113. 11.74	768.0
6-6CW	38. 11.32	113. 11.72	764.0
6-5CW	38. 11.32	113. 11.70	760.0
6-4CW	38. 11.32	113. 11.68	760.0
6-3CW	38. 11.32	113. 11.66	758.0
6-2CW	38. 11.32	113. 11.64	760.0
6-1CW	38. 11.32	113. 11.62	762.0
6-0	38. 11.32	113. 11.60	762.0
6-2KW	38. 11.32	113. 12.00	837.0
3-.3W	38. 11.53	113. 11.93	898.0
3-.2W	38. 11.53	113. 11.82	830.0
3-.1W	38. 11.53	113. 11.71	787.0
3-0	38. 11.53	113. 11.60	770.0
3-.1E	38. 11.53	113. 11.49	752.0
3-.2E	38. 11.53	113. 11.38	747.0
3-.3E	38. 11.53	113. 11.27	732.0
3-.4W	38. 11.53	113. 12.04	924.0
3-.5W	38. 11.53	113. 12.16	942.0
3-.6W	38. 11.53	113. 12.27	972.0

STATION NUMBER	LATITUDE	LONGITUDE	REDUCED MAGNETIC VALUE
3-.7W	38. 11.53	113. 12.38	995.0
3-.8W	38. 11.53	113. 12.49	1009.0
3-.9W	38. 11.53	113. 12.60	1038.0
3-1W	38. 11.53	113. 12.71	1058.0
9-0	38. 10.38	113. 12.16	714.0
9-1CE	38. 10.38	113. 12.15	728.0
9-2CE	38. 10.36	113. 12.13	728.0
9-3CE	38. 10.36	113. 12.11	747.0
9-4CE	38. 10.35	113. 12.10	759.0
9-5CE	38. 10.34	113. 12.07	757.0
9-6CE	38. 10.34	113. 12.05	784.0
9-7CE	38. 10.34	113. 12.03	767.0
9-8CE	38. 10.34	113. 12.01	773.0
9-9CE	38. 10.34	113. 11.99	778.0
9-1KE	38. 10.33	113. 11.97	799.0
911CE	38. 10.33	113. 11.95	789.0
912CE	38. 10.33	113. 11.93	784.0
913CE	38. 10.33	113. 11.90	777.0
914CE	38. 10.32	113. 11.88	770.0
915CE	38. 10.32	113. 11.86	751.0
916CE	38. 10.31	113. 11.84	743.0
917CE	38. 10.31	113. 11.82	746.0
918CE	38. 10.30	113. 11.80	739.0
919CE	38. 10.29	113. 11.78	722.0
9-2KE	38. 10.28	113. 11.76	708.0
9-1CW	38. 10.39	113. 12.18	704.0
9-2CW	38. 10.40	113. 12.20	701.0
9-3CW	38. 10.42	113. 12.20	701.0
9-4CW	38. 10.44	113. 12.21	703.0
9-5CW	38. 10.45	113. 12.23	709.0

STATION NUMBER	LATITUDE	LONGITUDE	REDUCED MAGNETIC VALUE
9-6CW	38. 10.46	113. 12.25	718.0
9-7CW	38. 10.46	113. 12.27	727.0
9-8CW	38. 10.46	113. 12.29	734.0
9-9CW	38. 10.46	113. 12.32	738.0
9-1KW	38. 10.46	113. 12.33	755.0
911CW	38. 10.46	113. 12.36	766.0
912CW	38. 10.46	113. 12.38	763.0
913CW	38. 10.48	113. 12.40	782.0
914CW	38. 10.48	113. 12.42	796.0
915CW	38. 10.49	113. 12.44	805.0
.3-1K	38. 10.67	113. 12.22	789.0
.311C	38. 10.67	113. 12.24	795.0
.312C	38. 10.67	113. 12.26	800.0
.313C	38. 10.67	113. 12.28	800.0
.314C	38. 10.67	113. 12.30	818.0
.315C	38. 10.67	113. 12.32	808.0

VITA

NAME	Robert Frank Sawyer
Birthplace	Brooklyn, New York
Birthdate	March 9, 1947
High School	John Glenn High School Elwood, New York
Military Service 1969-1970	U. S. Army
University 1971-1974	University of Arizona Tucson, Arizona
Degree 1974	B.S. in Geosciences University of Arizona Tucson, Arizona
Professional Organization	Society of Exploration Geophysicists
Professional Positions Summer 1974	Geologist, Cities Service Minerals Corporation Tucson, Arizona
Summer 1975	Geophysicist, Cities Service Minerals Corporation Salt Lake City, Utah
Graduate Student Geophysics Major 1975-1977	Department of Geology and Geophysics University of Utah Salt Lake City, Utah
Research Assistant Summer 1976	Department of Geology and Geophysics University of Utah Salt Lake City, Utah

Thangsuphanich, I., 1976, Regional gravity survey of the Southern Mineral Mountains, Beaver County, Utah; unpublished M. S. thesis, University of Utah, 38 p.

Ward, S. H., 1977, Geothermal exploration architecture: Technical Report ERDA Grant EY-76-S-07-1601, v. 77-2, 19 p.

Ward, S. H., 1977, Workshop on electrical methods in geothermal exploration: Geothermal Workshop U. S. Geological Survey 14-08-0001-G-359, 177 p.

Welsh, J. E., 1973, Paleozoic and Mesozoic stratigraphy of the Milford area, Beaver County, Utah: Utah Geological Association Publication 3, p. 9-12.

White, D. E., and Williams, D. L., 1975, Assessment of Geological Survey Circular 726, 155 p.

Woodward, L. A., 1973, Upper Precambrian and Lower Cambrian rocks of the Milford area, Utah: Utah Geological Association Publication 3, p. 5-8.

Zietz, Isodore, Shuey, Ralph, and Kirby, J. R., Jr., 1976, Aeromagnetic map of Utah: U. S. Geological Survey Map GP-907.

Oppenheim, A V., and Schafer, R. W., 1975, Digital Signal Processing, Prentice-Hall Inc., New Jersey, 585 p.

Parry, W. T., Benson, N. L. and Miller, C. D., 1976, Geochemistry and hydrothermal alteration at selected Utah Hot Springs: Final Report NSF Grant GI-43741, v. 3, 131 p.

Petersen, C. A., 1973, Roosevelt and Thermo Hot Springs, Beaver County, Utah: Utah Geological Association Publication 3, p. 73-74.

Peterson, D. L., 1972, Complete Bouguer anomaly map of parts of Beaver, Iron, and Millard Counties, Southwestern Utah; U. S. Geological Survey Open-File Map.

Rowley, R. D., 1975, Geologic Setting of the Thermo KGRA (KNOWN GEOTHERMAL RESOURCE AREA), BEAVER COUNTY, UTAH (abs.): Program with Abstracts Geol. Soc. America Annual Meeting, Salt Lake City, Utah, Oct. 20-22, p. 1254.

Schmoker, J. W., 1972, Analysis of gravity and aeromagnetic data, San Francisco Mountains and vicinity, Southwestern Utah: Utah Geological and Mineralogical Survey Bulletin 98, 24 p.

Shuey, R. T., and Pasquale, A. S., 1973, End corrections in magnetic profile interpretation: Geophysics, vol. 38, no. 3, p. 507-512.

Snow, J. H., 1977, Gravity and magnetic interpretation using one-dimensional direct search and Marguardt linear inversion: University of Utah GGS 628 class project, 56 p.

Sontag, R. J., 1965, Regional gravity survey of parts of Beaver, Millard, Piute, and Sevier Counties, Utah; unpublished M. S. thesis, University of Utah, 30 p.

Swick, D. H., 1942, Pendulum gravity measurements and isostatic reductions: U. S. Coast and Geodetic Special Publication 232, 82 p.

Talwani, Manik, 1965, Computation with help of a digital computer of magnetic anomalies caused by bodies of arbitrary shape: Geophysics, v. 30, p. 797-817.

Talwani, Manik, and Ewing, Maurice, 1960, Rapid computation of gravitational attraction of three-dimensional bodies of arbitrary shape: Geophysics, v. 25, p. 203-225.

Talwani, M., Worzel, J. L., and Landisman, M., 1959, Rapid computation for two-dimensional bodies with application to the Mendocino Submarine fracture zone: Jour. Geoph. Research, vol. 64, p. 49-59.

Hochstein, M. P., and Hunt, T. M., 1970, Seismic, gravity and magnetic studies, Broadlands geothermal field, New Zealand. Geothermics, Special Issue, 2, v. 2, pt. 1, p. 333-346.

Isherwood, W. F., 1975, Gravity and magnetic studies of the Geyers-Clear Lake Geothermal region, California; United States Department of the Interior Geological Survey. Open-file Report 75-368, 37 p.

Lavin, P. M., and Devane, J. F., 1970, Direct design of two-dimensional digital wave number filters: Geophysics, v. 35, no. 6, p. 1073-1078.

Lemmon, D. M., Silberman, M. L. and Kistler, R. W., 1973, Some K-Ar ages of extrusive and intrusive rocks of the San Francisco and Wah Wah Mountains, Utah: Utah Geological Association Publication 3, p. 23-26.

Miller, G. M., 1958, Post Paleozoic structure and stratigraphy of Blue Mountain area, Southwest Utah; unpublished M. S. thesis, University of Washington, 58 p.

Mitchell, C. M., and others, 1966, Aeromagnetic map of the San Francisco Mountains and vicinity, Southwestern Utah; U. S. Geological Survey Map GP-598.

Montgomery, J. R, 1973, A regional gravity survey of western Utah; unpublished Ph.D. dissertation, University of Utah, 142 p.

Mower, R. W., and Cordova, R. M., 1974, Water resources of the Milford area, Utah, with emphasis on ground water: State of Utah Department of Natural Resources Technical Publication No. 43, 106 p.

Mudgett, P. M., 1963, Regional gravity survey of parts of Beaver and Millard Counties, Utah; unpublished M. S. thesis, University of Utah, 19 p.

Mundorff, J. C., 1970, Major thermal springs of Utah: Utah Geological and Mineralogical Survey Water-Resources Bulletin 13, 60 p.

Nettleton, L. L., 1940, Geophysical Prospecting for Oil: McGraw-Hill Book Company, New York, 444 p.

__________, 1976, Gravity and Magnetics in Oil Prospecting: McGraw-Hill Book Company, New York, 464 p.

Odegard, M. E., and Berg, J. W., 1965, Gravity interpretation using Fourier integral: Geophysics, v. 30, no. 3. p. 424-438.

Cook, K. L., Nilsen, T. H., and Lambert, J. F., 1971, Gravity base station network in Utah -- 1967: Utah Geological and Mineralogical Survey Bulletin 92, 57 p.

Crebs, T. J., 1976, Gravity and Ground Magnetic Surveys of the Central Mineral Mountains, Utah; unpublished M. S. thesis, University of Utah, 129 p.

Crosby, G. W., 1973, Regional structure in southwestern Utah: Utah Geological Association Publication 3, p. 27-32.

Darby, E. K., and Davies, E. B., 1967, The analysis and design of two-dimensional filters for two-dimensional data: Geophysical Prospecting, v. 15, p. 383-406.

Elkins, T. A., 1951, The second vertical derivative method of gravity interpretation: Geophysics, v. 16, no. 1, p. 29-50.

Erickson, M. P., and Dasch, E. J., 1963, Geology and hydrothermal alteration in Northwestern Black Mountains and Southern Shauntie Hills, Beaver and Iron Counties, Utah: Utah Geological and Mineralogical Survey Special Studies 6, 32 p.

Erickson, M. P., 1973, Volcanic rocks of the Milford area, Beaver County, Utah: Utah Geological Association Publication 3, p. 13-22.

Fuller, B. D., 1967, Two-dimensional frequency analysis and design of grid operators: Mining Geophysics, v. 2, Society of Exploration Geophysicists, Tulsa, p. 658-708.

Grant, F. S., 1972, Review of data processing and interpretation methods in gravity and magnetics, 1964-71: Geophysics, v. 37, no. 4, p. 647-661.

Hardman, Elwood, 1964, Regional gravity survey of central Iron and Washington Counties, Utah; unpublished M. S. thesis, University of Utah, 107 p.

Henderson, R. G., and Zietz, Isidore, 1949, The upward continuation of anomalies in total magnetic intensity fields: Geophysics, v. 14, p. 517-534.

Hintze, L. F., 1963 (compiler), Geologic map of southwestern Utah: Utah Geological and Mineralogical Survey.

Hintze, L. F., 1973, Geologic history of Utah: Brigham Young University Geology Studies, v. 20, pt. 3, 181 p.

REFERENCES

Abou-Zied, M. S., 1968, Geology and mineralogy of the Milford Flat quadrangle and the Old Moscow Mine, Star District, Beaver County, Utah; unpublished Ph.D. dissertation, University of Utah, 150 p.

__________, 1973, Geology of the Milford Flat quadrangle, Star District, Beaver County, Utah: Utah Geological Association Publication 3, p. 43-48.

__________, and Whelan, J. A., 1973, Geology and Mineralogy of the Milford Flat quadrangle, Star District, Beaver County, Utah: Utah Geological and Mineralogical Survey Special Studies 46, 23 p.

Baer, J. L., 1962, Geology of the Star Range, Beaver County, Utah: Brigham Young University Geology Studies, v. 9, pt. 2, p. 29-52.

__________, 1973, Summary of stratigraphy and structure of the Star Range, Beaver County, Utah: Utah Geological Association Publication 3, p. 33-38.

Baetcke, G. B., 1969, Stratigraphy of the Star Range and reconnaissance study of three selected mines; unpublished Ph.D. dissertation, University of Utah, 184 p.

Black, D. I., and Scollar, I., 1969, Spatial filtering in the wave-vector domain: Geophysics, v. 34, no. 6, p. 916-923.

Carter, J. A., 1977, M. S. thesis in preparation; University of Utah.

Chapman, R. H., 1975, Geophysical study of the Clear Lake Region: California Special Report 116, California Division of Mines and Geology, 23 p.

Combs, J. H., and Muffler, L. J. P., 1973, Exploration for geothermal resources: Geothermal Energy, Resources, Production, Stimulation, Edited by Kruger, P., and Otte, C., Stanford University Press, Stanford, California, p. 95-129.

Cook, K. L., Montgomery, J. R, Smith, J. T., and Gray E. F., 1975, Simple Bouguer gravity anomaly map of Utah: Utah Geological and Mineralogical Survey, Map 37.